

การบำบัดไอออนปรอทจากน้ำทิ้งที่ได้จากหลุมขุดเจาะปิโตรเลียมโดยใช้เยื่อแผ่นเหลวที่พองด้วยเส้น
ใยกลางในระบบกึ่งต่อเนื่อง



นายเศรษฐา จตุระบูล

จุฬาลงกรณ์มหาวิทยาลัย

CHULALONGKORN UNIVERSITY

บทคัดย่อและแฟ้มข้อมูลฉบับเต็มของวิทยานิพนธ์ตั้งแต่ปีการศึกษา 2554 ที่ให้บริการในคลังปัญญาจุฬาฯ (CUIR)
เป็นแฟ้มข้อมูลของนิสิตเจ้าของวิทยานิพนธ์ ที่ส่งผ่านทางบัณฑิตวิทยาลัย

The abstract and full text of theses from the academic year 2011 in Chulalongkorn University Intellectual Repository (CUIR)
are the thesis authors' files submitted through the University Graduate School.

วิทยานิพนธ์นี้เป็นส่วนหนึ่งของการศึกษาตามหลักสูตรปริญญาวิศวกรรมศาสตรดุษฎีบัณฑิต

สาขาวิชาวิศวกรรมเคมี ภาควิชาวิศวกรรมเคมี

คณะวิศวกรรมศาสตร์ จุฬาลงกรณ์มหาวิทยาลัย

ปีการศึกษา 2557

ลิขสิทธิ์ของจุฬาลงกรณ์มหาวิทยาลัย

TREATMENT OF MERCURY IONS FROM PETROLEUM CO-PRODUCED WATER VIA SEMI-
CONTINUOUS HOLLOW FIBER SUPPORTED LIQUID MEMBRANE SYSTEM

Mr. Srestha Chaturabul



A Dissertation Submitted in Partial Fulfillment of the Requirements
for the Degree of Doctor of Engineering Program in Chemical Engineering

Department of Chemical Engineering

Faculty of Engineering

Chulalongkorn University

Academic Year 2014

Copyright of Chulalongkorn University

Thesis Title	TREATMENT OF MERCURY IONS FROM PETROLEUM CO-PRODUCED WATER VIA SEMI- CONTINUOUS HOLLOW FIBER SUPPORTED LIQUID MEMBRANE SYSTEM
By	Mr. Srestha Chaturabul
Field of Study	Chemical Engineering
Thesis Advisor	Professor Ura Pancharoen, D.Eng.Sc.

Accepted by the Faculty of Engineering, Chulalongkorn University in Partial
Fulfillment of the Requirements for the Doctoral Degree

.....Dean of the Faculty of Engineering
(Professor Bundhit Eua-arporn, Ph.D.)

THESIS COMMITTEE

.....Chairman
(Associate Professor Siriporn Damrongsakkul, Ph.D.)

.....Thesis Advisor
(Professor Ura Pancharoen, D.Eng.Sc.)

.....Examiner
(Assistant Professor Suphot Phatanasri, D.Eng.)

.....Examiner
(Doctor Chutimon Satirapipathkul, D.Eng.)

.....External Examiner
(Assistant Professor Prakorn Ramkul, D.Eng.)

เศรษฐา จตุระบูล : การบำบัดไอออนปรอทจากน้ำทิ้งที่ได้จากหลุมขุดเจาะปิโตรเลียมโดยใช้เยื่อแผ่นเหลวที่พุงด้วยเส้นใยกลวงในระบบกึ่งต่อเนื่อง (TREATMENT OF MERCURY IONS FROM PETROLEUM CO-PRODUCED WATER VIA SEMI-CONTINUOUS HOLLOW FIBER SUPPORTED LIQUID MEMBRANE SYSTEM) อ.ที่ปรึกษาวิทยานิพนธ์
 หลัก: ศ. ดร.อุรา ปานเจริญ, 282 หน้า.

งานวิจัยนี้ ศึกษาการแยกไอออน ปรอท ออกจากน้ำทิ้งจากหลุมขุดเจาะแก๊สธรรมชาติผ่านระบบเยื่อแผ่นเหลวที่พุงด้วยเส้นใยกลวง ปัจจัยที่ศึกษา ได้แก่ ชนิดและความเข้มข้นของสารสกัด/สารละลายนำกลับ เช่น Aliquat 336/ไทโอยูเรีย และ Calix[4]arene nitrile/ Deionized -water ค่าความเป็นกรด-เบส ในสารละลายป้อน รูปแบบการไหล ระยะเวลาปฏิบัติการ และอัตราการไหลสถานะที่ดีที่สุด สำหรับ Aliquat 336/ไทโอยูเรีย คือ ความเป็นกรด-เบส ในสารละลายป้อนมีค่าเท่ากับ 1 สารสกัด Aliquat 336 ที่ความเข้มข้น 4% (v/v) สารละลายนำกลับไทโอยูเรียที่ความเข้มข้น 0.1 โมลต่อลิตร ที่อุณหภูมิ 301 K สำหรับ Calix[4]arene nitrile/ Deionized คือ ความเป็นกรด-เบส ในสารละลายป้อนมีค่าเท่ากับ 4.5 สารสกัด of Calix[4]arene nitrile ที่ความเข้มข้น 0.004 โมลาร์ โดยใช้ Deionized-water เป็นสารละลายนำกลับ ที่อุณหภูมิ 313 K อัตราการไหลของสารละลายป้อนและสารละลายนำกลับเท่ากับ 100 มิลลิลิตรต่อนาที สารละลายป้อนไหลผ่านมอดูลเส้นใยกลวงครั้งเดียว ส่วนสารละลายนำกลับให้ไหลวน นอกจากนี้ ได้พัฒนาแบบจำลองทางคณิตศาสตร์สำหรับทำนายผลความเข้มข้นของไอออนปรอทโดยอาศัยความหนาแน่นของการไหล (flux) ซึ่งพิจารณาเทอมของการพา การแพร่ ปฏิกริยาที่ผิวสัมผัสของเยื่อแผ่นเหลว และการสะสมของไอออนปรอทพบว่าผลการทำนายความเข้มข้นของไอออนปรอททั้งในสารละลายป้อนและสารละลายนำกลับสอดคล้องกับค่าที่ได้จากการทดลอง ค่าเบี่ยงเบนมาตรฐานของการทำนายผลความเข้มข้นของไอออนปรอทในการสกัดและนำกลับมีค่าเท่ากับ 1.5% and 1.8% ตามลำดับ ซึ่งแบบจำลองนี้ทำให้เข้าใจกลไกการเคลื่อนที่ของไอออนปรอทจากสารละลายป้อนไปยังสารละลายนำกลับ และยังนำไปใช้ในการออกแบบเพื่อขยายขนาดสำหรับภาคอุตสาหกรรมต่อไป

ภาควิชา วิศวกรรมเคมี

ลายมือชื่อนิสิต

สาขาวิชา วิศวกรรมเคมี

ลายมือชื่อ อ.ที่ปรึกษาหลัก

ปีการศึกษา 2557

5271840021 : MAJOR CHEMICAL ENGINEERING

KEYWORDS: TREATMENT / PRODUCED WATER / MERCURY / SEMICONTINUOUS

SRESTHA CHATURABUL: TREATMENT OF MERCURY IONS FROM PETROLEUM CO-PRODUCED WATER VIA SEMI-CONTINUOUS HOLLOW FIBER SUPPORTED LIQUID MEMBRANE SYSTEM. ADVISOR: PROF. URA PANCHAROEN, D.Eng.Sc., 282 pp.

This study investigated the separation of mercury ions from produced water via hollow fiber supported liquid membrane (HFSLM). The influences of types and concentration of extractant / stripping agent, i.e. Aliquat 336 / Thiourea and Calix[4]arene nitrile / DI- water, pH in feed solution, flow patterns, operating time, and flow rates were investigated. The optimum condition was identified and reported: Aliquat 336/Thiourea hybrid at 1 pH of feed solution, 4% (v/v) Aliquat 336, 0.1 M Thiourea an operating temperature of 301 K; Calix[4]arene nitrile/DI-water at 4.5 pH of feed solution, 0.004 M of Calix[4]arene nitrile, DI-water as stripping solution and an operating temperature of 313 K. A single-pass flow pattern of feed solution and circulating flow pattern of the stripping solution of 100 mL/min were found to be the most practical setup to deal with continuous and large feed of the produced water, whilst, the mercury waste is manageable following the circulation of the stripping solution in a limited volume. In conjunction with experimental work, the new mathematical model to predict the concentration of mercury ions via HFSLM was developed by factoring mass transfer fluxes from convection, diffusion and reaction in the model. From the verification, the hypothetical concentrations of mercury ions aligned closely with the experimental results. Average standard deviations for predicting the extraction and recovery were 1.5% and 1.8%. The results imply that the combination of convection, diffusion and reaction is crucial for accurate prediction in this unsteady state model. This robust model with its high accuracy provides a greater understanding of transport mechanism across the feed to the stripping solution; a design scale-up for industrial application could prove useful.

Department: Chemical Engineering Student's Signature

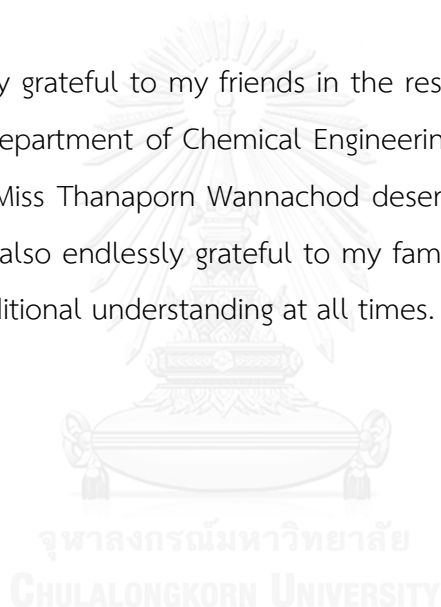
Field of Study: Chemical Engineering Advisor's Signature

Academic Year: 2014

ACKNOWLEDGEMENTS

I would like to express my grateful thanks to my advisor, Professor Dr. Ura Pancharoen, for his consistent kindness and support. He spent his time many years to advice me. I might never complete my doctoral dissertation without his encouragement. My deep appreciation also goes to the thesis committee, Assoc. Prof. Siriporn Damrongsakkul, Asst. Prof. Suphot Phatanasri, Doctor Chutimon Satirapipathkul and Asst. Prof. Prakorn Ramkul for many useful comments and suggestions.

I am deeply grateful to my friends in the research group, the Separation Laboratory at the Department of Chemical Engineering, Chulalongkorn University, Bangkok, Thailand. Miss Thanaporn Wannachod deserves special mention for her great support. I am also endlessly grateful to my family for their encouragement, support and unconditional understanding at all times.



CONTENTS

	Page
THAI ABSTRACT	iv
ENGLISH ABSTRACT	v
ACKNOWLEDGEMENTS	vi
CONTENTS	vii
LIST OF TABLES	xiii
LIST OF FIGURES	xv
CHAPTER 1.....	1
1.1 Rationale of research problem	1
1.1.1 Toxicity of mercury	5
1.1.2 Extractants	5
1.1.3 Stripping solutions.....	9
1.1.4 Transport in Hollow Fiber Supported Liquid Membrane	11
1.1.5 Patterns of HFSLM operations	16
1.1.6 Feed and its impurity.....	20
1.1.7 Diluents.....	21
1.2 Objectives of the dissertation	22
1.3 Scopes of the dissertation	23
1.4 Expected results.....	24
1.5 Dissertation overview	24
CHAPTER 2.....	30
2.1 Abstract.....	31
2.2 Introduction	32

	Page
2.3 Theory	37
2.3.1 Extraction Reaction flux model for transport in HF LSM tube	38
2.3.2 Recovery reaction flux model for transport in HF LSM	41
2.3.3 Transport across the hollow fiber tube (membrane phase)	47
2.4 Experimental	51
2.4.1 The reagents and the feed	51
2.4.2 Apparatus	52
2.4.3 Procedure	53
2.5 Results and discussion	56
2.5.1 Effect of extractant concentration	56
2.5.2 Synergistic extractant	60
2.5.3 Selective recovery	62
2.5.4 Effect of operating cycle	64
2.5.5 Determining rate of Pd(II) extractant	67
2.5.6 Reaction flux model for Pd(II) extraction and recovery	70
2.6 Conclusion	74
2.7 Notation	75
2.8 Acknowledgment	78
2.9 References	79
CHAPTER 3	84
3.1 Abstract	85
3.2 Introduction	85
3.3 Background and Theory	90

	Page
3.3.1 Reaction mechanisms.....	90
3.3.2 Transport in feed phase (extraction).....	95
3.3.3 Transport across the liquid membrane phase.....	100
3.3.4 Transport in the stripping phase (recovery).....	103
3.4 Experimental.....	106
3.4.1 The reagents and the feed solution.....	106
3.4.2 Apparatus.....	107
3.4.3 Procedure.....	108
3.5 Results and discussion.....	111
3.5.1 Effect of HCl concentration in feed solution.....	111
3.5.2 Effect of extractant concentration.....	113
3.5.3 Effect of stripping concentration.....	117
3.5.4 Effect of flow rate of both feed and stripping solutions.....	120
3.5.5 Parameters used in the model (Constants of rate reaction).....	122
3.5.6 Computation and evaluation of the model.....	124
3.6 Conclusions.....	127
3.7 Nomenclature.....	128
3.8 Acknowledgments.....	131
3.9 References.....	138
CHAPTER 4.....	147
4.1. Abstract.....	148
4.2. Introduction.....	148
4.3. Theory.....	154

	Page
4.3.1 Transport of mercury (II) across the liquid membrane phase.....	154
4.3.2 Mass transfer resistance of mercury (II) in HFSLM	156
4.4. Experimental.....	163
4.4.1 The reagents and the feed.....	163
4.4.2 Apparatus	164
4.4.3 Procedures	165
4.5. Results and discussion.....	168
4.5.1 Effect of pH of feed solution	168
4.5.2 Effect of concentration of Aliquat 336	170
4.5.3 Effect of concentration of stripping solution.....	172
4.5.4 Effect of types of diluents.....	174
4.5.5 Effect of the flow rate of feed and stripping solution.....	176
4.5.6 Effect of flow patterns of feed and stripping solutions	177
4.5.7 Mass transport resistance	181
4.5.8 Model for mass transfer of mercury (II)	182
4.6. Conclusions.....	184
4.7. Nomenclature.....	185
4.8. Acknowledgments	187
4.9. References.....	187
CHAPTER 5.....	192
5.1. Abstract.....	193
5.2. Introduction	194
5.3. Theory	198

	Page
5.3.1 Transport of mercury (II) ions across the liquid membrane phase.....	198
5.4. Experiment	199
5.4.1 Feed solution and reagent	199
5.4.2 Apparatus	201
5.4.3 Procedure.....	202
5.5. Result and discussion.....	204
5.5.1 Effect of pH of feed solution	204
5.5.2 Effect of compositions of feed solution.....	206
5.5.3 Effect of concentration of extractant.....	208
5.5.4 Effect of flow rates of both feed and stripping solutions	209
5.5.5 Effect of temperature.....	211
5.5.6 Stability.....	212
5.6. Conclusion.....	214
5.7. Nomenclatures	215
5.8. Acknowledgments	216
5.9. References.....	216
CHAPTER 6.....	221
6.1. Conclusions.....	221
6.1.1 Effects to the performance	221
6.1.2 Prediction from mathematical model.....	229
6.2. Recommendations for future studies.....	232
REFERENCES	235

	Page
APPENDIX.....	243
Appendix A.....	244
A.1 Abstract.....	245
A.2 Introduction	247
A.3 Theory	250
A.4 Experimental.....	257
A.4.1 The Feed Condensate and the Reagents.....	257
A.4.2 Apparatus	259
A.4.3 Procedures	260
A.4.4 Analytical Instrument.....	261
A.5 Results and Discussion.....	261
A.5.1 Extractant Effect.....	261
A.5.2 Synergistic Effect.....	265
A.5.3 Pulse Velocity Effect	267
A.5.4 Feed-to-Extractant Flowrate Effect.....	270
A.5.5 Cycle Effect.....	273
A.6 Conclusion.....	274
A.7 Acknowledgments	276
A.8 Nomenclature.....	276
A.9 Reference	278
VITA.....	282

LIST OF TABLES

TABLE	PAGE
Table 1.1	Properties of the hollow fiber module.....11
Table 1.2	Composition of petroleum produced 21
Table 1.3	Effect of dielectric constant and dipole moment of diluents 22
Table 2.1	Summary of previous research on palladium..... 35
Table 2.2	Properties of the hollow fiber module 53
Table 2.3	Metal distribution between phases while using NaNO_2 64
Table 2.4	Analysis of reaction order and rate constants 68
Table 2.5	Model computation results for the varying flow rate case..... 72
Table 2.6	Model computation results for the repeat cycle scenario. 74
Table 3.1	Summary of previous research on mercury (II)..... 89
Table 3.2	Literature review of mathematical models for HFSLM..... 90
Table 3.3	Composition of petroleum produced water..... 107
Table 3.4	Properties of the hollow fiber module 108
Table 3.5	Analysis of reaction order and rate constants..... 124
Table 4.1	summary of previous research on mercury (II) separation..... 152
Table 4.2	Composition of petroleum produced water..... 154
Table 4.3	Source and mass fraction purity of materials 164

Table 4.4	Properties of the hollow fiber module	165
Table 4.5	Validation of overall mass transfer coefficient (K) of mercury (II).....	172
Table 4.6	Effect of dielectric constant and dipole moment of diluents on the extraction and overall mass transfer coefficient (K)	175
Table 4.7	Mass transfer resistances under optimum conditions.....	181
Table 4.8	The average deviation in feed side	183
Table 5.1	Summary of previous research on mercury (II) ions separation.....	196
Table 5.2	The composition of petroleum produced water	200
Table 5.3	Source and mass fraction purity of materials	200
Table 5.4	Properties of the hollow fiber module	201
Table A.1	Arsenic Removal from Researches.....	258
Table A.2	Characteristics of the Pulsed Sieve-Plate Column in this Study	259
Table A.3	Physical properties	267
Table A.4	Calculated interfacial area from varied volumetric flowrate ratio	273

LIST OF FIGURES

FIGURE	PAGE
Figure 1.1	Thailand Petroleum Concessionaire Map..... 2
Figure 1.2	Schematic of liquid membrane systems..... 13
Figure 1.3	Schematic diagram of batch operation HFSLM..... 17
Figure 1.4	Schematic diagrams of continuous operation HFSLM. 19
Figure 1.5	Schematic diagrams of semi-continuous operation HFSLM 20
Figure 2.1	Schematic of transport flux within HFSLM..... 37
Figure 2.2	Transport schematic for the plug flow reaction in a HFSLM tube..... 41
Figure 2.3	Metal complex transport across the membrane phase..... 49
Figure 2.4	Counter-current flow diagram of a one-through-mode separation by hollow fiber supported liquid membrane. 54
Figure 2.5	Effect of a) TRHCl and b) OA concentrations on the extraction yield. ... 58
Figure 2.6	Effect of varying NaNO_2 concentration 62
Figure 2.7	Effect of repeat operating cycles metal 67
Figure 2.8	Integral concentrations of Pd (II) extraction 69
Figure 2.9	Integral concentrations of Pd (II) recovery 69
Figure 2.10	The model computation results against experimental data for the case of varying flowrate. 72

Figure 2.11	The model computation results against experimental data.....	74
Figure 3.1	Schematic representation of the complex-forming reactions.	93
Figure 3.2	Schematic transport flux within HFSLM.....	95
Figure 3.3	Schematic flow in the HFSLM tube (feed phase).....	97
Figure 3.4	Axis reference for the model.....	105
Figure 3.5	HFSLM in counter-current flow diagram.....	109
Figure 3.6	Effect of HCl concentrations.....	113
Figure 3.7	Effect of Aliquat 336 concentrations.....	115
Figure 3.8	FT-IR spectrum.....	116
Figure 3.9	Effect of thiourea concentrations.....	118
Figure 3.10	(a) concentration effects on extraction yield (b) concentration effects on recovery yield.....	120
Figure 3.11	Effect of flow rate on the extraction and recovery yield.....	121
Figure 3.12	Integral concentrations of mercury (II) (a) extraction (b) recovery.....	123
Figure 3.13	The model computation results against experimental data f.....	127
Figure 4.1	Schematic of mass transport of mercury (II) across the liquid membrane phase using Aliquat 336.....	156
Figure 4.2	Schematic representation of the counter-current flow diagram.....	167
Figure 4.3	Percentages of mercury (II) vs pH value.....	170
Figure 4.4	Percentages of mercury (II) vs concentration of Aliquat 336.....	171
Figure 4.5	Percentage of mercury (II) vs concentration of thiourea.....	174

Figure 4.6	Percentage of mercury (II) vs flow rate.....	177
Figure 4.7	Concentration of mercury (II) plotted as a function of time.....	180
Figure 4.8	Concentration of mercury (II) in the feed solution, plotted as a function of time at different concentrations of Aliquat 336.....	183
Figure 5.1	Schematic representation of the chemical reaction.....	198
Figure 5.2	HFSLM in counter-current flow diagram.....	203
Figure 5.3	Percentages of mercury (II) ions vs pH value.	206
Figure 5.4	Percentages of mercury (II) ions vs metal ions of feed solutions.	207
Figure 5.5	Percentages of mercury (II) ions vs Calix[4]arene nitrile.....	209
Figure 5.6	Percentage of mercury (II) ions vs flow rate	211
Figure 5.7	Effect of temperature.....	212
Figure 5.8	Comparison of stability of extractant.....	214
Figure A.1	(a) Schematic flow diagram of a pulsed sieve plate column.....	251
Figure A.2	Schematic flow patterns of continuous and dispersed phase in a pulsed sieve-plate column	252
Figure A.3	Flow patterns of continuous and dispersed phase.....	253
Figure A.4	The diagram for continuous countercurrent flow.	254
Figure A.5	The effects of <i>HCl</i> concentration on the percentage of arsenic removal	263
Figure A.6	The effects of methanol and ethanol concentration on the percentage of arsenic removal.....	265

Figure A.7	The effects of the mixture of HCl solution and CH ₃ OH on the percentage of arsenic removal.....	266
Figure A.8	The effects of pulse velocity and operating time	268
Figure A.9	The equilibrium diagram of the condensate and the extractant.....	269
Figure A.10	The relation of the calculated HTU _{oy} from arsenic removal.	270
Figure A.11	The effects of volumetric-flowrate ratio	271
Figure A.12	The effects of removal cycle.....	274



CHAPTER 1

INTRODUCTION

1.1 Rationale of research problem

Mercury is a natural trace component found in the petroleum reservoir. Its concentration levels vary widely, depending on the production area. It is produced with petroleum hydrocarbon and associated water –so-called “produced water” – in both elemental mercury and ionic mercury Hg(II) form^[1]. The presence of mercury is detrimental to petroleum production facilities as it forms corrosion induced through mercury amalgamates. Moreover, it has an effect on human beings if it is discharged into the atmosphere leading to severe, acute and chronic poisoning^[2-6].

In the Gulf of Thailand, petroleum development and upstream production have been growing following an increasing domestic energy demands. Numbers of operator, ranging from national, international leading and independent oil companies, have established operations in the Gulf for an interest of petroleum exploration and production. Figure 1.1 presents 2014 updated petroleum concessionaire map where total gross production per day from the Gulf has been

reported at circa 206,000 barrels of oil equivalent^[7] and million barrels daily for the produced water are generated.

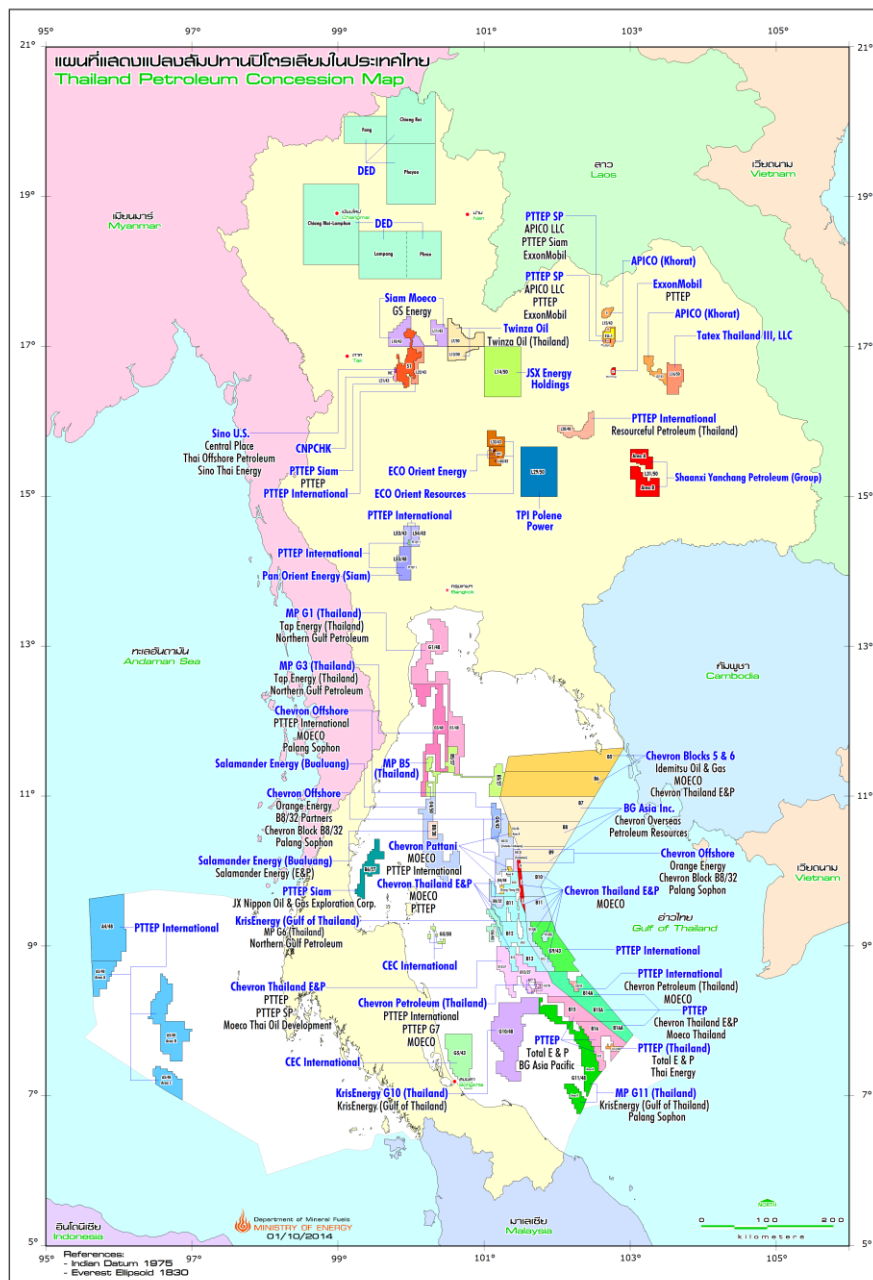


Figure 1.1 Thailand Petroleum Concessionaire Map^[8]

Trend for produced water production is increasing exponentially in relation to maturity of production reservoir itself. Some matured production field, the water cut, which is the ratio of water produced compared to the volume of total liquids produced, was reported up to 90%.

To handle this massive daily generated amount of produced water, oil company operators in the Gulf undertake an enduring path to pursue a “zero discharge” program enforced by Thai local authorities by injection of the produced water back into the formations. Nevertheless, overboard discharge of the produced water into an ocean is still necessitated when the re-injection facilities are in breakdown state or for some production fields where uncertainties in geological formations to receive such great volume of produced water hinder the feasibility. Pollution and biological impact to local marine environment is of concern when overboard discharge of mercury contaminating produced water into the ocean. Various aspects of the potential environment effects of mercury have been assessed by local environmental control authorities.

Conventionally, a mercury treatment unit based on chemical production aids precipitation^[1] ion exchange^[9, 10] sorption^[11] ultrafiltration^[12] adsorption^[13-16] solid phase extraction^[17] or liquid-liquid extraction^[18]. It deals excellently with elementary mercury at bulk concentration but not with ionic mercury^[14]. Ionic mercury usually

remains as residue after conventional treatment^[19] which may render a still high mercury content in the produced water above the environmental discharge limit. An alternative technique, such as hollow fiber supported liquid membrane (HFSLM) technology, is therefore considered to take care of the residual ionic mercury.

HFSLM has attracted interest from many researchers on its unique simultaneous extraction and recovery operation for promising ionic metal removal and wastewater treatment. It is an innovative separation technique which combines the advantages of liquid-to-liquid extraction and mass transfer area within the membrane micro-pore structure^[20]. It has other advantages, notably lower capital and operating costs^[21] less energy consumption, less extractant used^[22] and a larger surface area per unit for mass transfer^[23, 24].

In this work, the removal of ionic mercury or Hg (II) from petroleum-produced water via HFSLM was studied. The removal threshold was targeted to be less than 5 ppb which is the permissible discharge limit of industrial wastewater imposed by the government regulator in the Kingdom of Thailand^[1, 25].

1.1.1 Toxicity of mercury

Mercury poisoning damage the tissue of any organ to which it makes bone marrow produce less red blood cells. Mercury mostly accumulates in the cerebellum and cerebral cortex quickly during exposure but it is released from the brain very slowly. The liver and kidneys may also be damaged by mercury accumulation. Organic mercury compounds are the most toxic. It could slip through Blood-Brain-Barrier, which protects the brain from toxic, and causes neurological damage to the brain. Inorganic mercury compounds or mercury salts has limited effect to the brain unless continuous or heavy exposure. It could not cross the Blood-Brain-Barrier easily. However, it could still cause severe damage at the kidneys via digestive tract. It is absorbable through skin and inhalation. The presence in vapour is the most dangerous to human life as it cause acute poisoning ^[26].

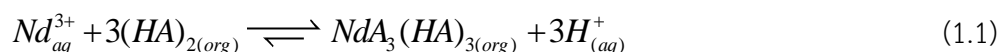
1.1.2 Extractants

The extractants for HFSLM system are grouped into 5 classes according to their functional groups, extraction mechanism and types of metal ions extracted (cation, neutral complex and anion), i.e., acidic extractants, chelating extractants,

neutral extractants (or solvating type extractants), ligand substitution extractants, and basic extractants (or ion-pair extractants)^[27, 28].

Acidic Extractants

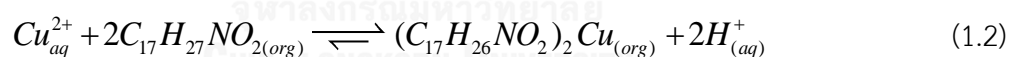
Acidic extractant contains a functional group of carboxyl (RCOOH), phosphate (HOPO(OR)₂) or sulfo (RSO₃H) where R is alkyl group^[27, 28]. The acidic extractant reacts with metal cation in the feed phase. In an organic solvent or liquid membrane, the carboxyl, sulfo or phosphate groups of the acidic extractant deprotonates to an anion species RCOO⁻, OPO(OR)₂⁻, or RSO₃⁻, respectively. The anion species subsequently form organo-metal complexes with the cation species. Acidic extractant which is widely used is D2EHPA (di-2-ethylhexylphosphoric acid, HOPO(OC₈H₁₇)₂)^[27]. The extraction of Nd³⁺ by D2EHPA is shown in Eq. (1.1)^[29].



where (aq) represents the species in the aqueous phase and (org) represents the species in the liquid membrane phase

Chelating extractants

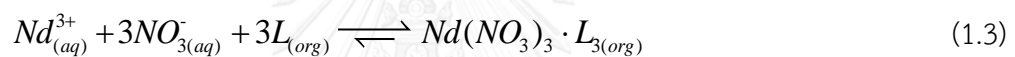
Chelating extractants are often derived from analytical reagents, such as LIX 84-I or 2'-hydroxy-5'-nonylacetophenone ketoxime ($C_{17}H_{27}NO_2$). They react with cation species same as the acidic extractants. The chelating extractants chemically bond to cation species at two sites in a manner similar to holding an object between the ends of the thumb and the index finger^[27]. When the chelating extractant bonds to cation species, it releases hydrogen ion into the feed solution. Extractability of the chelating extractant increases with the pH of the feed solution. Decreasing of the pH promotes back-extraction or stripping. The extraction of Cu^{2+} is shown in Eq. (1.2)^[30].



Neutral extractants (Solvating type extractants)

Neutral extractant contains a functional group of phosphate ester ($PO(OR)_3$), phosphine oxide (R_3PO) or phosphine sulphide (R_3PS). Tributyl phosphate ($L=TBP$, $PO(OC_4H_9)_3$) or tri-isobutylphosphine sulfide (Cyanex 471, $(C_4H_9)_3PS$) is a good example to the neutral extractant. The neutral extractants are basic in nature and will coordinate

to certain neutral metal ions in the feed solution by replacing water molecules of hydration around neutral metal ions; thereby altering the targeted metal to hydrophobic ions^[27]. The extraction reaction of Nd(III) with neutral donor) is shown in Eq. (1.3). The neutral donor (L) captures the inorganic anion (NO_3^-) in the feed phase to form the extractant. Subsequently, it reacts with Nd(III) to produce complex ions^[29].



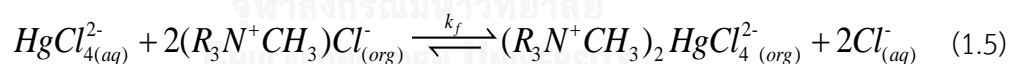
Ligand substitution extractants

Ligand substitution extractants donate an electrical pair to metal anion ions in similar mechanism to the neutral extractants. But, it forms inner shell complex and subsequently displace other ligands. A ligand substitution extractant includes mono-oxime (R_2CNOH) and dialkyl sulfides (R_2S), for example, di-n-hexyl sulfide ($(\text{C}_6\text{H}_{13})_2\text{S}$). Eq. (1.4) shows the extraction of PdCl_4^{2-} using mono-oxime^[31].



Basic extractants (Ion-pair extractants)

Basic extractants contain a functional group of primary amine (RNH_2) or secondary amine (R_2NH) or tertiary amine (R_3N) or quaternary amine (R_4N^+). In general, the commercial basic extractants contain a functional group of tertiary amine or quaternary amine. The quaternary amines are usually in the form of alkyl ammonium salts (or amine salts). Metal anions in the feed solution can react with quaternary amine to form organo-metal complexes by replacing the common anions (e.g., Cl^- , SO_4^- , and F^-) of the quaternary amines^[27, 32]. Equation (1.5) shows the extraction of HgCl_4^{2-} by Aliquat 336^[33].



1.1.3 Stripping solutions

The selection of stripping solution for removal of metal ions from the organo-metal complexes depends on types of metal ions extracted (cation, neutral complex, and anion) and types of extractants (acidic extractants, chelating

extractants, neutral extractants, ligand substitution extractants, and basic extractants) used in the extraction of metal ions.

In the extraction of metal cations, an acidic extractant or a chelating extractant is used. In order to strip metal cations from the organo-metal complexes, an acidic stripping solution is required. Hydrogen ions from the acidic stripping solution work to replace metal cations in the (organo) metal complex. As a consequence, the metal cations will become free and captured by the stripping solution.

For the extraction of neutral metal complexes, a neutral extractant is used. Neutral metal complexes can be stripped from the organo-metal complexes by a neutral stripping solution.

In the case of extraction of metal anions, a basic extractant or a neutral extractant is used. In order to strip metal anions from the organo-metal complexes, a basic stripping solution is required. Anions from the basic stripping solution replace metal anions in the organo-metal complexes. As a result, metal anions are released to the stripping solution.

1.1.4 Transport in Hollow Fiber Supported Liquid Membrane

HFSLM module, deployed in this study, is a Liqui-Cel®Extra-Flow Laboratory, supplied by CELGARD LLC (Charlotte, NC; formerly Hoechst Celanese). It is engineered from micro-porous polypropylene woven into fabric and wrapped around a central-tube feeder to supply the shell side fluid, thus, creating an immiscible layer between feed and stripping phases from an organic extractant in microporous hollow fibers. It has properties as shown in Table 1.1.

Table 1.1 Properties of the hollow fiber module

Material	Polypropylene
Inside diameter of hollow fiber (cm)	0.024
Outside diameter of hollow fiber (cm)	0.03
Effective length of hollow fiber (cm)	15
Number of hollow fibers	35,000
Average pore size (cm)	3×10^{-6}
Porosity (%)	30
Effective surface area (cm^2)	1.4×10^4
Area per unit volume ($\text{cm}^2 \cdot \text{cm}^{-3}$)	29.3
Module diameter (cm)	6.3
Module length (cm)	20.3
Tortuosity factor	2.6
Operating temperature (K)	273–333

The target component is dissolved in the liquid membrane at the interface and then preferentially diffuses through that immiscible layer to the stripping solution where it is recovered. In this phenomenon of diffusion transport, it can be either a simple facilitated transport or coupled facilitated transport. The simple facilitated transport occurs when the transport is independent of any other ions. It normally takes place in an application of neutral species extraction. While the case of ionic species extraction, the coupled transport will occur to maintain the solution electro neutrality^[34]. The driving force to determine transport rate is dependent on co-ion concentrations in the feed.

Fig. 1.2 schematically explains the transport of each case. The schematic depicts (A) as the target component, (B) co-ions, (C) the organic extractant, and (A-C or B-C or A-B-C) the organic complex. In our study, the target component (A) can be arsenic and/or mercury ions. The straightforward mechanism is observed with the simple facilitated transport (Figure 1.2 (a)) since the organic complex (A-C) is produced from the reaction between (A) and (C). Then, (A-C) is decomposed at the interface between liquid membrane and the stripping phase, and (A) is recovered to the stripping solution. The coupled facilitated transport can be classified into co-transport (Figure 1.2 (b)) and counter-transport (Figure 1.2 (c)). For the coupled facilitated co-transport, the extractant reacts with the target component (A) and co-

ion (B) to form the organic complex (ABC). The (ABC) diffuses across liquid membrane to the stripping interface where both target component and co-ion are simultaneously recovered. This mechanism has co-ion transporting along with the target component from feed phase to stripping phase.

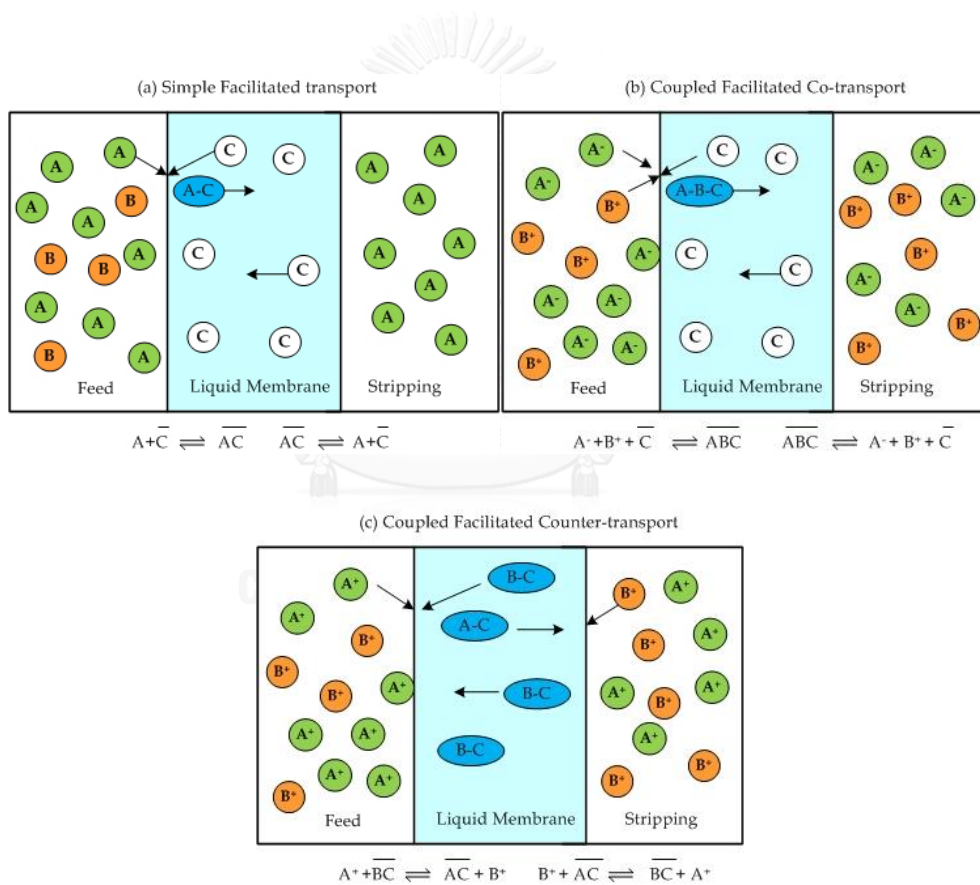


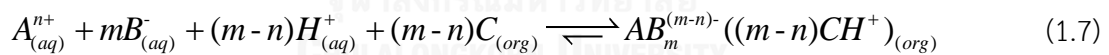
Figure 1.2 Schematic of liquid membrane systems ^[34]

This coupled facilitated co-transport is common for neutral and basic extraction as schematized in Equation (1.6) for the reaction with neutral organic extractant, and Equation (1.7) for the reaction with basic organic extractant. The aqueous pH phase or hydrogen ion in the system depicts with (H).

Coupled Co-transport, Neutral organic extractant



Coupled Co-transport, Basic organic extractant



The coupled facilitated counter-transport has reverse mechanism from the co-transport. The co-ion (B) transports from the stripping phase to feed phase, against the transport direction of the target component (A). The mechanism starts with the reaction between (A) and the organic extractant (BC) to form organic complex (AC) and release co-ion (B) to feed phase. The organic complex (AC), subsequently, diffuses across the liquid membrane to the stripping interface where the target

component is released to the stripping phase and co-ion is recovered to the organic extractant. The common case of counter-transport is the reaction using acidic extractant as schematized by Equation (1.8).

Coupled Counter-transport, Acidic organic extractant



Uphill transport where the target component can be transported across the membrane against the concentration gradient of the target component is usually observed from the coupled transport. The uphill effects can continue until the target component diffuses across liquid membrane to the stripping solution as long as the driving force in the coupled transport system is maintained. The driving force is often acquired from aqueous pH (H^+) and/or co-ion (B) gradient. Generally, research works within our laboratory for the removal of very dilute arsenic and mercury concentration from produced water follow the mechanism of coupled facilitated transport, and the uphill effects against the target component concentration is usually observed.

1.1.5 Patterns of HFSLM operations

The patterns of HFSLM operations for metal ions separation are mainly classified as follows: batch operation, continuous operation and semi-continuous operation.

I. Batch operation

The separation of metal ions by batch operation consists of a single HFSLM module, a feed reservoir, and a stripping reservoir, as shown in Figure 1.3. Feed and stripping solutions are circulated through the HFSLM module. Batch operation is suitable for the separation of metal ions from a small volume of feed solution, and slow extraction and stripping. By using batch operation, high percentage separation of the metal ions can be obtained.

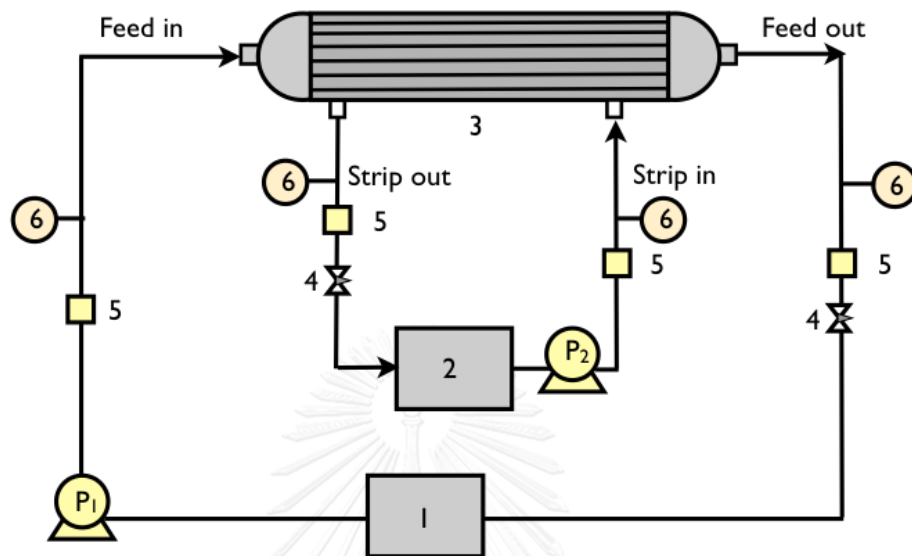


Figure 1.3 Schematic diagram of batch operation HFSLM: (1) inlet feed reservoir (2) stripping reservoir (3) HFSLM (4) flow regulator valve (5) flow indicator (6) pressure indicator.

II. Continuous operation

Continuous operation is suitable for the separation of metal ions from a large volume of feed solution and can be performed by connecting the HFSLM modules in series or in parallel as shown in Figure 1.4. The feed and stripping solutions are supplied in single-pass flow or one-through-mode.

Continuous operation by connecting the HFSLM modules in series provides higher residence time of feed and stripping solutions in the HFSLM modules. Therefore, the continuous operation with the HFSLM modules in series is recommended for slow extraction and stripping as they require long residence time to complete the reactions.

On the other hand, continuous operation by connecting the HFSLM modules in parallel provides shorter residence time than that in series. Therefore, continuous operation connecting the HFSLM modules in parallel is suitable for fast extraction and stripping.

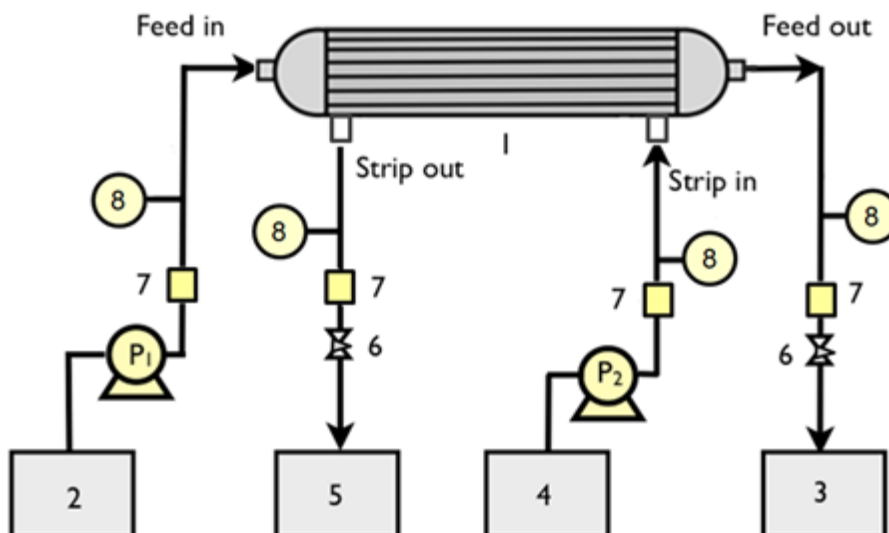


Figure 1.4 Schematic diagrams of continuous operation HFSLM : (1) HFSLM (2) inlet feed reservoir (3) outlet feed reservoir (4) stripping feed reservoir (5) stripping return reservoir (6) flow regulator valve (7) flow indicator (8) pressure indicator.

III. Semi-continuous operation

The separation of metal ions by semi-continuous operation is carried out by using single-pass flow of feed solution but circulating flow of stripping solution. By using this pattern operation, the metal ions in the stripping solution can be concentrated until its concentration is constant and the reaction reaches the equilibrium. Figures 1.5 show semi-continuous operation by connecting the HFSLM in series or in parallel. The operation using HFSLM modules in series is preferable for the selective separation of metal ions which the extraction reaction is slow. In case of fast extraction reaction, the separation of metal ions does not need long residence time. Therefore, using HFSLM modules in parallel is suitable.

From the application perspective, the semi-continuous setup offers continuous treatment of the large volume produced water effluent. Whilst, the stripping solution, which is circulating in limited volume, offers a manageable volume for waste disposal after the solution becomes saturated.

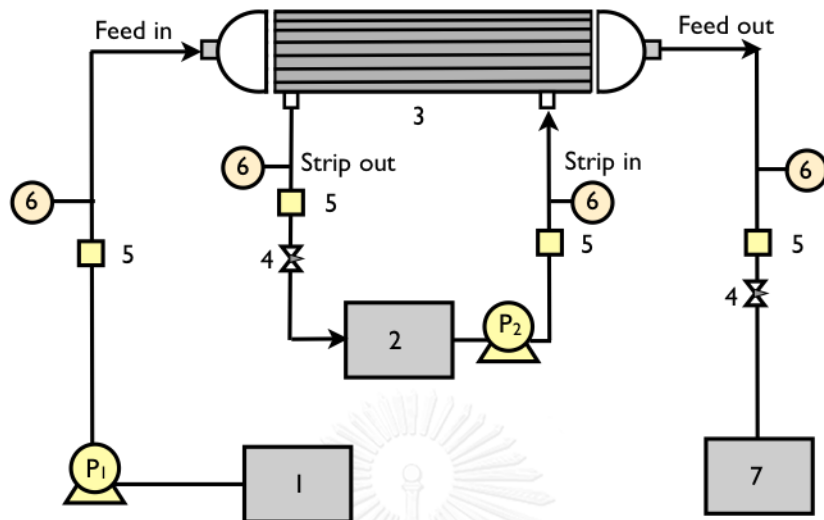


Figure 1.5 Schematic diagrams of semi-continuous operation HFSLM: (1) inlet feed reservoir (2) stripping reservoir (3) HFSLM (4) flow regulator valve (5) flow indicator (6) pressure indicator (7) outlet feed reservoir.

1.1.6 Feed and its impurity

Petroleum-produced water describes for the water that is produced as a by-product from upstream petroleum production. Hydrocarbon reservoirs often have water as well as oil and gas, sometimes in a zone that lies above or under the reservoir, and sometimes in the reservoir, same zone with the oil and gas.

Usually the petroleum-produced water is brine. It is not hydrocarbon free and has total dissolved solids, various heavy metal or even traces of naturally occurring radioactive material (NORM).

For the produced water that was adopted as the feed in this study, it has composition as provided in Table 1.2.

Table 1.2 Composition of petroleum produced

Metal ions	Concentration (ppm)
As	0.2
Ca	16
Fe	0.17
Hg	0.5
Mg	2
Na	1820

1.1.7 Diluents

Diluent is necessary in separation via HFSLM. Generally, it is solvent that shall be inert, low toxicity and high boiling point^[35]. Its application is to dissolve an extractant which is either solid or viscous liquid that will render suitability in term of mobility and capillary tension for working in microporous hollow fibers. Diluents, such

as nitrobenzene, dichloromethane, chloroform, xylene and toluene, are widely used for this HFSLM application^[36]. They have different characters in dielectric and dipole as demonstrated in Table 1.3.

Table 1.3 Effect of dielectric constant and dipole moment of diluents

Diluents	Nitrobenzene	Dichloromethane	Chloroform	Xylene	Toluene
Dielectric constant	34.82	10.42	4.81	2.54	2.39
Dipole moment	4.22	1.20	1.01	0.62	0

1.2 Objectives of the dissertation

1. To study the influences of variables on the efficiency of extraction and stripping of mercury (II) ions from petroleum produced water from the Gulf of Thailand via HFSLM in semi-continuous operation.
2. To develop, respectively, a high accuracy model for computation of the extraction and stripping result of mercury (II) ions.

1.3 Scopes of the dissertation

This dissertation presents the separation of mercury (II) ions via HFSLM as well as the model to predict the extraction and stripping. The scopes of this dissertation are as follows:

1. Separation of mercury (II) ions from petroleum produced water via HFSLM in semi-continuous operation.
2. Supply feed and stripping solutions counter-currently with equal flow rates to tube and shell sides of the HFSLM, respectively.
3. The investigated parameters were
 - a) optimum pH of the petroleum produced water feed.
 - b) concentration of extractant solution
 - c) concentration of stripping solutions
 - d) operating time and stability
 - e) flow rate
4. Development of the prediction model for the extraction and stripping of mercury ions via HFSLM.
5. Verification of the model by comparing the model results with the experimental data.

1.4 Expected results

The expected results are as follows:

1. The outlet concentration of mercury (II) ions from HFSLM modules complies with the regulatory discharge limits by the Ministry of Industry and the Ministry of Natural Resources and Environment, Thailand.
2. High stripping of mercury (II) ions.
3. High accuracy model.

1.5 Dissertation overview

This dissertation records results and discussions from thorough study on separation of mercury ions (II) from petroleum produced water via HFSLM. The HFSLM is a hybrid application that combines different processes from chemical reaction, to liquid-liquid extraction, to continuous-contact mass transfer and to pseudo-end-of-pipe separation. Moreover, it is an integrated unit of operations that allow extraction and (stripping) recovery simultaneously.

Chapters II to V consolidates article detail that is the results from dissertation progress. It covers different perspectives from the experiment, to mathematical modelling and to alternative system. Discussion for mass transfer mechanism by various driving fluxes is also addressed. For the benefit of dissertation readers, following outlines are provided to aids understanding.

CHAPTER II

SELECTIVE TRANSPORT OF PALLADIUM THROUGH A HOLLOW FIBER SUPPORTED LIQUID MEMBRANE AND PREDICTION MODEL BASED ON REACTION FLUX

This Chapter describes the successful result from the mathematical model that was developed to predict palladium transport system. The transport was set up with a hollow fiber supported liquid membranes application on batch (full recycle) operation for the simultaneous extraction and recovery of low-concentration palladium from waste aqua regia solutions. The optimum conditions in this system were pH 2 in the feed with 0.005M thioridazine and 0.05M oleic acid in liquid membrane, 0.03M NaNO_2 in the stripping solution and an operating flowrate of 100 mL/min. By employing a 3-cycle operation in repeated operating cycle mode, the cumulative palladium extraction and recovery was 82% and 78% respectively. A

remark was made that synergistic enhanced extraction was observed by using thioridazine and oleic acid as the extractant carrier. For the transport prediction, a reaction flux was the main basis in the model. The reaction order and the rate constant were determined and reported at 0.0140 s^{-1} and 0.0248 s^{-1} for extraction rate constant (k_f) and the stripping rate constant (k_s) respectively. We revealed that the first order rate law governed the reaction system both the extraction and the recovery. The model was plugged in with the calculated rate constants and subsequently solved by Laplace transform solution. Verification was made from the scenarios of a varying flowrate and a repeated operating cycle mode. The results showed good agreement with theoretical data (curve fittings gave $R^2 > 0.9$). Details are available in Chapter II and the article in Separation Science and Technology^[37]. At the outset of successful outcome in this study, it drove us to pursue the next and more advancing model that will be described further in Chapter III.

CHAPTER III

SEPARATION OF MERCURY (II) FROM PETROLEUM PRODUCED WATER VIA HOLLOW FIBER SUPPORTED LIQUID MEMBRANE AND MASS TRANSFER MODELING

The progression from the preceding success, a sophisticated mathematical model was developed, aiming to enhance the prediction result. The model was built from full or combined mass transfer fluxes, which are convection flux, diffusion flux and kinetic flux. It applied to a separation of mercury (II) from petroleum-produced water via HFSLM in semi-continuous operation where the optimum condition was reported at 0.2M HCl pre-feed treatment, 4% (v/v) Aliquat 336 for extractant carrier and 0.1 M thiourea for stripping solution. It yielded correspondingly best performance at 99.73% extraction, 90.11% recovery and 94.92% as an overall by taking account of both extraction and recovery prospects.

From the model, the results exhibited excellent agreement with theoretical data at an average Standard Deviation of 1.5%. It was radiant enhancement in comparison to the result from the previous model that had deviation at circa 10%. Apparently, the full fluxes contributed to the prediction accuracy. Full details are available in Chapter III and the article in Chemical Engineering Journal^[38].

CHAPTER IV

MASS TRANSFER RESISTANCE OF SIMULTANEOUS EXTRACTION AND STRIPPING OF MERCURY (II) FROM PETROLEUM PRODUCED WATER VIA HFSLM

We conducted further study to expand the knowledge on mercury separation system via HFSLM into mass transfer resistant perspectives. Different resistant layers were identified and quantified by appropriated hypothetical correlations. As a result, the mass transfer resistant coefficients were calculated and verified. Dominant resistance was learnt to have originated from the extraction reaction. Supplementing to the main objective, we varied different type of extraction diluent and recorded the corresponding effect. For more detail and discussion, it is available in Chapter IV and the article in Journal of Industrial and Engineering Chemistry^[39].

CHAPTER V

AN INVESTIGATION OF CALIX[4] ARENE NITRILE FOR MERCURY TREATMENT IN HFSLM APPLICATION

Proposing as an alternative to Aliquat 336-Thiourea system to overcome the requirement of strong acid condition in the feed phase and performance decline at higher operating temperature, Calix[4]arene nitrile was deployed as mercury (II) ions extractant. Calix[4]arenes is used in various applications such as purification, chromatography, catalysis, enzyme mimics, ion selective electrodes, phase transfer and transport across the liquid membranes. A variety of Calix[n]arene derivatives is

known for its effective use in the selective removal of metal ions from wastewater and has the capacity to capture Hg^{2+} in weak acid condition. The complex ions after the extraction reaction are in co-ordination bond which is reasonably strong but not too hard for a neutral-based stripping solution such as deionized water to break the bond.

In this study, the transport of mercury ions (Hg^{2+}) through hollow fiber supported liquid membrane was examined using the extractant Calix[4]arene nitrile as mentioned-above. Optimum condition was achieved using 4.5 pH of feed solution, 0.004 M of Calix[4]arene nitrile as extractant, de-ionized water as stripping solution and an operating temperature of 313 K. The stability of the liquid membrane was investigated and showed stable performance over 24 hours. After treatment, mercury (II) ions from petroleum produced water in feed solution was found to be below the legislation limit of 5 ppb. Details are available in Chapter V and the article in Chemical Engineering Processing^[40].

CHAPTER 2

SELECTIVE TRANSPORT OF PALLADIUM THROUGH A HOLLOW FIBER SUPPORTED LIQUID MEMBRANE AND PREDICTION MODEL BASED ON REACTION FLUX

Srestha Chaturabul, Kraiwith Wongkaew and Ura Pancharoen,[†]



*Department of Chemical Engineering, Faculty of Engineering, Chulalongkorn
University, Bangkok 10330, Thailand*

This article has been published in Journal: Separation Science and
Technology.

Page: 93–104. Volume: 48. Year: 2013.

2.1 Abstract

This paper describes the application of hollow fiber supported liquid membranes for the simultaneous extraction and recovery of low-concentration palladium from waste aqua regia solutions. A mathematical model to predict the palladium transport was also developed and verified. We found that the optimum conditions for transport of palladium were pH 2 in the feed with 0.005M thioridazine and 0.05M oleic acid in liquid membrane, 0.03M NaNO₂ in the stripping solution and an operating flowrate of 100 mL/min. With thioridazine and oleic acid as the extractant carrier, a synergistic enhanced extraction was observed. By employing a 3-cycle operation in repeated operating cycle mode, the cumulative palladium extraction and recovery was 82% and 78% respectively. Our mathematical model was developed based on reaction flux. The reaction order and the rate constant were determined. It revealed that the first order rate law governed the reaction system both the extraction and the recovery. The extraction rate constant (k_f) and the stripping rate constant (k_s) were calculated to 0.0140 s⁻¹ and 0.0248 s⁻¹ respectively. The model was set up for scenario based on a varying flow rate and a repeated operating cycle mode. The results showed good agreement with theoretical data (curve fittings gave $R^2 > 0.9$).

Keywords: Palladium; aqua regia; reaction flux; selective; modeling; HFSLM

*Corresponding author: Tel. +66-022186891; Fax. +66-022186877

E-mail address: ura.p@chula.ac.th

2.2 Introduction

Aqua regia reagent is used commonly in gold refining. The reagent is a mixture between freshly concentrated nitric acid and hydrochloric acid, usually in a volume ratio of 1:3. The aqua regia reagent is used once and, following the treatment, residues contains the desired gold (Au (III)) but also traces of other precious transition metals, including palladium (Pd (II)) and platinum (Pt (IV)).

Palladium has been increasingly used [1] in the automotive and electronics industries, for dental tools, ornaments, wear-resistant alloys, and in petrochemical and catalyst processes [2]. It is economically wise, following gold extraction, to also recover the palladium from such aqua regia wastes. From an ecological perspective, it also makes sense to eliminate palladium from aqueous waste prior to its environmental discharge, since the metal is highly toxic.

Solvent extraction in combination with a liquid membrane has been recently studied for the separation of the precious and toxic metals. The main interest lies in its unique simultaneous extraction and recovery application. Other advantages include lower capital and operating costs, less energy and consumption of extractant solution, and high selectivity. Moreover, it has the capability to extract metals at very low concentrations. The technique is of considerable importance in medicine, water purification, and metallurgy [3, 4]. Patthaveekongka W. et al studied the transport of cerium, lanthanum, neodymium and palladium via hollow fiber supported liquid membrane based on equilibrium theory [5]. Ramakul, P. et al, modeled a membrane carrier system for the extraction of cerium from sulfate media using hollow fiber supported liquid membranes [6]. Sunsandee et al focused on the selective separation of (S)-amlodipine [7], Lothongkum, A.W. et al studied the synergistic extraction and separation of mercury and arsenic [8]. We have previously examined pure extraction and separation of mixture of cerium (IV) and lanthanum (III) [9]. Wannachod P. et al identified effective recovery of praseodymium from mixed rare earths, again via a hollow fiber supported liquid membrane and replicated the previous successful mathematical model in dimensionless form [10]. Although several researchers have recently investigated various liquid-membrane processes for

palladium recovery, very few researchers to date have applied hollow fiber supported liquid membrane to this end. Hence for the current study we sought to apply hollow fiber supported liquid membrane (HFSLM) for treating aqua regia effluents containing residual Au (III), Pt (IV) and Pd (II).

The extraction and recovery of Pd (II) in this study presents an extra challenge when the element is present with Pt (IV), such is the chemical similarity of the two metals. They resemble one another more closely than any other pair in the group of platinum metals. Fontas et al. separated Pd (II) and Pt (IV) from automotive catalytic converters by combining two HFSLMs. Both Pd (II) and Pt (IV) were effectively enriched, with the percentage of recoveries were 43% for Pd (II) and 57% for Pt (IV) [11]. Katsuta et al. studied selective extraction of Pd (II) and Pt (IV) from hydrochloric acid solutions by trioctylammonium-based mixed ionic liquids. It was found that 47% of Pd (II) and 86% of Pt (IV) were recovered from the ionic liquid phase with 8.0 mol dm³ HNO₃ in 1 hour [12].

Table 2.1 Summary of previous research on palladium extraction and recovery using liquid membranes

Author	Method	Feed solution	Extractant	Stripping solution
Kakoi et al. [2]	LSM	wastewater	Di-2-ethylhexyl monothio- phosphoric acid (MSP-8)	Thiourea
Fontas et al. [11]	FSSLM HFSLM	aqueous feed in chloride solutions containing SCN^-	Cyanex 471	NaSCN
Farhadi and Shamsipur [13]	BLM	aqueous feed with palladium chloride (5×10^{-4} M)	Thioridazine-HCl, Oleic acid in Chloroform	Sodium Nitrite
Antico et al. [14]	BLM	aqueous feed with palladium	N-benzoyl thiourea derivatives	Thiourea derivatives
Fu et al. [15]	FSSLM	wastewater	Trioctylamine in kerosene	Nitric acid
Rovira and Sastre [16]	FSSLM	aqueous feed with Pd (II), Pt (IV), Rh (III), Zn (II) and Fe (III)	Di-(2-ethylhexyl) thiophosphoric acid (DEHTPA) in kerosene	Thiourea / Thiocyanate in HCl
This work	HFSLM	aqua regia	Thioridazine-HCl, Oleic acid in Chloroform	Sodium Nitrite

Abbreviations: SE: Solvent Extraction, LSM: Liquid Surfactant Membrane, BLM: Bulk Liquid Membrane, FSSLM: Flat Sheet Supported Liquid Membrane, HFSLM: Hollow Fiber Supported Liquid Membrane

The study was conducted via two different approaches. The first involved an experimental design to determine the optimum operating conditions for Pd (II) extraction and recovery. The second required the development of a mathematical model, based on reaction flux, to characterize the transport of Pd (II).

To describe the behaviour of an operation in the membrane contactor, several mathematical models were created and evaluated. Considerable efforts were made to establish a reliable mathematical model and parameters for design, cost estimation, optimization and unit scale-up. We have previously proposed models involving the mass transport of solute or target species through resistance boundaries [6, 10]. The resistance could range from the interfacial film at feed-membrane phase, the membrane and the interfacial film at membrane-stripping phase. The reaction at the interface is rapid enough to ignore the influence on the resistance [17]. The model construction in this current study, however, assumes only reaction involvement in the transport within the aqueous phase. No interfacial film between the aqueous and the membrane phase was involved, thereby eliminating the need for laborious calculation steps to solve interface concentration variables. The reaction flux is in the axial direction along the hollow fiber contactor. It behaves as the ideal plug flow.

2.3 Theory

The mathematical model assumes the only mass transfer flux from reaction for metal transport within a hollow fiber tube (feed phase) and shell annulus (stripping phase). Across the micro-pore site of the hollow fiber (membrane phase), the transport model assumes the diffusion flux for complex ions.

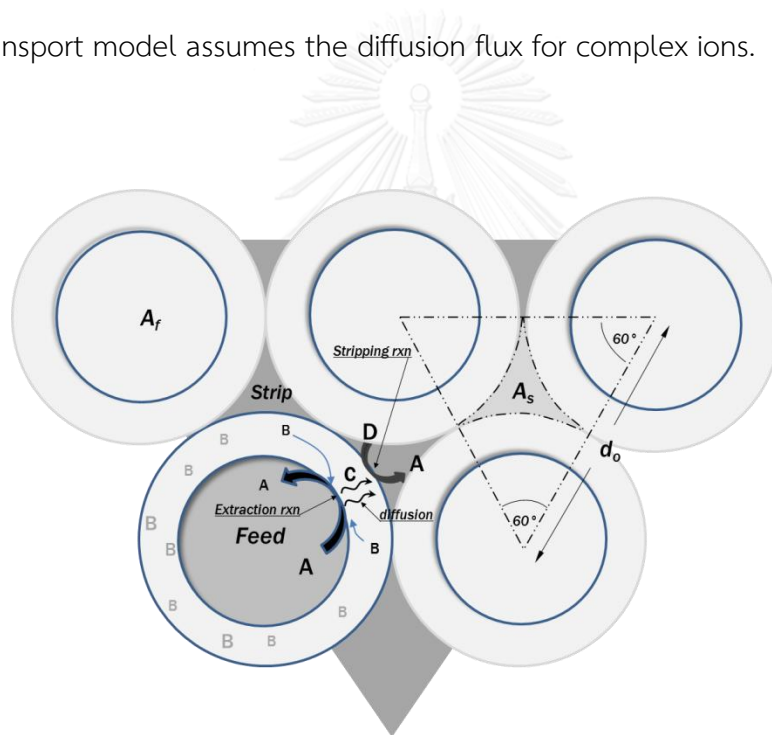


Figure 2.1 Schematic of transport flux within HFSLM (cross section view)

2.3.1 Extraction Reaction flux model for transport in HFSLM tube

Pancharoen U. et al. [18] modeled the metal ion transport in the feed phase with only reaction flux influence. The key assumption for the model is that perfect mixing occurs within the sheer small cross sectional area of the inner hollow fiber tube. In consequence, there is no variation in ion concentration across the cross-sectional area but only in the axial direction, arising from reaction flux along the hollow fiber tube.

The extraction reaction is summarized in Eq. (2.1) for target metal ions (A) reacting with the extractant solution (B) to produce a metal ion complex (C). The overall rate of reaction with respect to target metal concentration (C_A) is expressed by Eq. (2.2).



$$-r_f = k_f C_A^n(x, t) \quad (2.2)$$

The complete set of solutions for the feed phase model is as follows:

$$n = 0$$

$$\bar{C}_{A_f}(L,t) = \bar{C}_{A_f}(0,t-\tau_f) \cdot u(t-\tau_f) + k_f(t-\tau_f) - k_f t \quad (2.3)$$

$$n = 1$$

$$\bar{C}_{A_f}(L,t) = \exp(\tau_f k_f) \cdot \bar{C}_{A_f}(0,t-\tau_f) \cdot u(t-\tau_f) \quad (2.4)$$

$$n \neq 0, 1$$

$$\bar{C}_{A_f}(L,t) = e^{\beta_f} \cdot \bar{C}_{A_f}(0,t-\tau_f) \cdot u(t-\tau_f) \quad (2.5)$$

where:

$u(t-\tau_f)$ is a unit function

$$u(t - \tau_f) = 0, t < \tau_f$$

$$u(t - \tau_f) = 1, t \geq \tau_f$$

Let:

$$\bar{C}_{A_f}(x, t) = C_{A_f}(x, t) - C_{A_f}(x, 0)$$

$$\tau_f = \frac{A_f L}{q_f}$$

$$\beta_f = \left(\frac{A_f k_f n}{q_f \gamma} \right) \ln \left(\frac{\gamma L + \lambda}{\lambda} \right)$$

$$\lambda = C_{A_f}^{1-n}(0, 0)$$

$$\gamma = \frac{(1-n)k_f A_f}{q_f}$$

$$A_f = 35000 \cdot \pi (r_i)^2$$

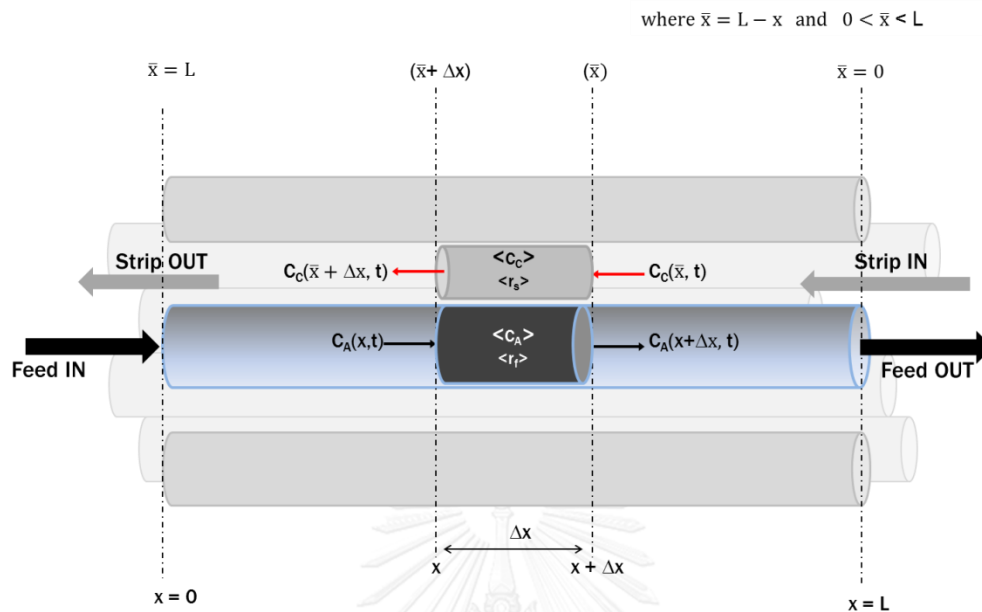


Figure 2.2 Transport schematic for the plug flow reaction in a HFSLM tube (feed phase) and shell annulus (stripping phase).

2.3.2 Recovery reaction flux model for transport in HFLSM

According to the aforementioned model of the feed flow, the same concept applies for the model of the stripping flow. The compilation of this model is possible given the following assumptions:

1. Operation is isothermal at constant pressure and volume.
2. Phase involved is homogeneous liquid.
3. Complete mixing occurs in each thin segment of the flow moving frame, thus no radial concentration distribution across the flow-cross-sectional area.
4. Recovery reaction takes place at the contact between the liquid membrane and the stripping phase, along the length of HFSLM. Hence it exhibits flux gradient in the axial direction.
5. The recovery reaction is irreversible. As a result, once the metal ion complex (C) decomposes to the original ions (A), the metal will be only transferred to the stripping phase.

จุฬาลงกรณ์มหาวิทยาลัย

The stripping flow moves through the shell and tube annulus as a series of infinitely thin coherent “plugs”. Following complete mixing, each plug has a uniform metal ion concentration. Each plug has a slightly different ion concentration to the plugs immediately preceding and following it, due to the progressive conversion of metal ions into their complexes.

The recovery reaction is basically the reverse of the extraction reaction in which the stripping solution agent (D) reacts with (C) to revert it back to (A).



$$+ r_s = k_s C_C^m(\bar{x}, t) \quad (2.7)$$

Let $0 < \bar{x} < L$ and $0 < \bar{x} < L$

Re-writing Eq. (2.7) to express the equation with a measurement concentration of target metal ions (C_A):

$$+ r_s = \frac{a}{c} k_s C_{A_s}^m(\bar{x}, t) \quad (2.8)$$

The mass conservation equation for the axial concentration distribution in stripping flow with respect to C_A is:

$$q_s C_{A_s}(\bar{x}, t) - q_s C_{A_s}(\bar{x} + \Delta x, t) + \langle r_s \rangle \cdot \Delta x A_s = \Delta x A_s \frac{\partial \langle C_{A_s} \rangle}{\partial t} \quad (2.9)$$

$$-\frac{q_s}{A_s} \left[\frac{C_{A_s}(\bar{x} + \Delta x, t) - C_{A_s}(\bar{x}, t)}{\Delta x} \right] + \langle r_s \rangle = \frac{\partial \langle C_{A_s} \rangle}{\partial t} \quad (2.10)$$

Take limit for Δx approaching to zero

$$-\frac{q_s}{A_s} \frac{\partial C_{A_s}(\bar{x}, t)}{\partial x} + r_s(\bar{x}, t) = \frac{\partial C_{A_s}(\bar{x}, t)}{\partial t} \quad (2.11)$$

A set of solution equations (Eqs. 2.12 to 2.17) is obtained as follows:

At an initial condition ($t = 0$):

$m = 0$

$$C_{A_s}(\bar{x}, 0) = C_{A_s}(0, 0) + \frac{k_s A_s}{q_s} \bar{x} \quad (2.12)$$

$m = 1$

$$C_{A_s}(\bar{x}, 0) = C_{A_s}(0, 0) \cdot \exp\left(\frac{k_s A_s}{q_s} \bar{x}\right) \quad (2.13)$$

$m \neq 0, 1$

$$C_{A_s}(\bar{x}, 0) = \left[C_{A_s}^{1-m}(0, 0) + \frac{(1-m)k_s A_s}{q_s} \bar{x} \right]^{\frac{1}{1-m}} \quad (2.14)$$

At any time (t):

$m = 0$

$$\bar{C}_{A_s}(L, t) = \bar{C}_{A_s}(0, t - \tau_s) \cdot u(t - \tau_s) + k_s(t - \tau_s) - k_s t \quad (2.15)$$

$m = 1$

$$\bar{C}_{A_s}(L, t) = \exp(\tau_s k_s) \cdot \bar{C}_{A_s}(0, t - \tau_s) \cdot u(t - \tau_s) \quad (2.16)$$

$m \neq 0, 1$

$$\bar{C}_{A_s}(L, t) = e^{\beta_s} \cdot \bar{C}_{A_s}(0, t - \tau_s) \cdot u(t - \tau_s) \quad (2.17)$$

where: $u(t - \tau_s)$ is a unit function

$$u(t - \tau_s) = 0, t < \tau_s$$

$$u(t - \tau_s) = 1, t \geq \tau_s$$

Let: $\bar{C}_{A_s}(\bar{x}, t) = C_{A_s}(\bar{x}, t) - C_{A_s}(\bar{x}, 0)$

$$\tau_s = \frac{A_s L}{q_s}$$

$$\beta_s = \left(\frac{A_s k_s m}{q_s \mu} \right) \ln \left(\frac{\mu L + \alpha}{\alpha} \right)$$

$$\alpha = C_{A_s}^{1-m}(0, 0)$$

$$\mu = \frac{(1-m)k_s A_s}{q_s}$$

$$A_s = 30000 \left(\frac{\sqrt{3}}{4} d_o^2 - \frac{\pi r_o^2}{2} \right)$$

For the case of $m \neq 0$ or 1 , a linearization is necessary to remove a non-linear term in Eq. (2.8) in order to obtain the solution equation of Eq. (2.17).

2.3.3 Transport across the hollow fiber tube (membrane phase)

The following assumptions stipulate the model construction of the ions transport within hollow fiber liquid membrane:

1. Target metal ions (A) are not allowed to enter micro-pore sites unless they are first converted to metal complexes (C).
2. The transport direction for the metal complex is in radial direction from the feed to the stripping phase.

3. The transport in axial direction is neglected due to the lack of lateral connection between adjacent micro-pore sites.
4. No reaction is involved in this model - only diffusion mass transport.
5. The system is considered to be in a pseudo steady state

The above assumptions imply that complex ions are the only species able to be transported within micro-pore sites in a radial direction.

Fick's law is used to describe the mass transport of metal complexes permeating through fiber micro-pores. Assuming there is no interface between the aqueous and membrane phases, concentration gradient can be determined directly from concentration of metal complex on the feed side (C_{c_f}) and on the stripping side (C_{c_s}).

The flux equation based on Fick's law is represented by Eq. (18) with the transport schematic shown in Fig. 2.3.

$$J_m = k_m(C_{c_f} - C_{c_s}) \quad (2.18)$$

Rewriting Eq. (2.18) in order to express the equation with measurement concentration of the target metal (C_A), gives:

$$J_m = \frac{a}{c} k_m \left\{ \left[C_{A_f} \left(x, t - \frac{A_f \Delta x}{q_f} \right) - C_{A_f} (x + \Delta x, t) \right] - \left[C_{A_s} \left(\bar{x} + \Delta x, t \right) - C_{A_s} \left(\bar{x}, t - \frac{A_s \Delta x}{q_s} \right) \right] \right\} \quad (2.19)$$

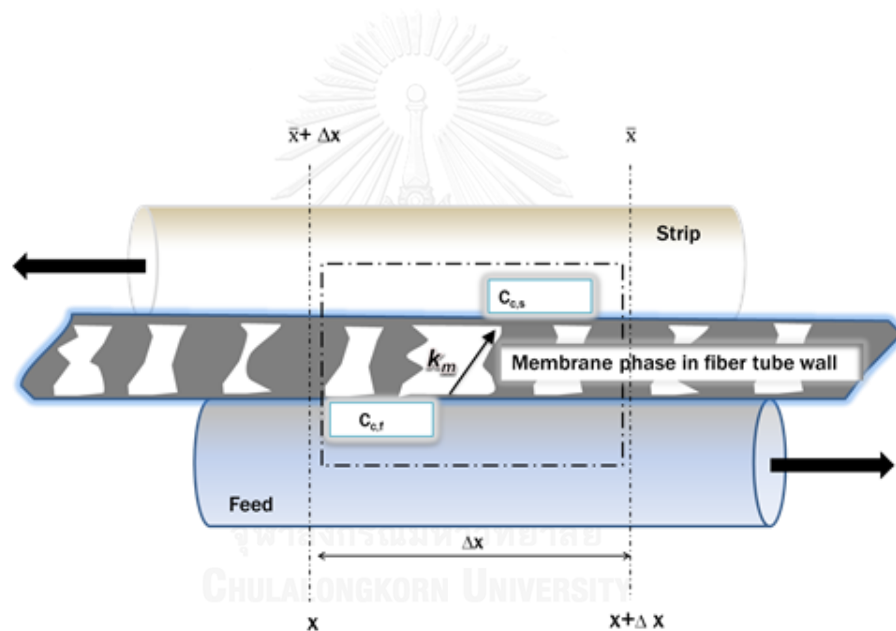


Figure 2.3 Metal complex transport across the membrane phase

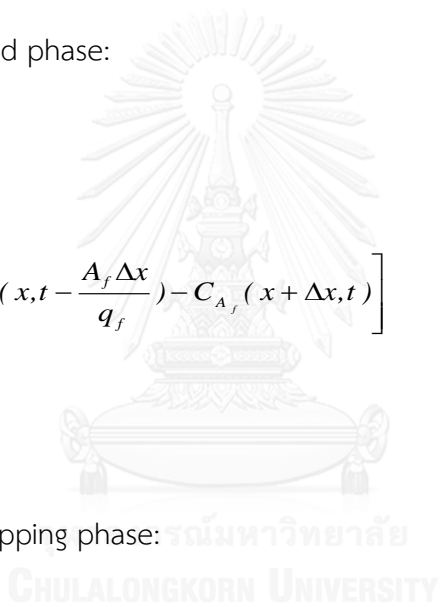
Under the pseudo-steady-state assumption, the mass transfer rates in membrane will equal the concentration flux in the feed phase and in the stripping phase, as described by Eq. (2.20).

$$J_f = J_m = J_s \quad J_f = J_m = J_s \quad (2.20)$$

However, the flux in the feed (J_f) and the flux in stripping phase (J_s) are largely functions of the concentration gradient (along the considered segment Δx).

Flux in the feed phase:

$$J_f = \Delta x \cdot \left[C_{A_f} \left(x, t - \frac{A_f \Delta x}{q_f} \right) - C_{A_f} (x + \Delta x, t) \right] \quad (2.21-a)$$

Flux in the stripping phase: 

$$J_s = \Delta x \cdot \left[C_{A_s} (\bar{x} + x, t) - C_{A_s} \left(\bar{x}, t - \frac{A_s \Delta x}{q_s} \right) \right] \quad (2.21-b)$$

Calculating the concentration gradient can be carried out by applying Eq. (2.3)

– (2.5) (the feed phase) and Eq. (2.15) – (2.17) (the stripping phase).

Corresponding to Eq. (2.20) - (2.21), the mass transfer coefficient in membrane phase (k_m) can be determined accordingly.

2.4 Experimental

2.4.1 The reagents and the feed

Reagent grade thioridazine-hydrochloric-acid solution and oleic acid were dissolved in analytical grade chloroform. Sodium nitrite (NaNO_2) was used as the stripping solution. Greatest Gold & Refinery Ltd. (Thailand) kindly supplied the waste aqua regia. The waste aqua regia reagent had residues containing Au (III) and other traces of other precious transition metals, including Pd (II) and Pt (IV). The initial concentration was 25.0, 18.7 and 51.4 $\text{mg}\cdot\text{L}^{-1}$ for Pd (II), Pt (IV) and Au (III) respectively. The waste aqua regia had been obtained with pH in the range of 1 to 2. Doubly distilled deionized water was used throughout the experiments.

2.4.2 Apparatus

All experiments were run with a Liqui-Cel[®] Extra-Flow 2.5X8 Laboratory Liquid Extraction System composed of two gear pumps, two variable speed controllers, two rota meters and four pressure gauges. The Liqui-Cel[®] Extra-Flow module, supplied by CELGARD LLC (Charlotte, NC; formerly Hoechst Celanese), was used as a support material. The fibers were put into a solvent-resistant polyethylene tube sheet featuring a shell casing of polypropylene. The properties of the hollow fiber module used are presented in Table 2.2. Metal concentration measurements in the aqueous phases were carried out by atomic absorption spectrophotometry (AAS) using a Shimadzu AA-670 spectrophotometer. All AAS measurements were carried out under recommended conditions specific for each metal. The pH measurements were made with a Metrohm 692 pH meter using a combined glass electrode.

Table 2.2 Properties of the hollow fiber module

Properties	Descriptions
Material	polypropylene
Inside diameter	240 μm
Outside diameter	300 μm
Effective length	15 cm
Number of hollow fibers	35,000
Pore size	0.03 μm
Porosity	25 %
Effective surface area	$1.4 \times 10^4 \text{ cm}^2$
Area per unit volume	$29.3 \text{ cm}^2/\text{cm}^3$
Module diameter	6.3 cm
Module length	20.3 cm
Tortuosity factor	2.6

2.4.3 Procedure

In the single-module operation (Fig. 2.4), the extractant was first diluted in chloroform. It was then circulated into the tube and the shell of HFSLM for 40 minutes to assure the extractant solution properly impregnated the micro-pores of hollow fiber. Thereafter, the feed solution was pumped into the tube side while the stripping solution was counter-currently pumped into the shell side. Samples for AAS analysis were taken from the feed flow outlet and the stripping flow outlet. The

static pressure across the membrane was kept higher on the feed and the stripping sides, to ensure that the solvent wetting the hydrophobic membrane remained in the pore.

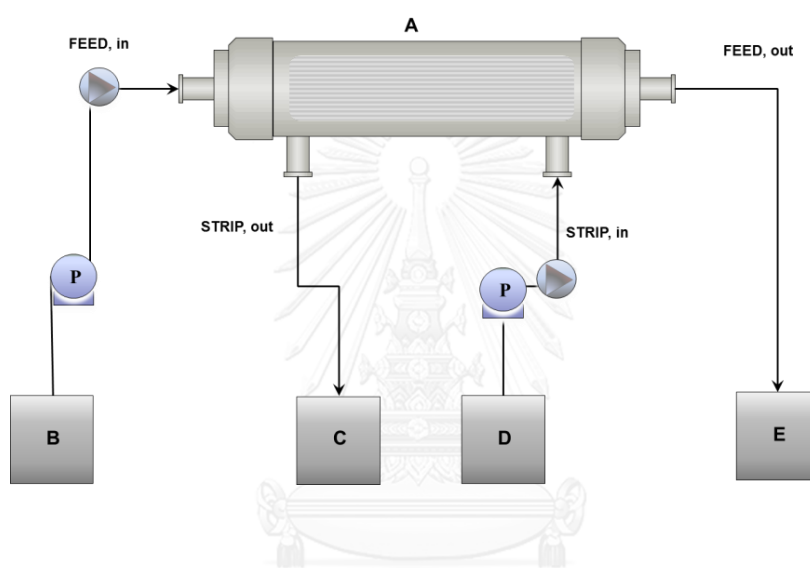


Figure 2.4 Counter-current flow diagram of a one-through-mode separation by hollow fiber supported liquid membrane: A-HFSLM; B-inlet feed reservoir; C-outlet strip reservoir; D-inlet strip reservoir; E-outlet feed reservoir.

In this study, key parameters to describe the performance are percentage of recovery and of extraction and the distribution ratio. The percentage of extraction (Eq. 2.22) serves quantitatively indicates to what extent the Pd (II) are extracted from

the used aqua regia solvent. The percentage of recovery (Eq. 2.23), by contrast, identifies how much the metal is drawn into the stripping solution. The overall distribution ratio (D.R.), therefore, indicates the propensity of Pd (II) to be transferred from the aqueous to the membrane phase (Eq. 2.24).

$$\text{Extraction} = \frac{C_{f_0} - C_f}{C_{f_0}} \% \quad (2.22)$$

$$\text{Recovery} = \frac{C_s - C_{s_0}}{C_{f_0}} \% \quad (2.23)$$

$$D.R. = \frac{C_m}{C_{aq}} \quad (2.24)$$

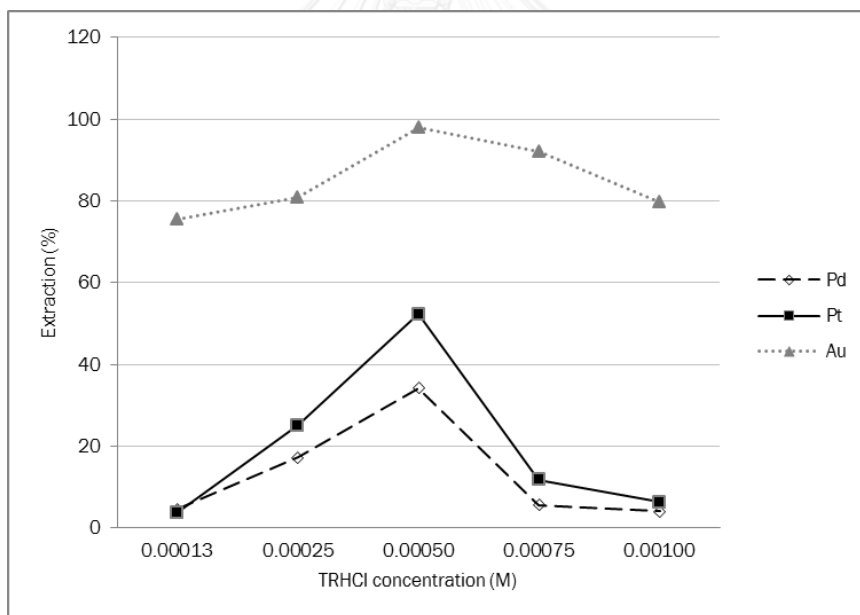
2.5 Results and discussion

2.5.1 Effect of extractant concentration

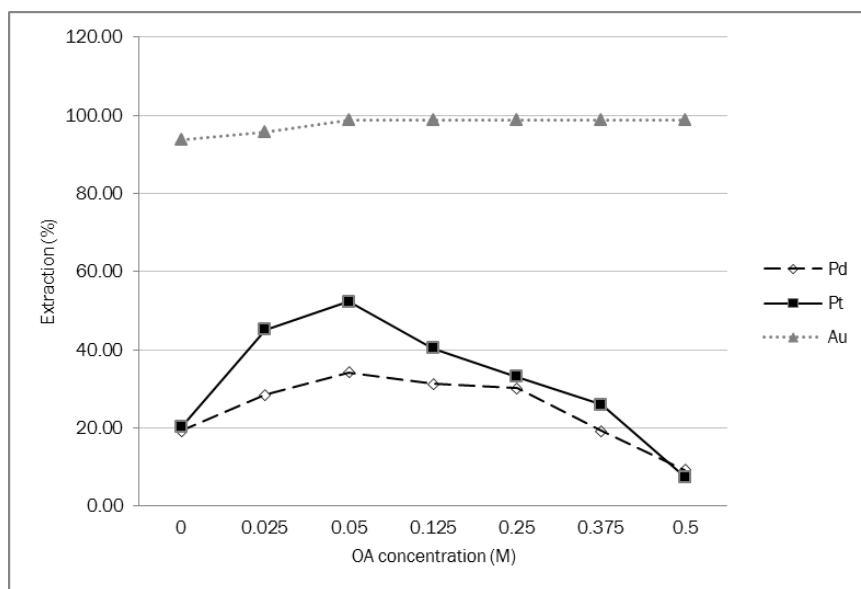
Metal ion concentration is the predominant factor affecting the efficacy of its extraction. The mixture of TRHCl and OA in chloroform served as the extractant carrier, a combination previously reported for successful Pd (II) extraction [13]. Thioridazine is a phenothiazine compound, believed to be become involved in metal complexation via hydrogen-bonding between its protonated nitrogen and a chlorine atom attached to the palladium ion [20, 21]. Oleic acid is a C₁₈ fatty acid whose inclusion, it has been suggested, substantially reduces leaching of thioridazine from the membrane phase into the aqueous phases. It is also thought to promote a synergistic effect resulting in the uphill transport of Pd (II) through the liquid membrane [22, 23].

Experimental runs were conducted at 28°C using 0.03 M NaNO₂ stripping solution, a feed pH of 2.0 and a feed/stripping flowrate of 100 mL·min⁻¹, a value shown to be successful in previous studies [5, 6].

The optimum pH in the feed was around 2. The pH influence is significant in this separation system. With pH less than 2, less system performance was observed. It made the system into highly acidic state which, in turn, compromised the integrity of the HFLSM fibers as the fibers became frayed. With pH greater than 2, the performance also dropped off, because corresponding metal complex with organic carrier became less stable at higher pH, resulting in less transport efficiency to stripping phase [13]. Moreover precipitation was observed.



(a) TRHCl

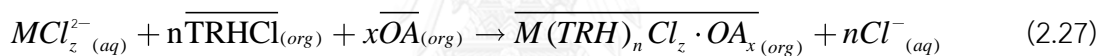
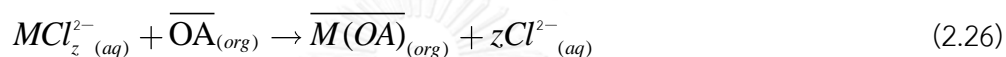
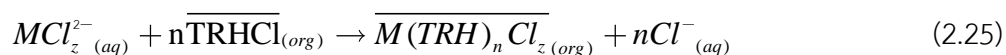


(b) OA mixing with 0.0005M TRHCl

Figure 2.5 Effect of a) TRHCl and b) OA concentrations on the extraction yield (28°C, feed: pH 2, strip: 0.03M NaNO₂, Flowrate: 100 mL·min⁻¹ in both the feed and the stripping, Operating time: 30 minutes).

Figure 2.5 shows how the concentration of TRHCl and OA affect the % extraction. Each plot exhibits a distinct peak for optimal extraction at concentration values that we adopted thereafter for the remainder of this study. The optimum concentration of TRHCl for this system was at 0.0005M (Fig. 2.5(a)). The optimum concentration of OA in conjunction with 0.0005M TRHCl was 0.05M (Fig. 2.5(b)).

The reactions involved in this extraction are summarised in Eq. (2.25) - (2.27).



The increase in extraction yield with concentration can be explained by Le Chatelier's Principle. Increasing the reactants' concentration favors their consumption and hence drives the reaction forwards. Thus, Pd (II) became more readily transported from the feed to the membrane and so the % extraction increases. After the point corresponding to maximum extraction, the steady decrease observed is due to the viscosity effect from high extractant concentration [24, 25]. It hinders effective diffusion of the metal complex through the liquid membrane phase, resulting in the drop in performance. The Nernst Equation for the diffusion coefficient

in Eq. (2.28) reveals the effect viscosity (η) has on the system; the higher the viscosity, the lower the rate of diffusion.

$$D = \frac{RT}{6\pi\eta r} \quad (2.28)$$

2.5.2 Synergistic extractant

The aspect of synergy effects was captured here. The optimal extraction of both Pd (II) and Pt (IV) occurred at extractant concentrations of 0.0005M TRHCl and 0.05M OA.

The effect of synergistic extraction (expressed as synergy coefficient S) as a function of the distribution ratios was deployed [26].

$$S = \frac{D.R._{12}}{(D.R._1 + D.R._2)} \quad (2.29)$$

where: $D.R._{12}$ is a distribution ratio from the synergistic extractant. $D.R._1$ or $D.R._2$ are distribution ratios obtained from a single extraction.

It was calculated that S for Pt (IV) was 3.1, 1.85 for Pd (II) and only 1.00 for Au (III), confirming that the extraction had synergy effect on Pt (IV) and Pd (II). No synergy effect on Au (III) as the calculated S was only 1 (neutral).

Fig. 2.5 (b) reveals that the extractant carrier by OA appeared to contribute negligibly towards Au (III) despite concentration increase. Only the extractant carrier by TRHCl appeared to play a significant role in Au (III) extraction, observations in accordance with its calculated S value of unity.

There were three reactions involved in this synergistic extraction. The reaction as shown in Eq. (2.25) and (2.26) were primary extractions from direct reaction with TRHCl (proton acceptor) and OA (proton donor) respectively.

The reaction in Eq. (2.27) was the secondary reaction where the reaction took place at the presence of proton acceptor-donor interactions (TRHCl-OA). It produced the derivative complex TRHCl-OA-metal ions, termed 'inverse micelles' by Farhadi

and Shamsipur [13]. These inverse micelles induce the cooperative transport of metal ions within the liquid membrane, thus augmenting the extraction performance.

2.5.3 Selective recovery

Recovery using NaNO_2 as the stripping solution was also investigated, the results from which are presented in Fig. 2.6. NaNO_2 was selected following reports by Farhadi and Shamsipur [13] detailing the nitrite ion's superlative selectivity for recovery of Pd (II).

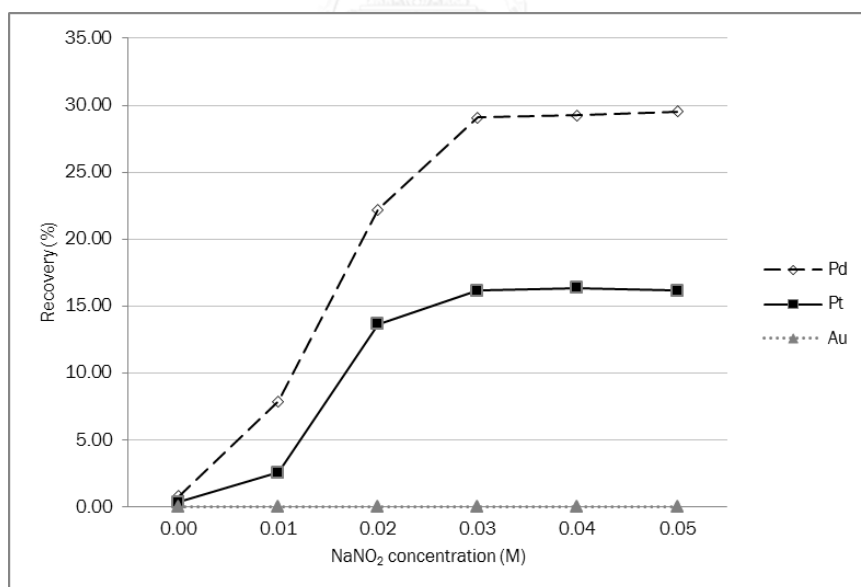


Figure 2.6 Effect of varying NaNO_2 concentration in the stripping phase (28°C, Feed: pH 2.0, extractant carrier: 0.0005M TRHCl and 0.05M OA in chloroform, Flowrate: 100 $\text{mL}\cdot\text{min}^{-1}$ in both the feed and the stripping, Operating time: 30 minutes).

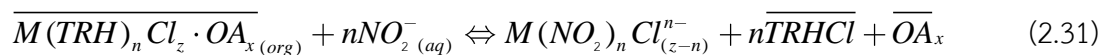
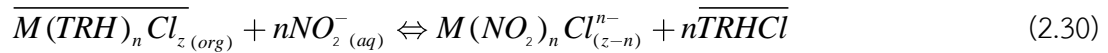


Fig. 2.6 is results after the 1st cycle operation (30 minutes). This intention is just to illustrate the point where an optimum concentration of NaNO₂ as a stripping agent was located. In this case, a NaNO₂ concentration of 0.03 M was found to give the best recovery yield and selected for use in further study.

In order to clearly illustrate the performance of NaNO₂, Table 2.3 presents the quantitative metal distributions between the phases. It was obvious that NaNO₂ preferentially captured Pd (II) complex from the liquid membrane and turned them to stay in the stripping phase. This fact is supported by the lowest distribution of Pd (II) in liquid membrane and the highest in the stripping phase as shown in Table 2.3.

Table 2.3 Metal distribution between phases while using NaNO_2 as the stripping solution

Metal ion	Feed inlet $\text{mg}\cdot\text{L}^{-1}$	Distribution in $\text{mg}\cdot\text{L}^{-1}$		
		Outlet feed phase	Liquid membrane phase	Outlet stripping phase
Pd (II)	25.0	16.5	1.2	7.3
Pt (IV)	18.7	8.9	5.3	4.5
Au (III)	51.4	1.1	50.3	0.0

From Table 2.3., it was obvious that significant quantities of residual of Au (III) remained in the liquid membrane. With different and proper stripping solutions other than NaNO_2 , those residuals could be recovered for further economic exploitation. However, it was not the scope in this study

2.5.4 Effect of operating cycle

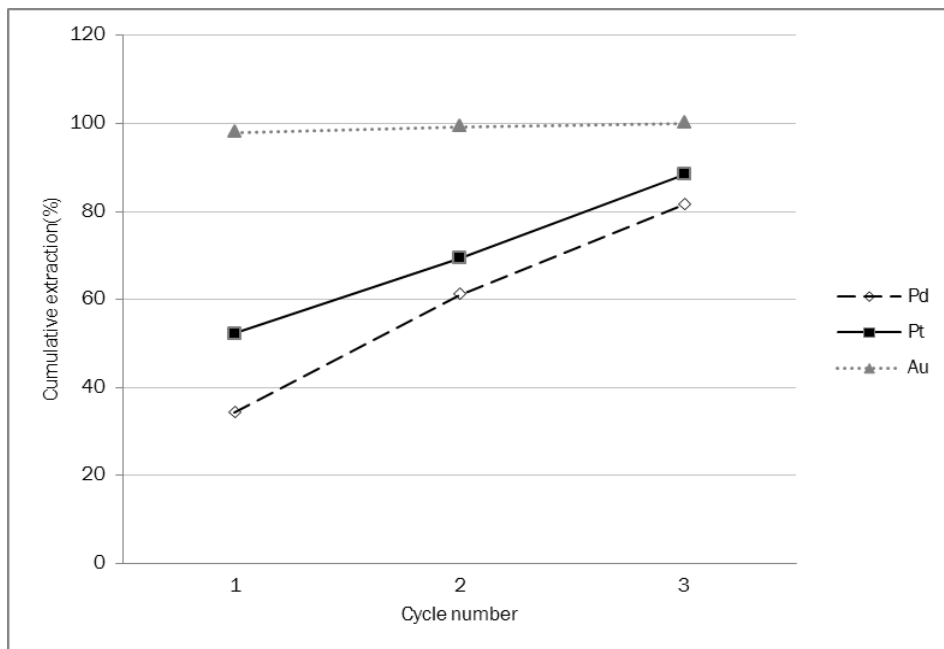
In once-through operations, the extraction yields of Pd (II), Pt (IV) and Au (III) were 34%, 52 and 98% respectively, whereas the percentages of recovery were 29%, 16% and 0% respectively. To further enhance the performance, we investigated the operation in repeated cycle mode which afforded the results shown in Fig. 2.7.

The cumulative Pd (II) extraction and recovery rose to 82% and 78%, respectively following the third cycle. The selectivity of Pd (II) recovery was also observed to improve with repetition of the extraction cycle. The selectivity index was calculated from Eq. (2.32):

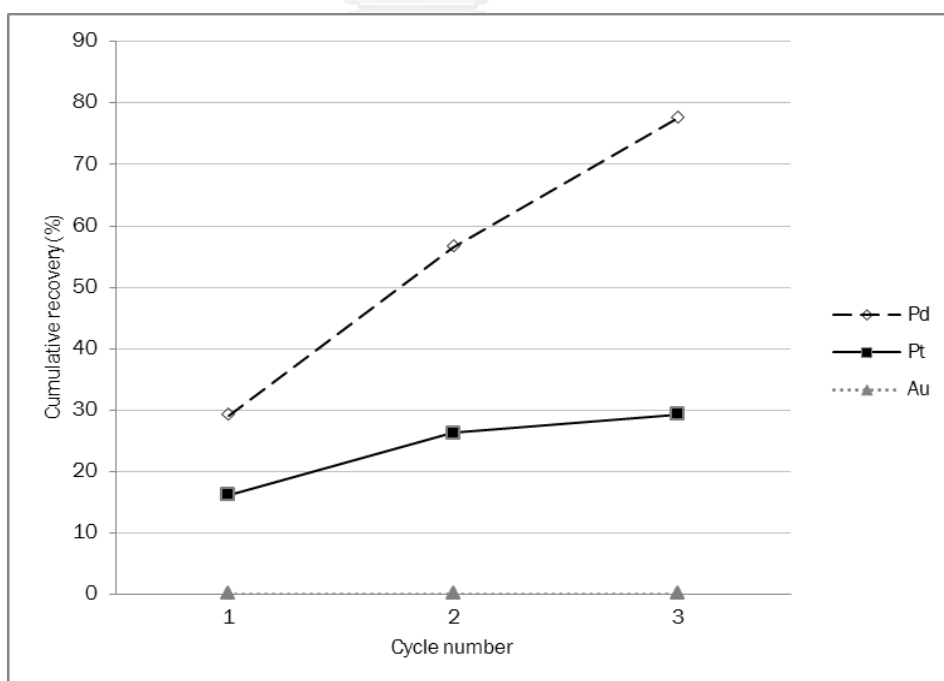
$$\text{Selectivity index} = \frac{C_{Pd(II)}}{C_{Pt(IV)}} \text{ for Pd (II) over Pt (IV)} \quad (2.32)$$

Selectivity indices of 1.8, 2.1 and 2.6 were obtained after the first, second and third cycles, respectively.

After the 1st cycle operation, the recovery (from the feed to the stripping phase) yielded 29% and 16% respectively for Pd (II) and Pt (IV). But after the 3rd cycle, 90 minutes in total, the recovery of Pd (II) became 78% while Pt (IV) only 29% - shown by Fig. 7(b). This pronounces the effectiveness of using NaNO₂ as the stripping agent to recover preferentially of Pd (II) over Pt (IV).



(a) Extraction



(b) Recovery

Figure 2.7 Effect of repeat operating cycles metal (a) extraction and (b) recovery. (28°C, Feed: pH 2.0, Extractant carrier: 0.0005M TRHCl and 0.05M OA in chloroform, Strip: 0.03M NaNO₂, Flowrate: 100 mL·min⁻¹ in both the feed and the stripping, Operating time: 90 minutes for 3 cycles)

2.5.5 Determining rate of Pd(II) extractant

The rate constant for Pd (II) extraction and recovery was determined for the model input. (Table 2.5). The best-fit result was obtained from the integrated first-order rate law at the semi natural logarithm plot between Pd (II) concentration and time. The linear curve was drawn tangentially along the plot, giving a calculated $R^2 > 0.99$ for the extraction reaction and $R^2 > 0.96$ for the recovery reaction (Figs. 2.8 and 2.9).

Table 2.4 Analysis of reaction order and rate constants

Rate	Determination			
Order	Relationship	Rate constant		R^2
Extraction				
0	C vs. Time ^{*1}	2.174×10^{-1}	$\text{mg}\cdot\text{L}^{-1}\cdot\text{min}^{-1}$	0.925
1	$\ln(C_0/C)$ vs. Time ^{*1}	1.400×10^{-2}	min^{-1}	0.995**
2	$1/C$ vs. Time ^{*1}	1.000×10^{-3}	$\text{L}\cdot\text{mg}^{-1}\cdot\text{min}^{-1}$	0.982
$n = 4.1$	$\ln(\partial C/\partial t)$ vs. $\ln C$ ^{*2}	8.584×10^{-6}	$\text{mg}^{1-n}\cdot\text{L}^{n-1}\cdot\text{min}^{-1}$	0.881
Recovery				
0	C vs. Time ^{*1}	2.020×10^{-1}	$\text{mg}\cdot\text{L}^{-1}\cdot\text{min}^{-1}$	0.883
1	$\ln(C_0/C)$ vs. Time ^{*1}	2.480×10^{-2}	min^{-1}	0.965**
2	$1/C$ vs. Time ^{*1}	4.900×10^{-3}	$\text{L}\cdot\text{mg}^{-1}\cdot\text{min}^{-1}$	0.671
$m = 2.2$	$\ln(\partial C/\partial t)$ vs. $\ln C$ ^{*2}	$2.803 \times 10^{+1}$	$\text{mg}^{1-n}\cdot\text{L}^{n-1}\cdot\text{min}^{-1}$	0.925

NB* (1) Integral analysis. (2) Differential analysis. ** Best Fit

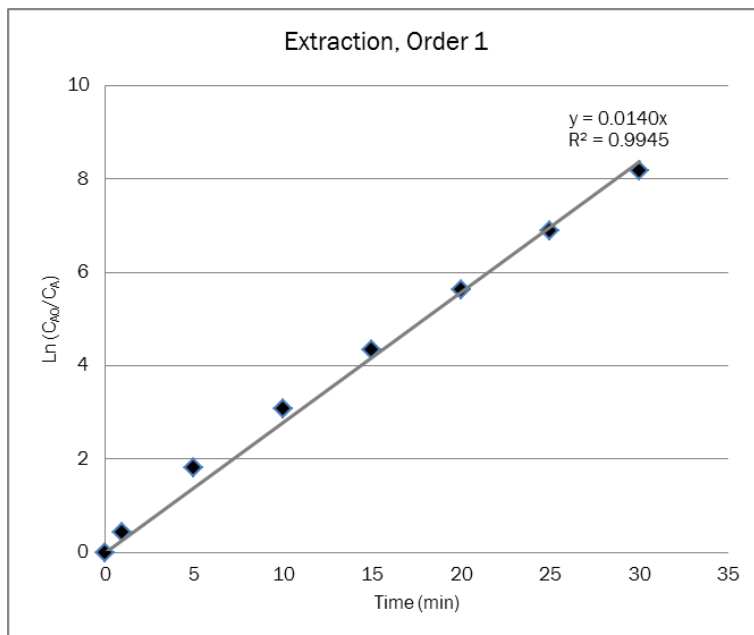


Figure 2.8 Integral concentrations of Pd (II) extraction

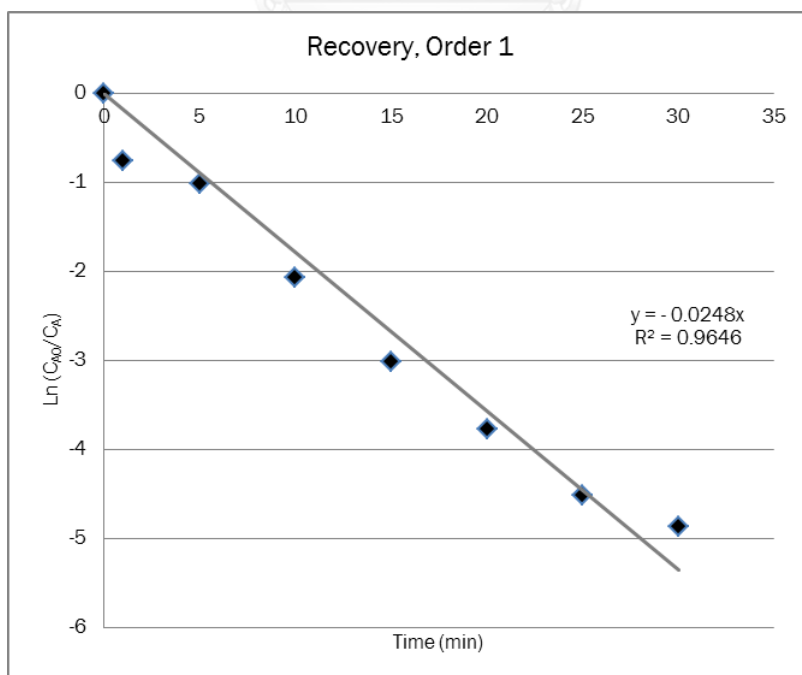


Figure 2.9 Integral concentrations of Pd (II) recovery

This system appears to obey a pseudo-first-order rate equation in which both extraction and stripping depends on the concentration of only one reactant.

The extraction reaction rate constant (k_f) and the stripping reaction rate constant (k_s) were read as 0.0140 s^{-1} and 0.0248 s^{-1} from the slopes of the respective plots at the controlled temperature of $28 \text{ }^\circ\text{C}$ and flowrate of $100 \text{ mL}\cdot\text{min}^{-1}$. These rate constants from this experiment and computation were deemed to be specific to the set of conditions (extractant carrier of 0.0005M TRHCl and 0.05M OA in chloroform, stripping solution 0.03M NaNO_2).

2.5.6 Reaction flux model for Pd(II) extraction and recovery

The computation model for Pd (II) transport within HF LSM was developed. It was composed of three flow transport paths. The paths in the feed phase (fiber tube) and the stripping phase (tube & shell annulus) were modeled with only axial concentration distribution. The k_f term was used to calculate the concentration profile of the feed phase in the tube. Similarly, the term k_s term was used to calculate the concentration profile in the stripping phase.

For the membrane, the k_m term was used to calculate the concentration profile following the transport of Pd (II) across the micropore sites of the membrane phase. From the equal flux relationship in Eq. (2.18), the mass transfer coefficient in membrane phase (k_m) was calculated as $0.198 \text{ cm}\cdot\text{min}^{-1}$, a value adopted for the model.

Running the model for the scenario of varying flowrate, the hypothetical results appeared to follow the same trend as the experimental data (Fig. 2.10 and Table 2.5).

In order to verify the model, an R-squared coefficient (R^2 or RSQ) and the average percentage deviation were calculated using:

$$\% \text{ Deviation} = \frac{\sum_{i=1}^j C_{Exp} - C_{Hypo}}{j} \% \quad (2.33)$$

In this instance, a good match was observed with the extraction case, as indicated by high R^2 and low % deviation. The recovery case showed also a good match as the hypothetical results corresponded well with the experimental data. Both the extraction and recovery commonly showed high deviation at high flowrates.

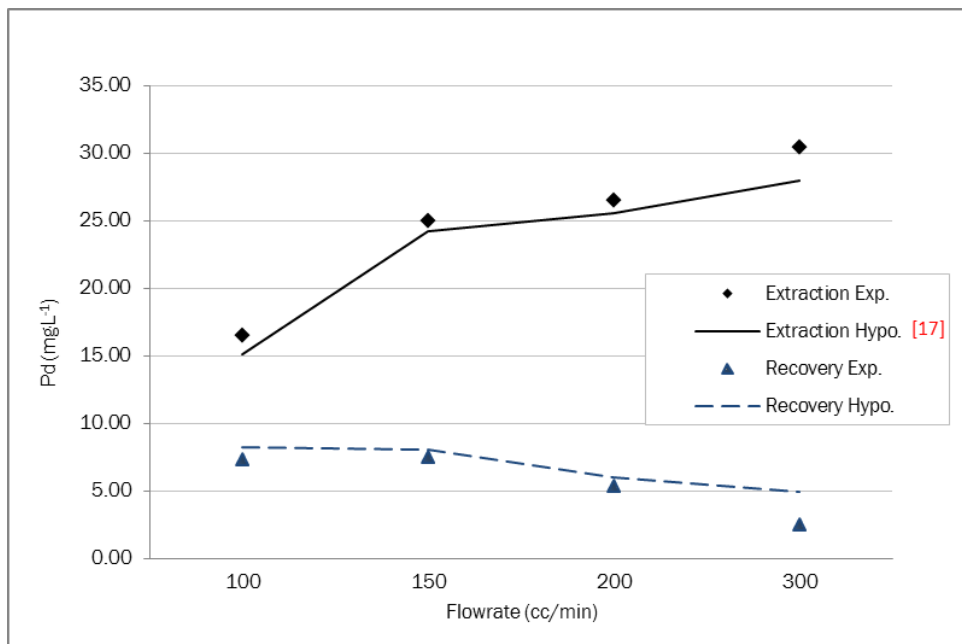


Figure 2.10 The model computation results against experimental data for the case of varying flowrate.

Table 2.5 Model computation results for the varying flow rate case

Flowrate (mL/min)	Extraction (%)		Recovery (%)	
	Exp.	Hypo. ^{*[17]}	Exp.	Hypo.
100	16.46	15.07	7.28	8.24
150	26.99	24.26	6.18	8.01
200	26.46	25.56	5.32	6.00
300	30.43	28.00	2.47	4.94
R ²	0.982		0.867	
Deviation	8.17%		24.33%	

NB*Pancharoen U. et al. [17]

The hypothetical result for the recycling scenario showed good agreement with experiment data (Fig. 2.11 and Table 2.6); the average percentage of deviation was 10.52% for the extraction case and only 1.66 % for recovery. It was consistent although the third cycle elapsed.

The results from the varying flowrate scenario were less satisfactory. At 300 mL·min⁻¹ flowrate, the deviation was large (> 90%), i.e. 2.47 mg·L⁻¹ (Exp.) vs. 4.94 mg·L⁻¹ (Hypo.). A mismatch from the model parameter is likely to have been a contributory factor. The reaction rate constant was one of the parameters subsequently considered for review, given that the constant was from the reaction data running through HFSLM at 100 mL·min⁻¹. The use of the same constant may not be appropriate in cases of higher flowrate.

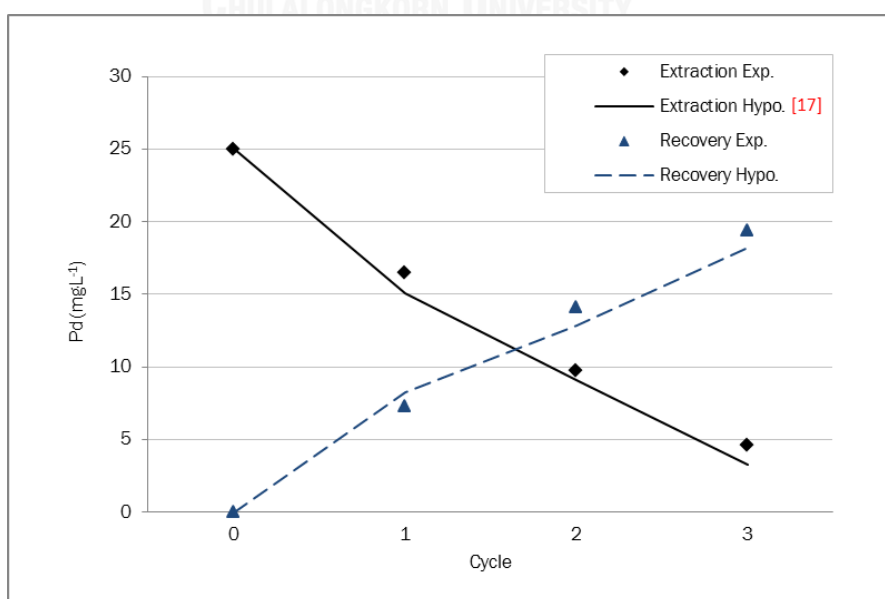


Figure 2.11 The model computation results against experimental data for the case of repeated operating cycles.

Table 2.6 Model computation results for the repeat cycle scenario.

Cycle	Extraction (%)		Recovery (%)	
	Exp.	Hypo. ^{*[17]}	Exp.	Hypo.
0	25.02	25.02	0	0
1	16.46	15.08	7.28	8.24
2	9.75	9.09	14.14	12.84
3	4.62	3.26	19.42	18.17
R ²	0.996		0.986	
Deviation	10.52%		1.66%	

NB*Pancharoen U. et al. [17]

2.6 Conclusion

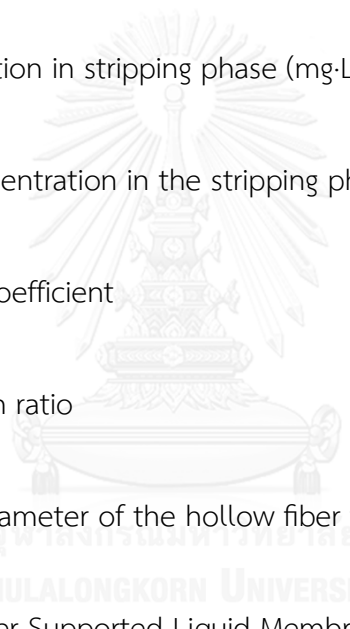
Our combined results show that a hollow fiber supported liquid impregnated with TRHCl–OA membrane can extract Pd (II) with a potentially useful degree of selectivity. The optimum conditions of transport were found at pH 2 in the feed (used aqua regia waste), 0.005M thioridazine and 0.05M oleic acid in the liquid membrane, 0.03M NaNO₂ in the stripping solution and operating flowrate of 100 mL a minute. Use of thioridazine and oleic acid in the extractant carrier results in a synergistic enhancement of Pd (II) and Pt (IV) extraction.

The performance was considerably enhanced by running the operation in repeated cycle mode. After the third repeat cycle, the cumulative extraction of Pd (II), Pt (IV) and Au (III) were reported to 82%, 88 and 100%; the percentages of recovery were 78%, 29% and 0% respectively. Selective recovery of Pd (II) over Pt (IV) was calculated to be 2.6.

The prediction model ran on the scenario of varying flowrate and the scenario of repeated cycle mode. The results demonstrated good agreement between the experiment and hypothetical data. Accordingly it is reasonable to conclude that the model shows potential for use in the application ^{คือ} design (at the same operating environment and reagents). The model is simple and it requires few inputs to plug in, such as the rate constants, the mass transfer coefficient and the flow rate.

2.7 Notation

A	Cross sectional area (cm ³)
A,B,C,D	Target metal ions (A), Extractant carrier (B), Complex ions (C) and Stripping solution (D)

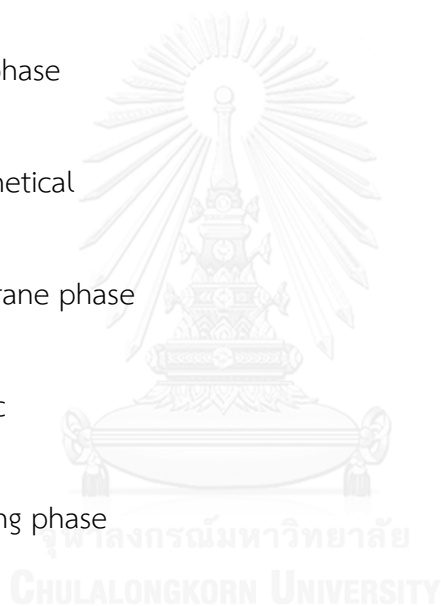


a, b, c, d	Stoichiometric coefficients
C_f	Concentration in the feed phase ($\text{mg}\cdot\text{L}^{-1}$)
C_{f0}	Initial concentration in the feed phase ($\text{mg}\cdot\text{L}^{-1}$)
C_m	Concentration in liquid membrane phase ($\text{mg}\cdot\text{L}^{-1}$)
C_s	Concentration in stripping phase ($\text{mg}\cdot\text{L}^{-1}$)
C_{s0}	Initial concentration in the stripping phase ($\text{mg}\cdot\text{L}^{-1}$)
D	Diffusion coefficient
D.R.	Distribution ratio
d_o	External diameter of the hollow fiber tube (cm)
HFSLM	Hollow fiber Supported Liquid Membrane
J	Flux ($\text{mg}\cdot\text{cm}^{-2}\cdot\text{min}^{-1}$)
k_f	Rate constant of “extraction” reaction in the feed phase (min^{-1})
k_m	Rate of mass transfer coefficient in the membrane phase ($\text{cm}\cdot\text{min}^{-1}$)
k_s	Rate constant of “recovery” reaction in the stripping phase (min^{-1})
L	Length of the hollow fiber (cm)

m	Order of recovery reaction
N	Numbers of hollow fibers in the module
n	Order of extraction reaction
OA	Oleic acid (secondary organic extractant in the study)
Q_f	Volumetric flowrate of feed solution ($\text{mL} \cdot \text{min}^{-1}$)
R^2	R-square coefficient
S	Synergistic coefficient
r_i	Internal radius of the hollow fiber tube (cm)
r_o	External radius of the hollow fiber tube (cm)
r_{lm}	Log-mean radius of the hollow fiber
r	Rate of reaction
$TRHCL$	Thioridazine (primary organic extractant in the study)
ϵ	Porosity of the hollow fiber (%)
μ	Viscosity (cp)

Subscripts

<i>A</i>	Target metal ion
<i>aq</i>	Aqueous
<i>C</i>	Complex metal ion
<i>Exp</i>	Experimental
<i>f</i>	Feed phase
<i>Hypo</i>	Hypothetical
<i>m</i>	Membrane phase
<i>org</i>	Organic
<i>s</i>	Stripping phase



2.8 Acknowledgment

This work was supported by the Graduate School of Engineering, Chulalongkorn University and the ASAHI Glass Foundation and Mass Separation Technology Laboratory, Department of Chemical Engineering, Faculty of Engineering, Chulalongkorn University

2.9 References

- [1] Rizvi, G.H., Mathur, J.N., Murali, M. S. and Iyers, R.H., "Recovery of Fission Product Palladium from Acidic High Level Waste Solution", *Separation Science and Technology*, 31(13), 1805-1816 (1996).
- [2] Kakoi, T., Horinouchi, N., Goto, M. and Nakashio, F., "Recovery of Palladium from an Industrial Wastewater using Liquid Surfactant Membranes", *Separation Science and Technology*, 31(3), 381-399 (1996).
- [3] Araki, T. and Tsukube, H. (Eds.), *Liquid Membranes: Chemical Applications*, CRC Press, Boca Raton, FL, 1990.
- [4] Mori, A., Kubo, K. and Takeshita, H., "Synthesis and metallophilic properties of troponoid thiocrown ethers", *Coord. Chem. Rev.*, 148, 71-96 (1996).
- [5] Patthaveekongka W., Prakorn, R., Suttichai, A., and Pancharoen, U., "Transport of cerium, lanthanum, neodymium and palladium via hollow fiber supported liquid membrane based on equilibrium theory", *Journal of the Chinese institute of Chemical Engineers*, 37(3), 227-238 (2006)
- [6] Ramakul, P., Pattaveekongka, W., and Pancharoen, U., "Mass transfer modeling of membrane carrier system for extraction of Ce(IV) from sulfate

- media using hollow fiber supported liquid membrane”, Korean Journal of Chemical Engineering, 23(1), 85-92 (2006)
- [7] Sunsandee N., Leepipatpiboon N., Ramakul P., Pancharoen U., “The Selective Separation of (S)-amlodipine via a Hollow Fiber Supported Liquid Membrane: Modeling and Experimental verification”, J. Chem. Eng., 180, 299–308 (2012)
- [8] Lothongkum, A.W., Suren, S., Chaturabul, S., Thamphiphit, N., Pancharoen, U., “Simultaneous Removal of Arsenic and Mercury from Natural-Gas-Co-Produced water from the Gulf of Thailand using Synergistic Extractant via HFSLM”, J. Membr. Sci., 369, 350-358 (2011).
- [9] Pancharoen, U., Ramakul, P., and Pattaveekongka, W., “Purely extraction and separation of mixture of cerium(IV) and lanthanum(III) via hollow fiber supported liquid membrane”, Journal of Industrial and Engineering Chemistry, 11(6), 926-931 (2005).
- [10] Wannachod P., Chaturabul, S., Pancharoen, U., Lothongkum, A. W. and Patthaveekongka, W. “The effective recovery of praseodymium from mixed rare earths via a hollow fiber supported liquid membrane and its mass transfer related”, Journal of Alloys and Compounds, 509 (2), 354-361(2011).

- [11] Fontàs, C., Salvadó, V., Hidalgo, M., “Selective enrichment of palladium from spent automotive catalysts by using a liquid membrane system”, *Journal of Membrane Science*, 223, 39–48 (2003)
- [12] Katsuta, S., Yoshimoto, Y., Okai, M., Takeda, Y., and Bessho K., “Selective Extraction of Palladium and Platinum from Hydrochloric Acid Solutions by Trioctylammonium-Based Mixed Ionic Liquids”, *Industrial & Engineering Chemistry Research*, 50, 12735–12740 (2011).
- [13] Farhadi, K. and Shamsipur, M., “Separation Study of Palladium through a Bulk Liquid Membrane Containing Thioridazine-HCl and Oleic Acid”, *Separation Science and Technology*, 35(6), 859-868 (2000).
- [14] Antico, E., Masana, A., Hidalgo, M., Salvado', V. and Valiente, M., “New Sulphur-containing Reagents as Carriers for the Separation of Palladium by Solid Supported Liquid Membranes”, *Hydrometallurgy*, 35(3), 343-352 (1994)
- [15] Fu, J., Nakamura, S. and Akiba, K., “Transport of Palladium (II) through Trioctylamine Liquid Membrane”, *Separation Science and Technology*, 30(5), 793-803 (1995).
- [16] Rovira, M. and Sastre, A.M., “Modeling of Mass Transfer in Facilitated Supported Liquid-membrane Transport of Palladium (II) using Di-(2-ethylhexyl) Thiophosphoric Acid”, *Journal of Membrane Science*, 149(2), 241-250 (1998).

- [17] Huang, D.; Huang, K.; Chen, S. & Liu, S., “Rapid Reaction-Diffusion Model for the Enantioseparation of Phenylalanine across Hollow Fiber Supported Liquid Membrane”, *Journal of Separation Science and Technology*, 43, 259–272 (2008)
- [18] U. Pancharoen, et al., *Separation Science and Technology* (2011), doi:10.1080/01496395.2011.595287
- [19] Rathorea, N.S., Sonawanea, J. V., Kumar, A., Venugopalana, A. K., Singha, R. K. , Bajpaia, D. D. and Shukla, J. P., “Hollow fiber supported liquid membrane: a novel technique for separation and recovery of plutonium from aqueous acidic wastes”, *Journal of Membrane Science*, 189(1),119-128 (2001).
- [20] Raber, G., Kalcher, K., Neuhold, C.G., Talaber, C. and Kölbl, G. “Adsorptive Stripping Voltammetry of Palladium(II) with Thioridazine- In Situ - Modified Carbon Paste Electrodes”, *Electroanalysis* 7(2), 138-142(1995).
- [21] Lindoy, L. F. and Baldwin, D. S., “Ligand design for selective metal-ion transport through liquid membranes”, *Pure and Applied Chemistry*, 61(5), 909-914(1989).
- [22] Dadfarnia, S. and Shamsipur, M., “Highly Selective Membrane Transport of Zn^{2+} Ion by a Cooperative Carrier Composed of 1,10-Diaza-18-crown-6 and

- Palmitic Acid”, Bulletin of the Chemical Society of Japan, 65, 2779-2783 (1992).
- [23] Akhond, M. and Shamsipur, M., “Specific uphill transport of Cd^{2+} ion by a cooperative carrier composed of aza-18-crown-6 and palmitic acid” Journal of Membrane Science, 117, 221-226 (1996).
- [24] Patthaveekongka, W., “Influence of Acetic Acid-sodium Acetate Solution Concentration on Extraction of Zinc Ions via a Hollow Fiber Supported Liquid Membrane,” Master’s thesis, Dept. of Chem. Eng., Chulalongkorn University (1999).
- [25] Sangtumrong, S., Ramakul, P., Satayaprasert, C., Pancharoen, U. and Lothongkum, A.W., “Purely separation of mixture of mercury and arsenic via hollow fiber supported liquid membrane”, Journal of Industrial and Engineering Chemistry 13 (5), 751-756 (2007).
- [26] Luo, F., Lia, D., Wei, P., “Synergistic extraction of zinc(II) and cadmium(II) with mixtures of primary amine N1923 and neutral organophosphorous derivatives”, Hydrometallurgy, 73, 31-40 (2004).

CHAPTER 3

SEPARATION OF MERCURY (II) FROM PETROLEUM PRODUCED WATER VIA HOLLOW FIBER SUPPORTED LIQUID MEMBRANE AND MASS TRANSFER MODELING

Srestha Chaturabul, Wanchalerm Srirachat, Thanaporn Wannachod, Ura Pancharoen[†]
and Soorathep Kheawhom^{††}

*Department of Chemical Engineering, Faculty of Engineering, Chulalongkorn
University, Bangkok 10330, Thailand*

This article has been published in Journal: Chemical Engineering Journal.

Page: 34–46. Volume: 265. Year: 2015.

3.1 Abstract

The separation of mercury (II) from petroleum-produced water from the Gulf of Thailand was carried out using a hollow fiber supported liquid membrane system (HFSLM). Optimum parameters for feed pretreatment were 0.2M HCl, 4% (v/v) Aliquat 336 for extractant and 0.1 M thiourea for stripping solution. The best percentage obtained for extraction was 99.73% and for recovery 90.11%, respectively. The overall separation efficiency noted was 94.92% taking account of both extraction and recovery prospects. The model for this separation developed along a combined flux principle i.e. convection-diffusion-kinetic. The results showed excellent agreement with theoretical data at an average Standard Deviation of 1.5% and 1.8%, respectively

3.2 Introduction

Mercury is a natural trace component found in the petroleum reservoir. Its concentration levels vary widely, depending on the production area. It is produced with petroleum hydrocarbon and associated water –so-called “produced water” – in both elemental mercury and ionic mercury Hg(II) form [1]. The presence of mercury is

detrimental to petroleum production facilities as it forms corrosion induced through mercury amalgamates. Moreover, it has an effect on human beings if it is discharged into the atmosphere leading to severe, acute and chronic poisoning [2-6].

Conventionally, a mercury treatment unit based on chemical production aids precipitation [1] ion exchange [9, 10] sorption [11] ultrafiltration [12] adsorption [13-16] solid phase extraction [17] or liquid-liquid extraction [18]. It deals excellently with elementary mercury at bulk concentration but not with ionic mercury [14]. Ionic mercury usually remains as residue after conventional treatment [19] which may render a still high mercury content in the produced water above the environmental discharge limit. An alternative technique, such as hollow fiber supported liquid membrane (HFSLM) technology, is therefore considered to take care of the residual ionic mercury.

HFSLM has attracted interest from many researchers on its unique simultaneous extraction and recovery operation for promising ionic metal removal and wastewater treatment. It is an innovative separation technique which combines the advantages of liquid-to-liquid extraction and mass transfer area within the membrane micro-pore structure [20]. It has other advantages, notably lower capital and operating costs [21] less energy consumption, less extractant used [22] and a larger surface area per unit for mass transfer [23, 24].

The application of HFSLM in this study follows on previous success in precious metal and toxic metal separation in our research groups [41-45]. Huang et al. [46] demonstrated successful pharmaceutical wastewater treatment by membrane separation. Yeung's team [47-50] deployed LUS membrane to enhance selectivity of Cu(II) in the Cu(II)/Au(III) system [50]. Güell et al. [51] succeeded in the removal of Cr(VI) at trace concentration from different aqueous samples via HFSLM using Aliquat 336. It reported high efficient separation and stability over 8-days continuous operation. Wannachod et al. [52] separated Nd(III) from mixed rare earths. The percentage of Nd(III) extraction was 95% using 0.5 M D2EHPA and 0.3M TOPO being the synergistic extractant and 1M H₂SO₄ the stripping solution. Mafu et al. [53] conducted a separate study of As (III) from wastewater via HFSLM. An extractant was made with n-undecane and di-n-hexyl ether mixtures (3:1 %v/v) while the stripping solution was H₂SO₄; satisfactory removal was reported. Mtibe et al. [54] treated wastewater which was contaminated with dibutyl phthalate (DBP), benzyl butyl phthalate (BBP) and diethylhexyl phthalate (DEHP). High performance liquid chromatography (HPLC) has also been used in conjunction with HFSLM for separation processes. Fontàs et al. [55] simultaneously separated mercury via HFSLM by using N-benzoyl-N', N'-diheptadecyl thiourea as extractant and thiourea as stripping agent.

In this work, the removal of ionic mercury or Hg (II) from petroleum-produced water via HFSLM was studied. The removal threshold was targeted to be less than 5 ppb which is the permissible discharge limit of industrial wastewater imposed by the government regulator in the Kingdom of Thailand [1, 25]. The extractant used was Aliquat 336 (a quaternary ammonium salt) while the stripping solution used was an aqueous solution with Thiourea (an organosulfur compound). Fábrega et al. [33] successfully used Aliquat 336 and thiourea to separate mercury (II) by liquid–liquid extraction. Previous successful researches on the separation of mercury (II) are shown in Table 3.1.

The experiment was set up with a single-pass feed and circulating stripping solution through HFSLM. This setup offers continuous treatment of the produced water effluent. The stripping solution, which is circulating in limited volume, offers a manageable volume for waste disposal after the solution becomes saturated [56].

Along with the experiments, a mathematical model was developed and presented. The model followed the schema taking combined fluxes i.e. convection–diffusion–kinetic into account. This is a significant feature posed by the proposed model in order to provide a more realistic unsteady time dependent. A summary of previous works on the mathematical models for HFSLM is as follows in Table 3.2.

Table 3.1 Summary of previous research on mercury (II)

Authors	Types of feeds	Metals	Extractants	Diluents	Stripping	Methods
Minhas et al. [2]	Synthetic water	Hg(II)	Calix-6-arene hexaester	Dichloro Methane	DI-water	BLM
Sangtumrong et al. [19]	Synthetic water	Hg(II)	TOA	Toluene	NaOH	HFSLM
Fontàs et al. [55]	Synthetic water, sea water	Hg(II)	N-benzoyl, N, N-diheptadecyl thiourea	Cumene	Thiourea	HFSLM
Fàbrega et al. [33][39]	Synthetic water	Hg(II)	Aliquat 336	Kerosene	Thiourea	L-L
Quanmin et al. [57]	Synthetic water	Hg(II)	TOA+span 80	Toluene	NaOH	ELM
Jabbari et al. [58]	Synthetic water	Hg(II)	DC18C6	Chloro - form	DI-water	ELM
Meera et al. [59]	Synthetic water	Hg(II)	Cyanex 923	Xylene	Thiourea	L-L
Huebra et al. [60]	Wastewater	Hg(II)	LIX 34	Toluene	N/A	L-L
Francis et al. [61]	Industrial wastewater	Hg(II)	Cyanex 471X	Xylene	Na ₂ S ₂ O ₃	L-L
Chakrabarty et al. [62]	Synthetic water	Hg(II)	TOA	Dichloro-ethane	NaOH	FSLM
This work	Petroleum produced water	Hg(II)	Aliquat 336	Toluene	Thiourea	HFSLM

Abbreviations: BLM: Bulk Liquid Membrane, ELM: Emulsion Liquid Membrane, HFSLM: Hollow Fiber Supported Liquid Membrane

Table 3.2 Literature review of mathematical models for HFSLM

Authors	Metals	Extractants	Stripping	Considered parameters				Methods	Ref.
				(1)	(2)	(3)	(4)		
Pancharoen et al.	Cu(II)	LIX84	H ₂ SO ₄	✓	-	✓	✓	Laplace	[56]
Vernekar et al.	Co(II)	D2EHPA	H ₂ SO ₄	✓	✓	-	-	Successive substitution	[63]
Kandwal et al.	Cs(I)	CNC	Di-water	✓	✓	-	-	Integral	[64]
Yang et al.	Cu(II)	LIX54	H ₂ SO ₄	✓	-	✓	-	Empirical correlation	[65]
Suren et al.	Hg(II)	Aliquat 336	Thiourea	✓	-	✓	✓	Generating	[66]
Chaturabul et al.	Pd(II)	TRHCL-OA	NaNO ₂	✓	-	✓	✓	Laplace	[37]
This work	Hg(II)	Aliquat 336	Thiourea	✓	✓	✓	✓	Numerical	This work

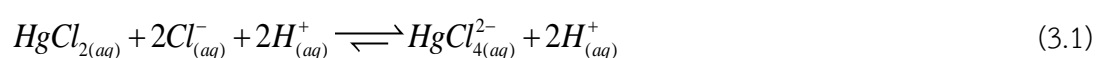
Abbreviations: (1) convection transport (2) diffusion transport (3) reaction (4) mass accumulation

3.3 Background and Theory

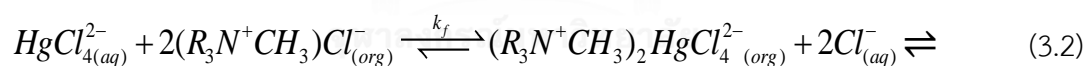
3.3.1 Reaction mechanisms

Research has proved that an extractant plays an important role in separation processes. Trioctyl methyl ammonium chloride (Aliquat 336) extractant, for example, can extract mercury (II). The reactions involved are as follows in Eq. (3.1) and (3.2).

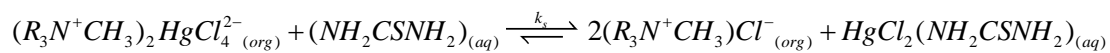
In Eq. (3.1) mercury chloride compound in produced water is deprotonated to ($HgCl_2$) in the presence of excess chloride ions:



Then, $HgCl_2$ exchanges Cl^- with Aliquat 336 and generates mercury complex as in Eq. (3.2). Aliquat 336 has been used extensively for the extraction of metal chloride complexes [67-69].



Once the complex has formed, it will selectively diffuse to the opposite side of the liquid membrane and react with thiourea for decomposition, as shown in Eq. (3.3):



(3.3)

where *(aq)* represents the species in the aqueous phase and *(org)* represents the species in the liquid membrane phase. The complex-forming reactions with the feasible structure of complexes are illustrated in Fig.3.1.

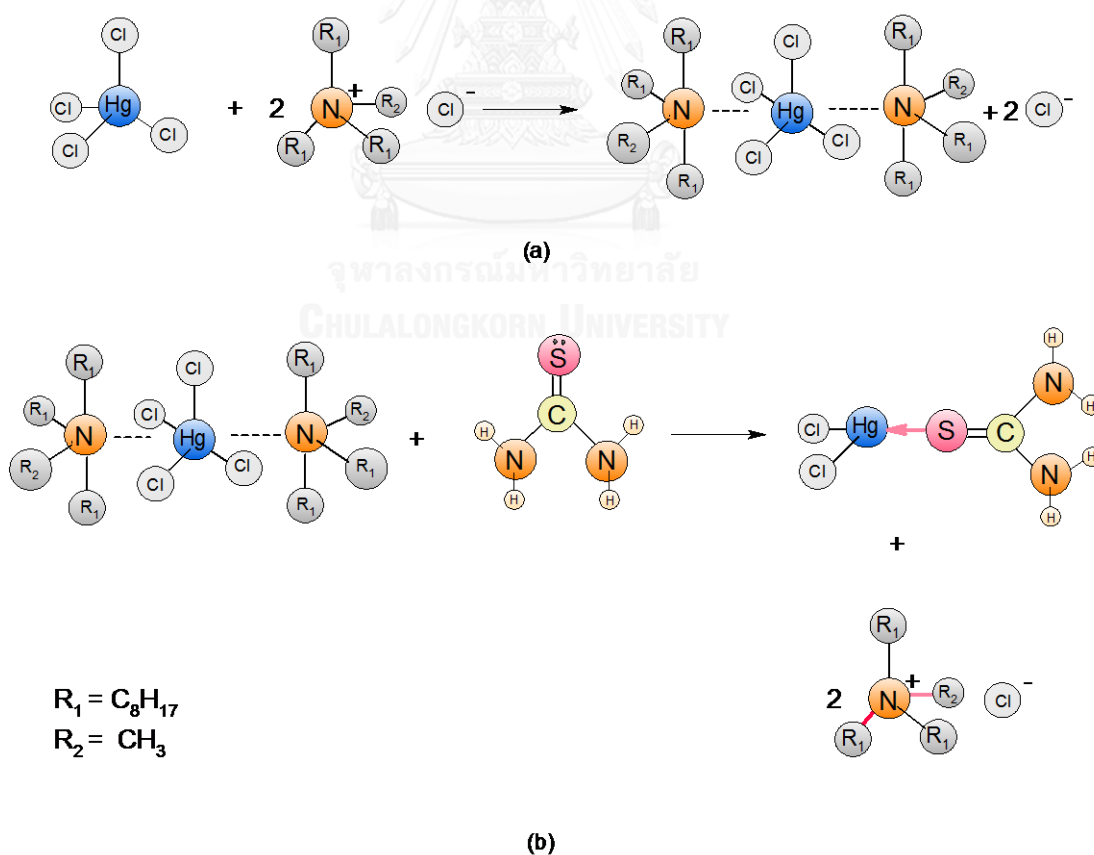


Figure 3.1 Schematic representation of the complex-forming reactions with the feasible structure of complexes (a) mercury (II) with Aliquat336 forms the complex species and (b) metal–extractant complex with thiourea.

In Eq. (3.4), and as shown below in Fig. 3.2, extraction reaction is summarized for target metal ions (A) which react with the extractant solution (B) to produce metal ions complex (C):



In Eq. (3.5), the overall rate of reaction with respect to target metal concentration (C_f) is given. Thereby, the simplified rate equation with respect to A -component concentration (C_f) is:

$$r_f(x,t) = k_f C_f^n(x,t) \quad (3.5)$$

where the term k_f is the extraction rate constant that occurs in the HFSLM tube, t is the extraction time, C_f is the concentration of metal ions in the feed solution (mg/L),

n is the reaction order of extraction and x is any distance along the axis of the hollow fiber in the feed phase.

In Eq. (3.6), the recovery reaction is a basic reverse of the extraction reaction in which the stripping solution agent (D) reacts with (C) to generate a new mercury compound (E) in the stripping solution; again as shown below in Fig. 3.2.



Similarly, in Eq. (3.7), with the model for extraction reaction, the rate of recovery reaction is simplified with respect to E-component concentration (C_s):

$$r_s(\bar{x}, t) = k_s C_s^m(\bar{x}, t) \quad (3.7)$$

where k_s is the reaction rate constant of stripping, t is the stripping time, C_s is the concentration of metal ions in the stripping solution (mg/L), m is the reaction order of stripping and \bar{x} is any distance along the axis of the hollow fiber in the stripping phase and equal to $L - x$.

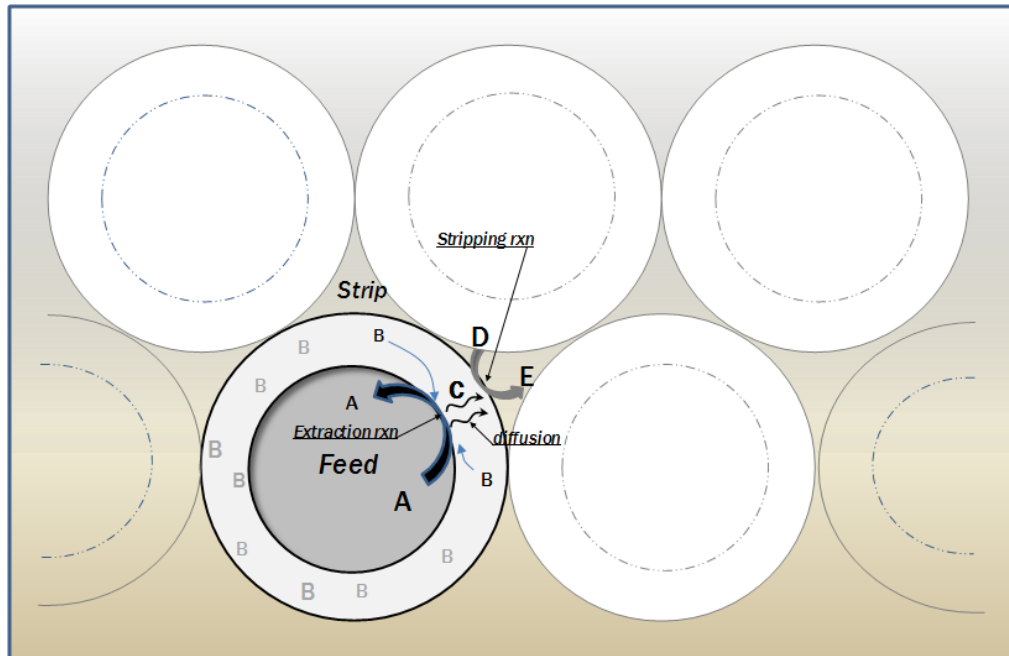


Figure 3.2 Schematic transport flux within HFSLM (cross section view)

3.3.2 Transport in feed phase (extraction)

The transport of target ions across HFSLM corresponds to the combined flux principle i.e. convection–diffusion–kinetic and accumulation. The transport schema for the flow in the HFSLM tube is given in Fig. 3.3. The creation of this model is based upon the following assumptions:

1. Operation is isothermal at constant pressure and volume.
2. The HFSLM tube is very small. Thus, the concentration distribution across the tube–cross–sectional area is uniform regardless of flow pattern.
3. Extraction reaction takes place at the contact between the liquid membrane and feed phase along the length of HFSLM. Hence, it exhibits a gradient in the axial direction according to the combined fluxes from the reaction and the flow convection.
4. The extraction reaction is irreversible. As a result, once the metal ion complex (C) forms, the metal ion complex will not decompose back to original metal ions (A).

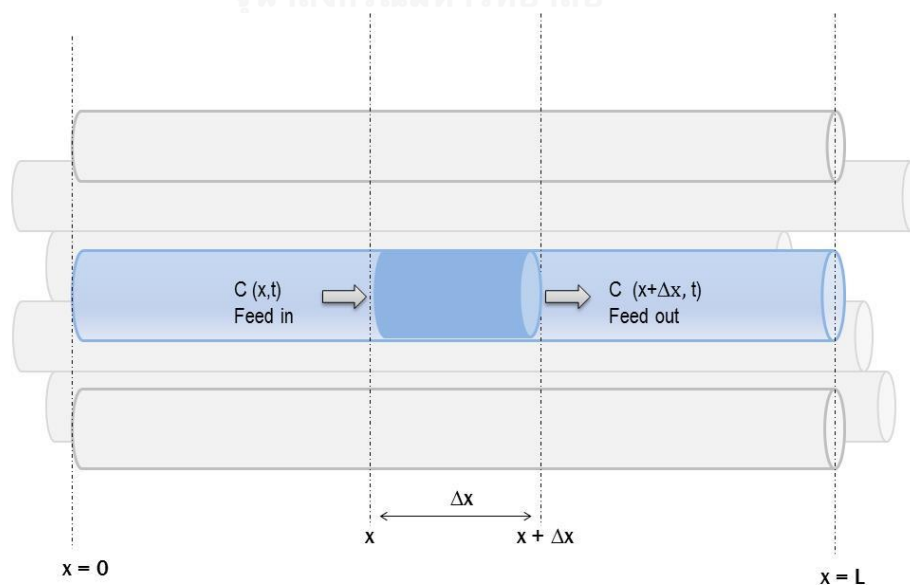


Figure 3.3 Schematic flow in the HFSLM tube (feed phase)

Conservation of mass with respect to extraction reaction operation in HFSLM provides the general mass balance as follows:

$$\left[\begin{array}{l} \text{Rate of mass} \\ \text{accumulation} \\ \text{in the system} \end{array} \right] = \left[\begin{array}{l} \text{Rate of mass} \\ \text{transport according} \\ \text{to convection flux} \end{array} \right] + \left[\begin{array}{l} \text{Rate of mass} \\ \text{transport according} \\ \text{to diffusion flux} \end{array} \right] + \left[\begin{array}{l} \text{Rate of mass} \\ \text{transport according} \\ \text{to reaction flux} \end{array} \right]$$

$$\begin{aligned} A_f \cdot \Delta x \frac{d\langle C_f \rangle}{dt} = & \left\{ q_f C_f(x, t) - q_f C_f(x + \Delta x, t) \right\}_{convection} \\ & + \left\{ (-A_f J_{Df}(x, t)) - (-A_f J_{Df}(x + \Delta x, t)) \right\}_{diffusion} \\ & + \left\{ \varepsilon \cdot A_p \cdot \Delta x \cdot k_f \langle C_f \rangle^n \right\}_{reaction} \end{aligned}$$

(3.8)

where:

ε is the porosity of the hollow fiber (%)

A_f is the total cross sectional area of hollow fiber ($35000 \cdot \pi r_i^2$)

A_p is the total cross sectional area of hollow-fiber ring ($35000 \cdot \pi(r_o^2 - r_i^2)$)

$\langle C_f \rangle$ is average concentration over the interested segment (Δx).

$C_f(x, t)$ is a concentration at the point (x) and time (t) of interest.

$J_f(x, t)$ is a diffusion flux in the feed phase.

Eq. (3.8) can be redefined by relocating term $A_f \cdot \Delta x$ to the right side of the equation and converting it to a discrete equation format:

$$\begin{aligned} \frac{d\langle C_f \rangle}{dt} = & -\frac{q_f}{A_f} \left\{ \frac{C_f(x + \Delta x, t) - C_f(x, t)}{\Delta x} \right\}_{convection} \\ & + \left\{ \frac{J_{Df}(x + \Delta x, t) - J_{Df}(x, t)}{\Delta x} \right\}_{diffusion} \\ & + \left\{ \varepsilon \cdot \frac{A_p}{A_f} k_f \langle C_f \rangle^n \right\}_{reaction} \end{aligned}$$

(3.9)

when $\Delta x \rightarrow 0$, Eq. (3.9) above can be simplified to an unsteady state equation:

$$\frac{\partial C_f(x,t)}{\partial t} = -\frac{q_f}{A_f} \frac{\partial C_f(x,t)}{\partial x} + \frac{\partial J_{Df}(x,t)}{\partial x} + \varepsilon \cdot \frac{A_p}{A_f} k_f C_f^n(x,t) \quad (3.10)$$

Substituting the diffusion flux term J_{Df} to the concentration parameter by the use

of Fick's first law where $J_{Df}(x,t) = \mathcal{D}_f \frac{\partial C_f(x,t)}{\partial x}$ and \mathcal{D}_f is the diffusion coefficient

of mercury (II) in feed phase, the following equation is obtained:

$$\frac{\partial C_f(x,t)}{\partial t} = -\frac{q_f}{A_f} \frac{\partial C_f(x,t)}{\partial x} + \mathcal{D}_f \frac{\partial^2 C_f(x,t)}{\partial x^2} + \varepsilon \cdot \frac{A_p}{A_f} k_f C_f^n(x,t) \quad (3.11)$$

Solving Eq. (3.11) by the concept of the finite difference using an explicit integral method, the equation for estimating the concentration of metal ions in the outlet feed solution is obtained as shown below:

$$\begin{aligned}
C_f(x, t + \Delta t) = & C_f(x, t) + \mathcal{D}_f \cdot \Delta t \left(\frac{C_f(x + \Delta x, t) - 2C_f(x, t) + C_f(x - \Delta x, t)}{(\Delta x)^2} \right) \\
& - \frac{q_f \cdot \Delta t}{A_f} \left(\frac{C_f(x, t) - C_f(x - \Delta x, t)}{\Delta x} \right) + \varepsilon \cdot \frac{A_p}{A_f} k_f \Delta t (C_f(x, t))^n
\end{aligned}
\tag{3.12}$$

Appendix A shows the above in more detail.

3.3.3 Transport across the liquid membrane phase

Following extraction reaction at the interface between the feed and the liquid membrane phase, the reaction product which is the complex ions between mercury (II) and the organic extractant, will selectively enter the liquid membrane phase. Then, in the stripping phase, it is transported freely to the opposite side at the boundary. Under a pseudo-steady-state, mass transfer rates in the liquid membrane will equal the concentration flux in the feed phase and in the stripping phase, as described by Eq. (3.13) [37].

$$J_m = J_f = J_s \tag{3.13}$$

Other assumptions that stipulate the model for transport within the liquid membrane phase are:

1. Target metal ions cannot enter micro-pore sites unless they are first converted to metal complexes.
2. The transport direction for the metal complex is in a radial direction from the feed to the stripping solution.
3. No reaction is involved in this model – only diffusion mass transport.
4. There is no interfacial layer between the aqueous and the membrane phase. By this, concentration input for the model can be read directly from the concentration of metal complex on the feed side (C_c) and on the stripping side (\bar{C}_c). Thus, the flux in the membrane phase can be expressed as in Eq.

(3.14):

$$J_m = k_m (C_c - \bar{C}_c) \quad (3.14)$$

5. The system is considered to be in a pseudo-steady state with other phases.

After the necessary assumptions are defined, fluxes in Eq. (3.13) can be broken down as follows:

J_m represents flux in the liquid membrane phase:

$$J_m = k_m \frac{a}{c} [C_f(x,t) - C_f(x + \Delta x, t)] - k_m \frac{c}{a} [C_s(\bar{x} + \Delta x, t) - C_s(\bar{x}, t)] \quad (3.15)$$

Eq. (3.15) has been redefined from Eq. (3.14) to present the equation in term of known concentrations from the feed phase.

J_f represents flux in the feed phase:

$$J_f = \frac{q_f}{A_f} [C_f(x,t) - C_f(x + \Delta x, t)] \quad (3.16)$$

J_s represents flux in the stripping phase:

$$J_s = \frac{q_s}{A_s} [C_s(\bar{x} + \Delta x, t) - C_s(\bar{x}, t)] \quad (3.17)$$

The flux in the feed (J_f) and stripping phase (J_s) represented in Eq. (3.16) and (3.17) respectively are largely functions of the concentration gradient (along the considered segment Δx). Eqs. (3.14) – (3.17) can be used to determine the mass transfer coefficient in the liquid membrane phase (k_m).

3.3.4 Transport in the stripping phase (recovery)

According to the model mentioned previously as regards the feed phase, the same concept applies to the model of the stripping phase. The model still assumes operation with isothermal conditions under constant pressure and controlled temperature at the laboratory (28°C). The stripping phase forms a homogenous liquid. Specific assumptions are as follows:

- 1 Complete mixing occurs in the annulus section between the HFLSM shell and tube. Thus, there is no radial concentration distribution across the annulus area.

- 2 Recovery reaction takes place at the contact between the liquid membrane and the stripping phase along the length of HFSLM. Hence, it exhibits flux gradient in the axial direction.
- 3 The recovery reaction is irreversible. As a result, once the metal ion complex (C) decomposes to the original ions (A), only the metal ions will be transferred to the stripping phase.

In this recovery system, when the stripping solution enters HFSLM at the opposite end of the feed inlet, the axis reference is therefore a reversal of the feed (Fig. 3.4). The term $\bar{x} = L - x$ represents a correlation between any point of interest in the stripping flow system i.e. \bar{x} and in the feed flow system i.e. x .

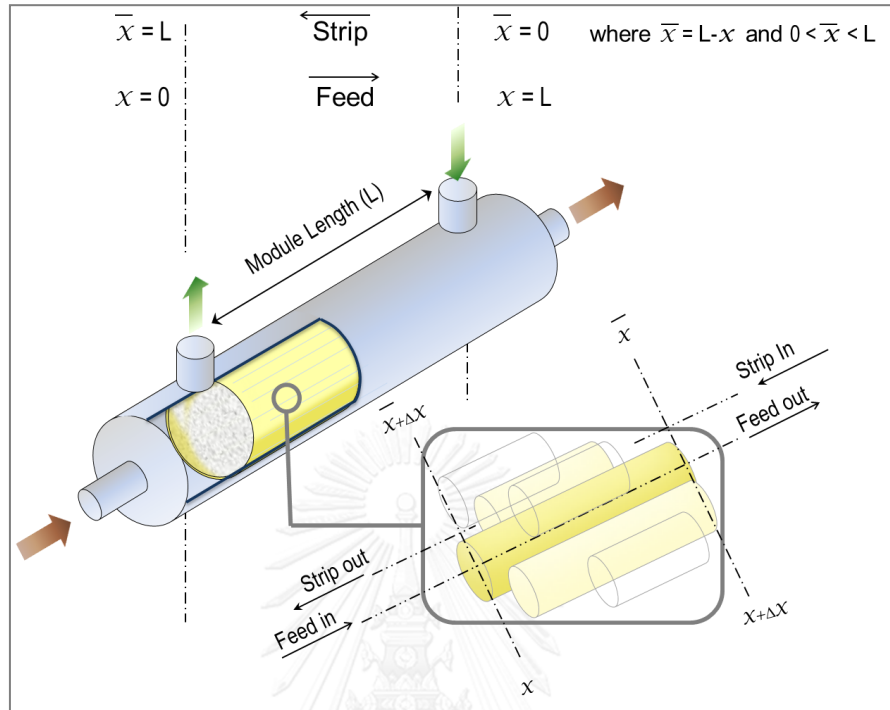


Figure 3.4 Axis reference for the model

Based on the conservation of mass, the equation for stripping phase is as follows:

$$\frac{\partial C_s(\bar{x}, t)}{\partial t} = -\frac{q_s}{A_s} \frac{\partial C_s(\bar{x}, t)}{\partial \bar{x}} + \mathcal{D}_s \frac{\partial^2 C_s(\bar{x}, t)}{\partial \bar{x}^2} + \varepsilon \cdot \frac{A_p}{A_s} k_s C_s^m(\bar{x}, t) \quad (3.18)$$

Solving Eq. (3.18) by the concept of finite difference using an explicit integral method, the concentration of metal ions in the outlet stripping solution can be estimated as shown below:

$$C_s(\bar{x}, t + \Delta t) = C_s(\bar{x}, t) + \mathcal{D}_s \cdot \Delta t \left(\frac{C_s(\bar{x} + \Delta x, t) - 2C_s(\bar{x}, t) + C_s(\bar{x} - \Delta x, t)}{(\Delta x)^2} \right) - \frac{q_s}{A_s} \cdot \Delta t \left(\frac{C_s(\bar{x}, t) - C_s(\bar{x} - \Delta x, t)}{\Delta x} \right) + \varepsilon \cdot \frac{A_p}{A_s} \cdot k_s \cdot \Delta t C_s(\bar{x}, t)^m \quad (3.19)$$

3.4 Experimental

3.4.1 The reagents and the feed solution

The feed solution was petroleum-produced water provided by one of the oil and gas operators in the Gulf of Thailand. For feed pre-treatment, hydrochloric acid (HCl) from Qrec New Zealand was used without further purification. The extractant trioctyl methyl ammonium chloride (94% Aliquat 336) was obtained from Sigma-Aldrich Germany and was dissolved in toluene from Qrec New Zealand. Thiourea, of

analytical grade from RFLC New Zealand, was used as stripping solution. The composition of the petroleum-produced water is given in Table 3.3.

Table 3.3 Composition of petroleum produced water

Metal ions	Concentration (ppm)
As	0.2
Ca	16
Fe	0.17
Hg	0.5
Mg	2
Na	1820

3.4.2 Apparatus

The HFSLM module was a Liqui-Cel®Extra-Flow Laboratory, supplied by CELGARD LLC (Charlotte, NC; formerly Hoechst Celanese). The hollow fibers were made from micro-porous polypropylene woven into fabric and wrapped around a central-tube feeder to supply the shell side fluid. The concentration of mercury (II) in the aqueous phases was determined by an inductively coupled plasma optical emission spectrometer (ICP-OES) by JY 2000, JY JOBIN YVON (HORIBA). The identity of Aliquat 336 (R_3NCH_3Cl) and Aliquat 336 – Hg(II) complex ($HgCl_4^{2-} 2(R_3N^+CH_3)Cl^-$)

was determined by Fourier transform infrared spectroscopy (FT-IR) from Perkin Elmer.

The properties of the hollow fiber module used are presented in Table 3.4.

Table 3.4 Properties of the hollow fiber module

Properties	Descriptions
Material	polypropylene
Inside diameter of hollow fiber	0.024 cm
Outside diameter of hollow fiber	0.03 cm
Effective length of hollow fiber	15 cm
Number of hollow fibers	35,000
Average pore size	3×10^{-6} cm
Porosity	25 %
Effective surface area	1.4×10^4 cm ²
Area per unit volume	29.3 cm ² /cm ³
Module diameter	6.3 cm
Module length	20.3 cm
Tortuosity factor	2.6
Operating temperature	273 – 333 K

3.4.3 Procedure

The extractant in the liquid membrane phase was prepared by dissolving Aliquat 336 in toluene. The extractant was then circulated throughout the HFSLM

system for at least 40 min. to ensure the hollow fibers were well impregnated. The stripping solution used was thiourea. The experimental setup was a single-pass feed with a circulating stripping solution. The feed and counter stripping flow circulated within their own reservoir. The flow rates for both feed and stripping solution were $100 \text{ cm}^3 \cdot \text{min}^{-1}$. Samples, each of 30 cm^3 , were taken from the feed and stripping outlet. A flow diagram is shown in Fig. 3.5.

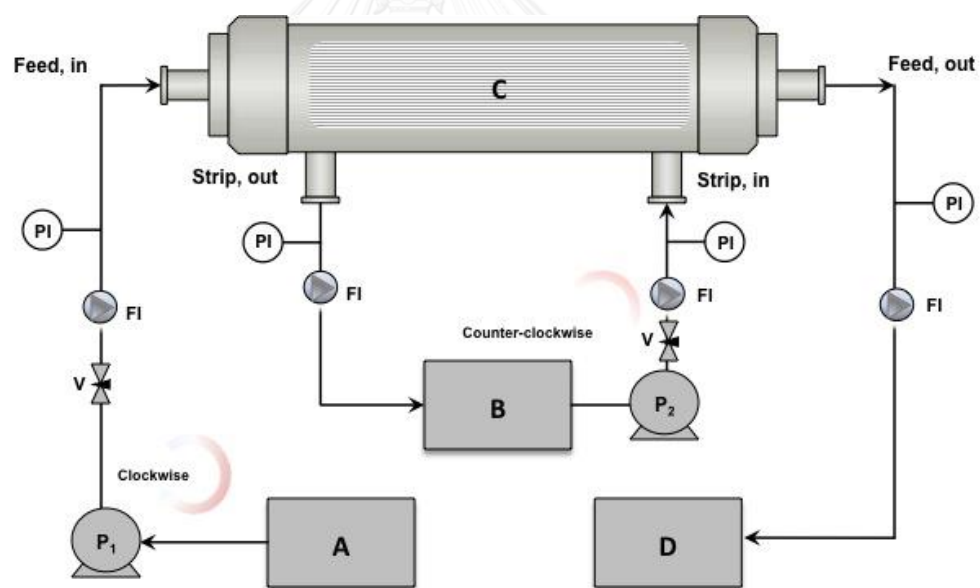


Figure 3.5 HFSLM in counter-current flow diagram of a single-pass of feed solution and circulating of stripping solution operation: A inlet feed reservoir, B stripping reservoir, C HFSLM, D outlet feed reservoir, V flow regulator valve, FI flow indicator and PI pressure indicator.

Key parameters describing performance can be denoted by the percentage of extraction and of recovery. In Eq. (3.20), the percentage of extraction indicates the extent mercury (II) was extracted from the produced water. In Eq. (3.21), by contrast, the percentage of recovery identifies how much metal was drawn into the stripping solution:

$$\% \text{Extraction} = \frac{C_f(0,0) - C_f(L,t)}{C_f(0,0)} \quad (3.20)$$

$$\% \text{Recovery} = \frac{C_s(L,t) - C_s(0,0)}{C_f(0,0)} \quad (3.21)$$

Subsequently, Eq. (3.22) describes HFSLM overall efficiency (*O.E.*):

$$\% \text{O.E.} = \frac{\text{Extraction} + \text{Recovery}}{2} \quad (3.22)$$

Further, the standard deviation can be calculated as follows:

$$\% S.D. = 100 \times \sqrt{\frac{\sum_{i=1}^n \left\{ \left(\frac{D_{Expt.}}{D_{Model}} \right) - 1 \right\}^2}{N - 1}} \quad (3.23)$$

where $D_{Expt.}$ is the experimental data, D_{Model} is the calculated value from the mathematical model and N is the number of experimental points.

3.5 Results and discussion

3.5.1 Effect of HCl concentration in feed solution

Fig. 3.6. shows the results of HCl concentration in the feed solution. The effect of HCl in the feed solution focused on a concentration range between 0.05 – 0.7 M. In the early stages, where HCl concentration ranged between 0.05 – 0.2 M, an increase of HCl concentration resulted in an increase in the extraction and recovery

of mercury (II). This was in accordance with Le Chatelier's Principle whereby increasing the concentration of the reactants drives the reaction forwards.

In later stages, mercury (II) extraction decreased when the concentration of HCl in feed solution was more than 0.2 M. This was simply because the system turned out to be highly acidic. The basic extractant Aliquat 336, in this case, was not in a suitable condition to extract mercury (II) [23].

From the above result, the optimum concentration of HCl in this system proved to be 0.2 M, which yielded the distinct percentage of mercury (II) extraction and recovery at 99.73% and 90.11% respectively. This constituted the highest overall efficiency, as calculated in Eq. (3.22), of 94.92 %.

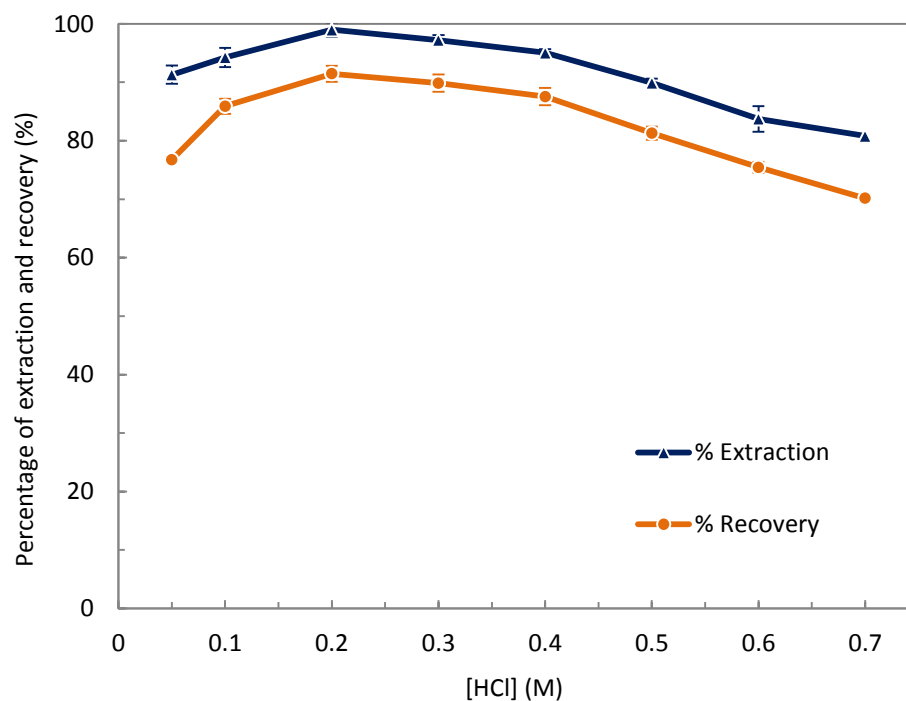


Figure 3.6 Effect of HCl concentrations on the extraction and recovery yield (extractant: 4% (v/v) Aliquat 336, stripping: 0.1M thiourea, flow rate: $100 \text{ cm}^3 \cdot \text{min}^{-1}$ in both feed and stripping solutions, operating time: 30 min. 28°C)

3.5.2 Effect of extractant concentration

For the extraction and recovery percentage of mercury (II), it was necessary to select a suitable extractant concentration. Aliquat 336 was investigated with respect to a concentration range between 0.5 – 5% (v/v). From Fig. 3.7, the results show that

when Aliquat 336 concentration increased in the range of 0.5 – 4 % (v/v), extraction and recovery percentage of mercury (II) was of a higher tendency. This was because Aliquat 336 as a reactant pushed the reaction further forwards generating more mercury complex ions in the liquid membrane. Therefore, the extraction rate was higher. Likewise, when more mercury complex ions formed in the liquid membrane, more mercury (II) could be recovered at the stripping phase.

In contrast, the percentage of extraction and recovery declined when concentration was more than 4% (v/v). This decline was due to the viscosity effect from higher extractant concentration [23]. This hindered effective diffusion of the metal complex through the liquid membrane phase resulting in the drop in performance.

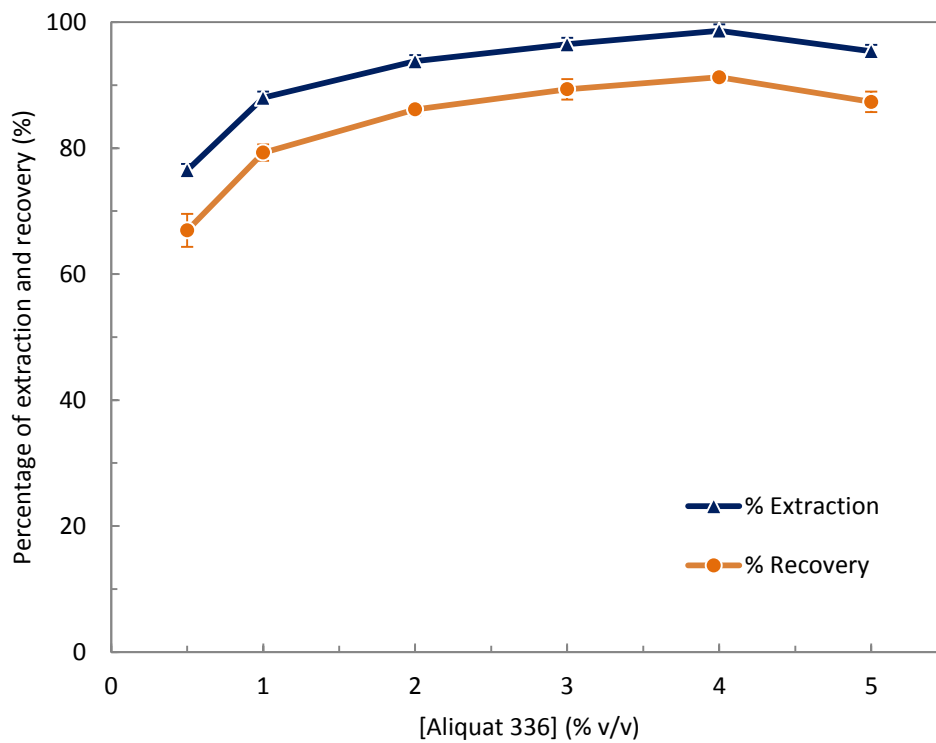


Figure 3.7 Effect of Aliquat 336 concentrations on the extraction and recovery yield

(pretreatment: 0.2M HCl, stripping: 0.1M thiourea, flow rate: $100 \text{ cm}^3 \cdot \text{min}^{-1}$ in both feed and stripping solutions, operating time: 30 min. 28°C)

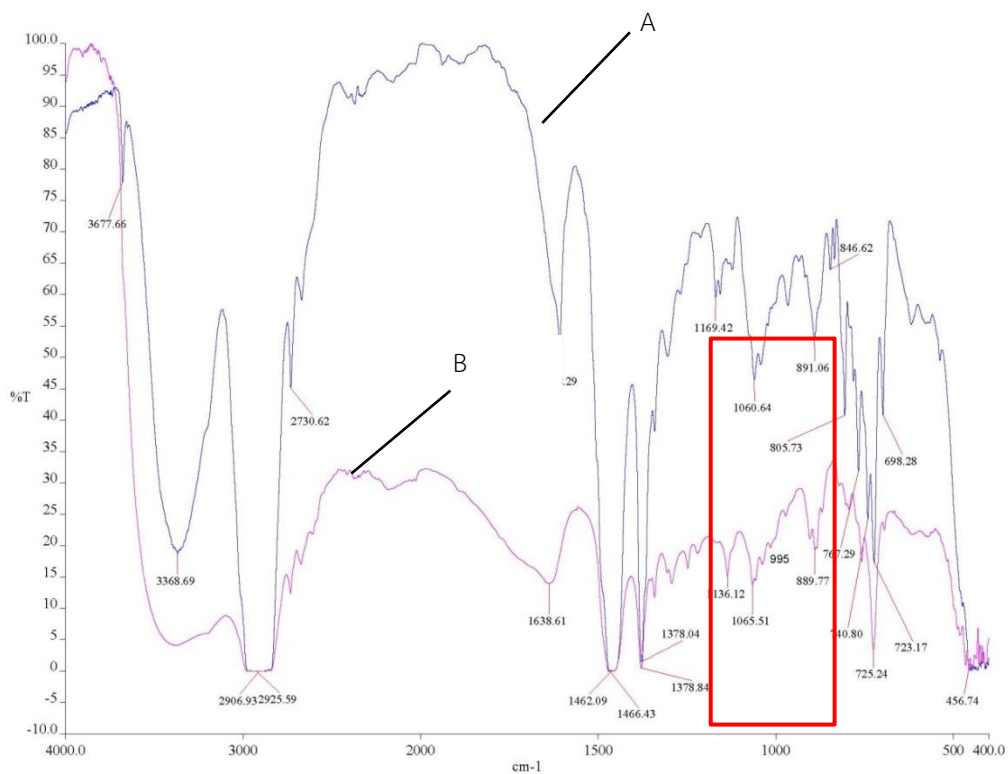


Figure 3.8 FT-IR spectrum of native Aliquat 336 (A) and loaded Aliquat 336 (B)

CHULALONGKORN UNIVERSITY

FT-IR was run to characterize Hg (II) complex post extraction. The result is present in Fig.3.8 from which new absorption bands at 1136 and 995 cm⁻¹ were observed. It indicates the location where the mercury complex formed after the (CH₃)N⁺ function group in Aliquat 336 captured the Hg (II) in stretching pattern [70].

3.5.3 Effect of stripping concentration

Thiourea was selected since it had been reported as having outstanding performance for use as a stripping solution for mercury (II) recovery [33]. Thiourea with large anions in the structure was strong enough to strip mercury complex ions from Aliquat 336, which was composed of a large organic cation associated with chloride ions [71, 72]. Using thiourea, no trace of precipitates was observed unlike NaOH which produced precipitates with mercury (II) resulting in membrane fouling and poor transport performance in the membrane phase [72]. Thiourea concentration varied between 0.05 – 0.5 M. In Fig. 3.9. results show that the percentage of mercury ions recovery increased until thiourea concentration reached 0.1 M. Subsequently, the percentage of recovery decreased due to concentration polarization [52]. Thus, in this case, Thiourea concentration of 0.1 M yielded the best recovery.

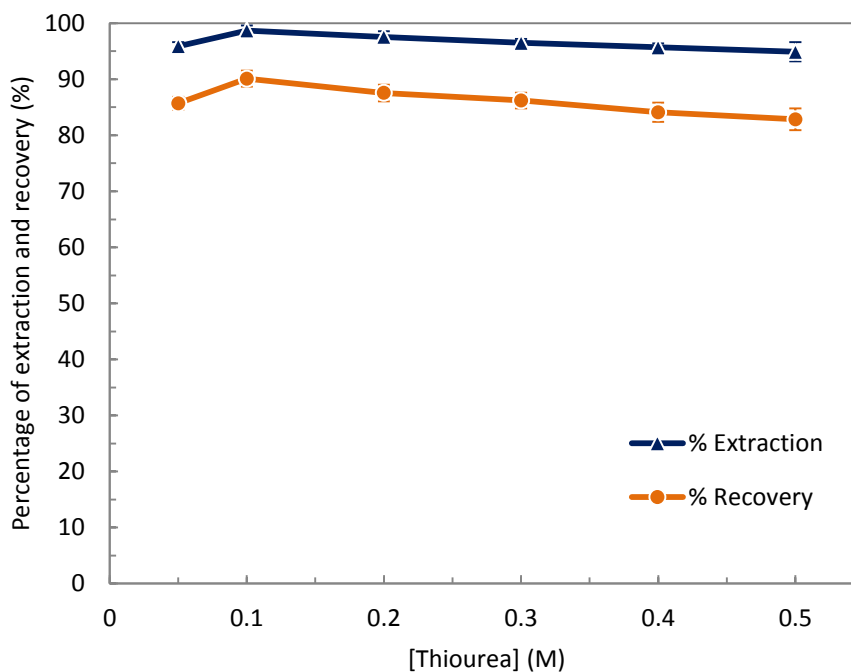
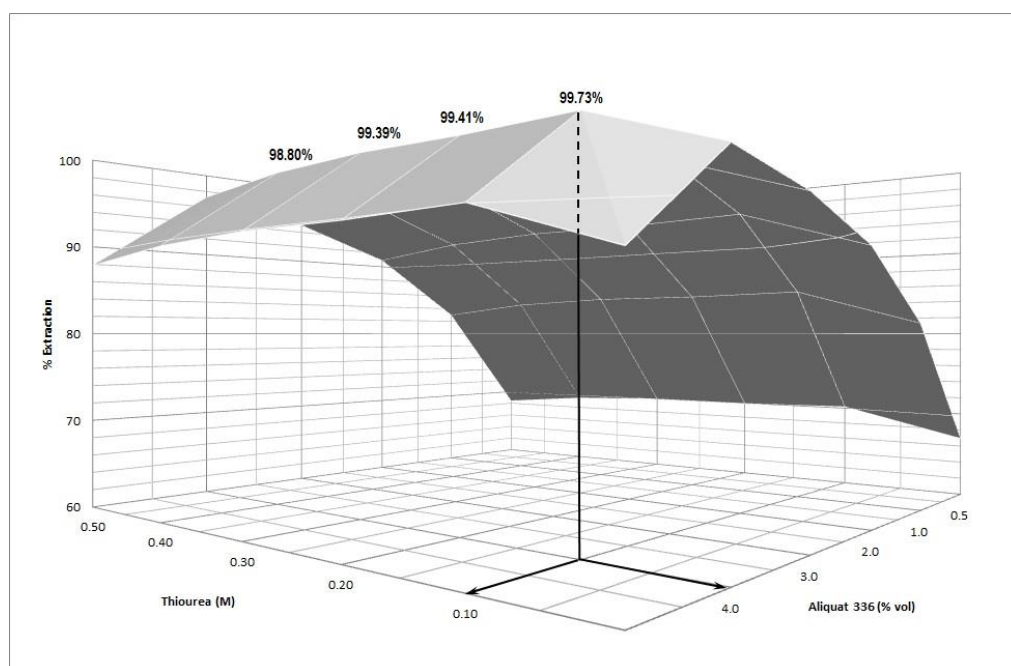


Figure 3.9 Effect of thiourea concentrations on the extraction and recovery yield (pretreatment: 0.2 M HCl, extractant: 4% (v/v) Aliquat 336, flow rate: $100 \text{ cm}^3 \cdot \text{min}^{-1}$ in both feed and stripping solutions, operating time: 30 min. 28°C)

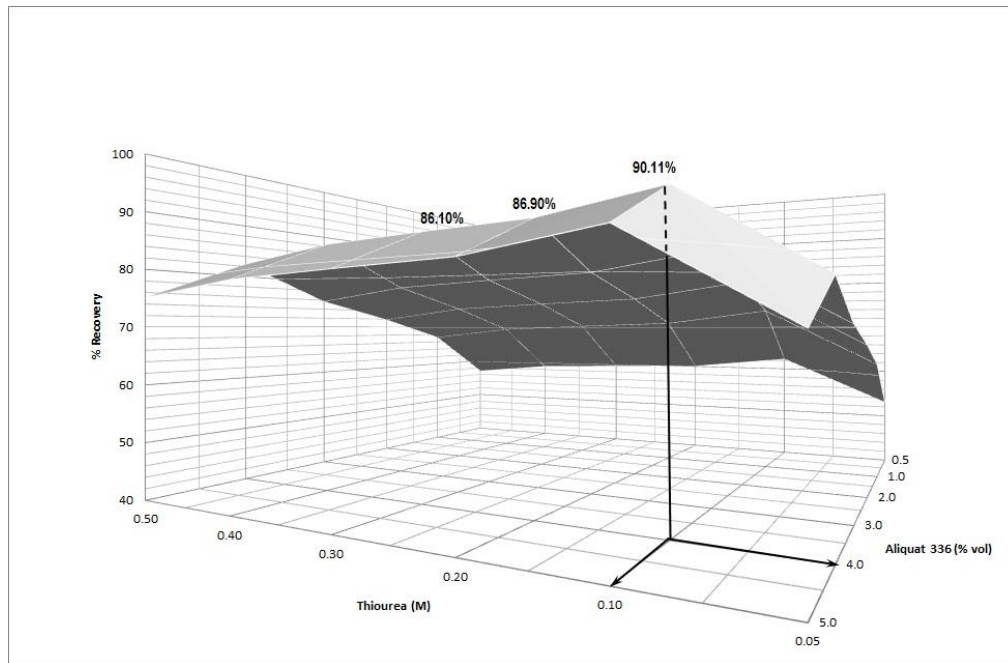
The investigation was expanded by generating a dimensional surface plot from the concentration effect data. The concentrations investigated were still Aliquat 336 in a range of 0.5 – 4 % (v/v) and thiourea in a range of 0.05 – 0.5 M. The plot in Fig.3.10 was set up to investigate the optimum concentration coordinate for this study. As demonstrated, the optimum concentration proved to be at 4% (v/v) Aliquat 336 and 0.1 M thiourea. This was the point which yielded the highest

percentage of extraction and recovery and was consistent with previous conclusions and illustrations in Fig. 3.7 and Fig. 3.9.



CHULALONGKORN UNIVERSITY

(a)



(b)

Figure 3.10 (a) concentration effects on extraction yield (b) concentration effects on recovery yield: (pretreatment: 0.2 M HCl, flow rate: $100 \text{ cm}^3 \cdot \text{min}^{-1}$ in both feed and stripping solutions, operating time: 30 min. 28°C)

3.5.4 Effect of flow rate of both feed and stripping solutions

The flow rate of both feed and stripping solution via HFSLM was undertaken. Flow rate influence is regarded as one of the most important parameters on the performance of mercury (II) extraction and recovery. The flow rates of both feed and

stripping solution varied from $75 - 300 \text{ cm}^3 \cdot \text{min}^{-1}$. The results are shown in Fig. 3.11. Apparently, the highest flow rate furnished less retention time for the reactants to work effectively inside the hollow fiber module. At a higher flow rate, performance declined. Consequently, the optimum flow rate was found to be at $100 \text{ cm}^3 \cdot \text{min}^{-1}$. Thus, the best percentage of extraction and recovery of mercury (II) was obtained at 99.73% and 90.11%, respectively.

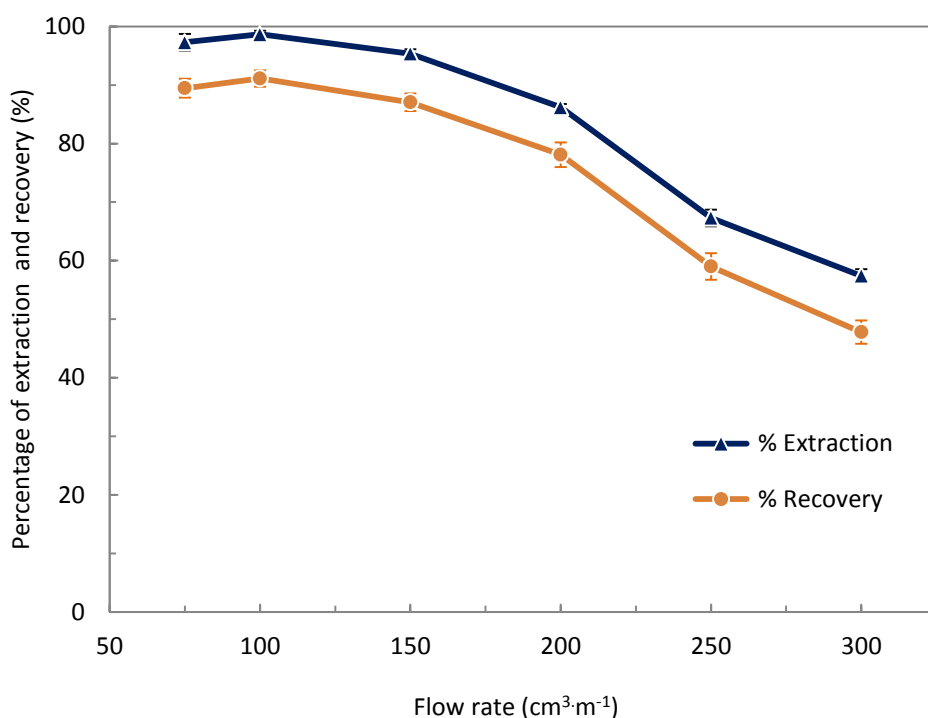
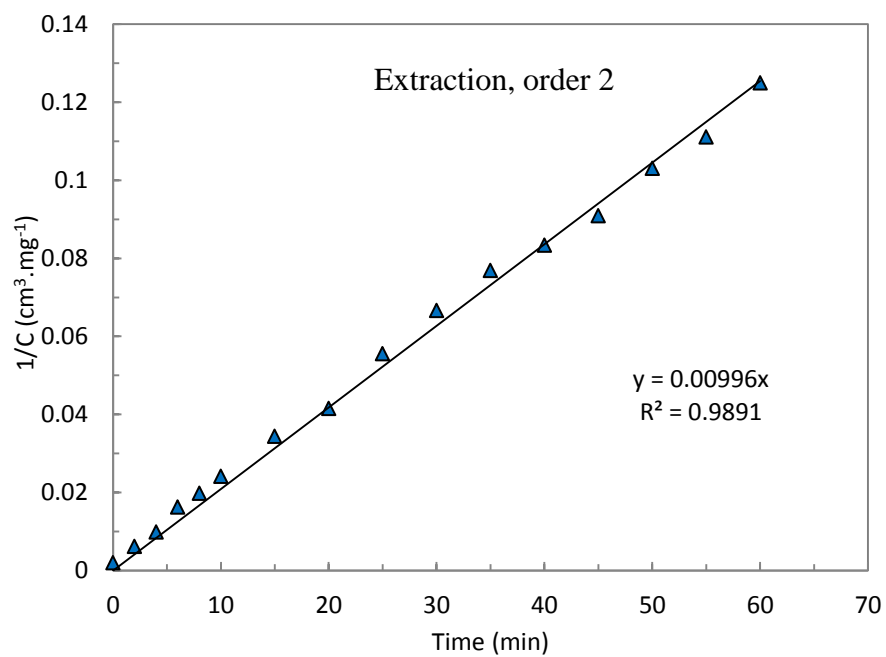


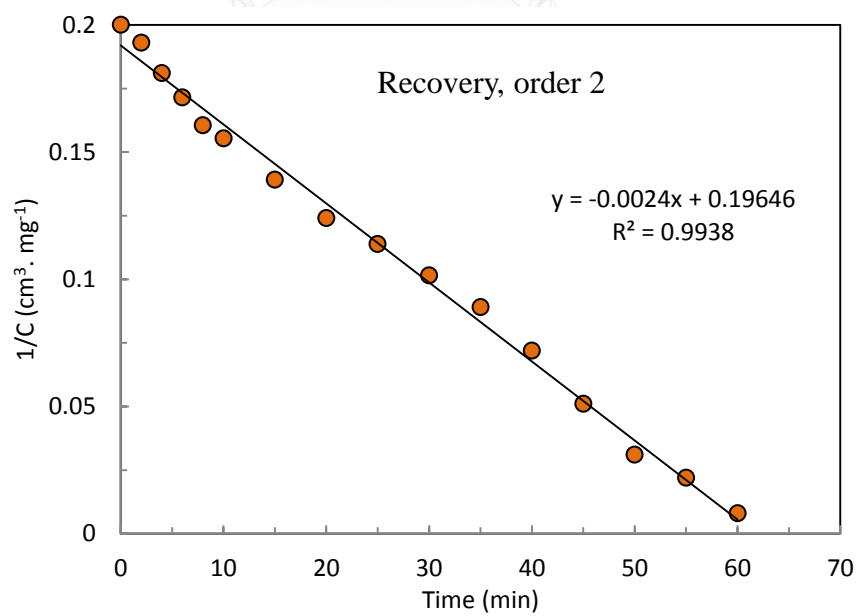
Figure 3.11 Effect of flow rate on the extraction and recovery yield (pretreatment: 0.2 M HCl, extractant: 4% (v/v) Aliquat 336, stripping: 0.1 M thiourea, operating time: 30 min. 28°C)

3.5.5 Parameters used in the model (Constants of rate reaction)

The rate constant for mercury (II) extraction and recovery was determined and presented in Table 3.5. Best-fit result proved to be the integrated second-order rate as shown in Fig. 3.12. This system appears to obey a pseudo-second-order rate equation in which both extraction and stripping depends on the concentration of only one reactant. The rate constants of extraction reaction (k_f) and the stripping reaction (k_s) were 9.96×10^{-3} and $2.39 \times 10^{-3} \text{ cm}^3 \cdot \text{mg}^{-1} \cdot \text{min}^{-1}$ from the slopes of the respective plots. For the membrane, the k_m term was applied in order to calculate the concentration profile following the transport of mercury (II) across the micro-pore sites of the membrane phase. From the equal flux relationship in Eq. (3.13), the mass transfer coefficient in the membrane phase (k_m) was calculated as $7.02 \text{ cm} \cdot \text{min}^{-1}$.



(a)



(b)

Figure 3.12 Integral concentrations of mercury (II) (a) extraction (b) recovery

Table 3.5 Analysis of reaction order and rate constants

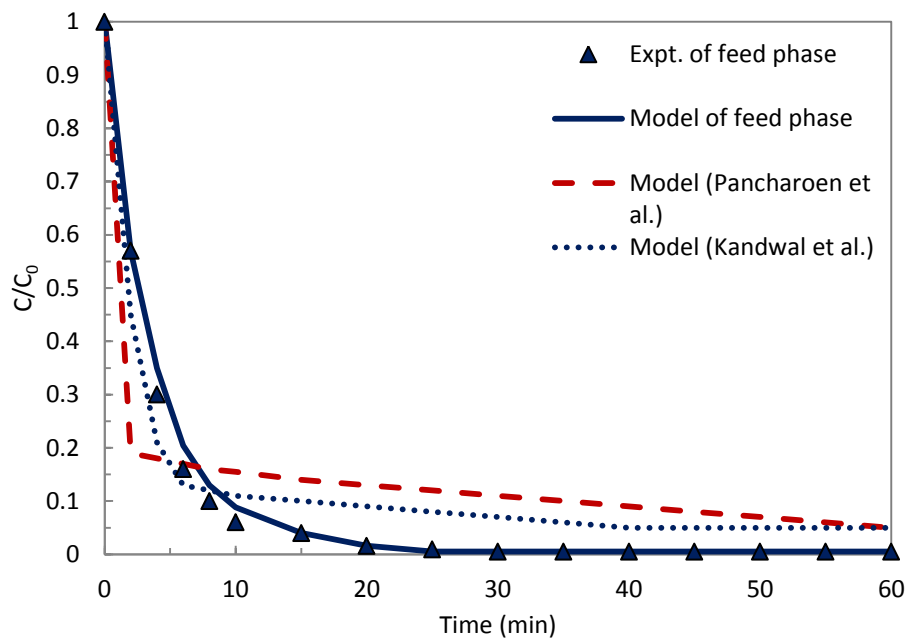
Rate Order	Determination			
	Relationship	Rate constant		R^2
Extraction				
0	C vs. Time	1.34×10^8	$\text{mg} \cdot \text{cm}^{-3} \cdot \text{min}^{-1}$	0.812
1	$\ln(C_0/C)$ vs. Time	1.75×10^{-1}	min^{-1}	0.795
2	$1/C$ vs. Time	9.96×10^{-3}	$\text{cm}^3 \cdot \text{mg}^{-1} \cdot \text{min}^{-1}$	0.989
Recovery				
0	C vs. Time	2.36×10^8	$\text{mg} \cdot \text{cm}^{-3} \cdot \text{min}^{-1}$	0.848
1	$\ln(C_0/C)$ vs. Time	1.45×10^{-1}	min^{-1}	0.788
2	$1/C$ vs. Time	2.39×10^{-3}	$\text{cm}^3 \cdot \text{mg}^{-1} \cdot \text{min}^{-1}$	0.993

** Best Fit

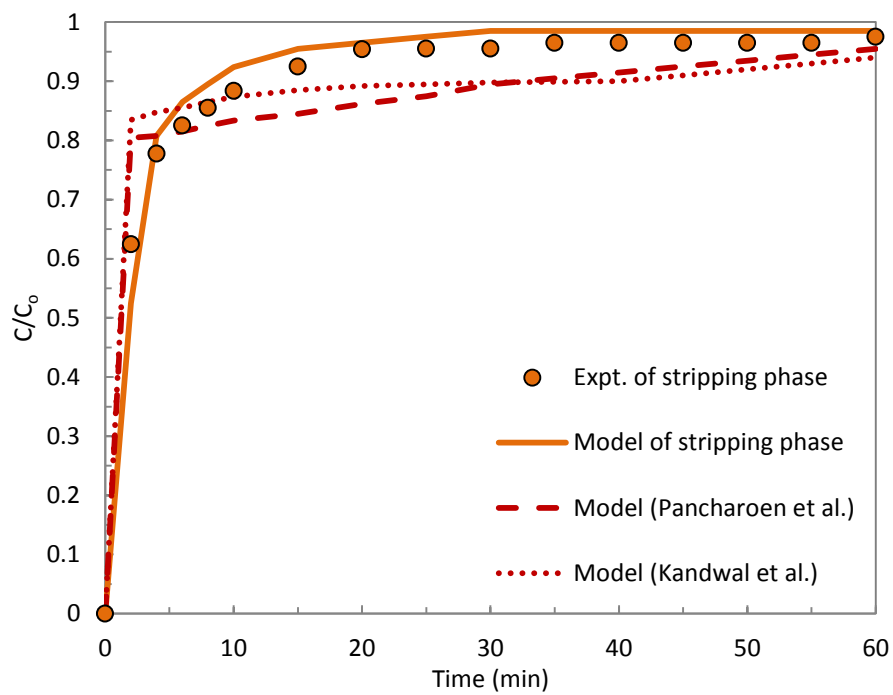
3.5.6 Computation and evaluation of the model

Fig. 3.13. presents a comparison between experimental results and model results regarding the concentration of mercury (II) in both feed and stripping solution; including the works of Pancharoen et al. [56] and Kandwal et al. [64]. Pancharoen et al. [56] developed a model based on chemical reaction and conventional flux (neglecting diffusion); average standard deviations for extraction and recovery were 8.5% and 9.1%, respectively. Kandwal et al. [64] developed their model based on

the principle of a facilitated diffusional transport mechanism (neglecting conventional and chemical reactions); average standard deviations for extraction and recovery were 9.8% and 8.4%, respectively. The model results from Pancharoen et al. and Kandwal et al. align with the experimental data to a great extent but still exhibit a high deviation. In contrast, the predicted results of this model, based on the combined convection–diffusion–kinetic flux in presence with mass accumulation term (non-steady), demonstrate very good agreement with the experimental results. For predictions in both feed and recovery solution, average percent deviations were low at 1.5% and 1.8%, respectively. This confirmed that the conservation of mass which consisted of convection, diffusion, reaction and accumulation were very important factors in controlling the rate of transport of mercury (II) along the hollow fibers. In conclusion, the set up by this study (a single-pass of feed solution and circulating of stripping solution) proved to be a viable solution for treating produced water with mercury (II) content less than 5 ppb.



(a)



(b)

Figure 3.13 The model computation results against experimental data for the case of (a) extraction and (b) recovery (pretreatment: 0.2 M HCl, extractant: 4% (v/v) Aliquat 336, stripping: 0.1 M thiourea, 28°C)

3.6 Conclusions

This work investigated the separation of mercury (II) from petroleum-produced water from Gulf of Thailand across a hollow fiber supported liquid membrane (HFSLM). The combined results showed that a hollow fiber supported liquid membrane impregnated with Aliquat 336 can treat mercury (II) contaminated petroleum-produced water quite satisfactorily. As the concentration in the aqueous phase changed sharply after a few minutes of separation, rapid reaction was observed. The highest percentages of extraction and recovery of mercury (II) were 99.73% and 90.11%, respectively, at the optimum condition as presented earlier. The produced water at post treatment had mercury (II) well below the discharge limit, per se 5 ppb.

A mathematical model was developed from the basis of a combined flux principle i.e. convection–diffusion–kinetic and accumulation of mercury (II). The prediction results proved to be in good agreement with the experimental results.

Average standard deviations for predicting the extraction and recovery were 1.5% and 1.8%, respectively. The results imply that the combination of convection, diffusion and reaction is crucial for accurate prediction in this unsteady state model. This robust model with its high accuracy provides a greater understanding of transport mechanism across the feed to the stripping solution; a design scale-up for industrial application could prove useful.

3.7 Nomenclature

A_f	Total cross sectional area of hollow fiber (cm^2)
A_p	Total cross sectional area of hollow-fiber ring (cm^2)
A_s	Total cross sectional area of stripping phase (cm^2)
A,B,C,D	Target metal ions (A), Extractant (B), Complex ions (C) and Stripping solution (D)
a, b, c, d	Stoichiometric coefficients
C_c	Metal complexes at the feed–membrane interface
$\overline{C_c}$	Metal complexes at the membrane–stripping interface
C_f	Concentration of target ions in the feed phase ($\text{mg}\cdot\text{cm}^{-3}$)
C_f^*	Concentration of complex ions next to the feed phase ($\text{mg}\cdot\text{cm}^{-3}$)

C_m	Concentration of complex ions in liquid membrane phase ($\text{mg}\cdot\text{cm}^{-3}$)
C_s	Concentration of target ions in stripping phase ($\text{mg}\cdot\text{cm}^{-3}$)
C_s^*	Concentration of complex ions next to the stripping phase ($\text{mg}\cdot\text{cm}^{-3}$)
D_f	The diffusion coefficient of mercury (II) in feed phase
$D_{\text{Expt.}}$	The experimental data
D_{Model}	The model data
d_o	External diameter of the hollow fiber tube (cm)
J	Flux ($\text{mg}\cdot\text{cm}^{-2}\cdot\text{min}^{-1}$)
J_f	Diffusion flux of mercury (II) in the feed phase ($\text{mg}\cdot\text{cm}^{-2}\cdot\text{min}^{-1}$)
J_m	Diffusion flux of complex species in the liquid membrane phase ($\text{mg}\cdot\text{cm}^{-2}\cdot\text{min}^{-1}$)
J_s	Diffusion flux of mercury (II) stripping solution in the stripping phase ($\text{mg}\cdot\text{cm}^{-2}\cdot\text{min}^{-1}$)
k_f	Rate constant of extraction reaction in the feed phase ($\text{cm}^3\cdot\text{mg}^{-1}\cdot\text{min}^{-1}$)
k_m	Mass transfer coefficient in the membrane phase ($\text{cm}\cdot\text{min}^{-1}$)
k_s	Rate constant of recovery reaction in the stripping phase ($\text{cm}^3\cdot\text{mg}^{-1}\cdot\text{min}^{-1}$)
L	Length of the hollow fiber (cm)

m	Order of recovery reaction
M_B	Molecular weight of liquid medium (g/mol)
N	Numbers of hollow fibers in the module
n	Order of extraction reaction
$O.E.$	Overall efficiency of HFSLM separation (%)
q_f	Volumetric flow rate of feed solution ($\text{cm}^3 \cdot \text{min}^{-1}$)
q_s	Volumetric flow rate of stripping solution ($\text{cm}^3 \cdot \text{min}^{-1}$)
R^2	R-square coefficient
r_i	Internal radius of the hollow fiber tube (cm)
r_o	External radius of the hollow fiber tube (cm)
r_f	Rate of extraction reaction in the feed phase ($\text{mg} \cdot \text{cm}^{-3} \cdot \text{min}^{-1}$)
r_s	Rate of recovery reaction in the stripping phase ($\text{mg} \cdot \text{cm}^{-3} \cdot \text{min}^{-1}$)
x	Longitudinal axis of the hollow fibers in the feed phase (cm)
\bar{x}	Longitudinal axis of the hollow fibers in the stripping phase (cm)
t	Time (min)
V_F, V_S	Volume of feed (and stripping) solution in the reservoir tank (cm^3)
V_f, V_s	Volume of feed (and stripping) solution in the HFSLM (cm^3)

Greek letters

ε Porosity of the hollow fiber (%)

μ Viscosity (cp)

Symbol

$\langle \rangle$ Average value of the concentration

Δ Small segment of longitudinal axis of the hollow fibers

Subscript

f Feed phase

s Stripping phase

จุฬาลงกรณ์มหาวิทยาลัย
CHULALONGKORN UNIVERSITY

3.8 Acknowledgments

The author would like to express sincere gratitude towards the Rachadapisek-Somphot Endowment Fund of Chulalongkorn University (RES560530215-EN) as well as Thailand Research Fund under the Royal Golden Jubilee Ph. D Program (Grant No.

PHD/0372/2552) and the Separation Laboratory, Department of Chemical Engineering, Faculty of Engineering, Chulalongkorn University who support this work

Appendix A. Mathematics for a transport model on separation of Mercury (II) via HFSLM

Based on Eq. (3.11) the conservation of mass for feed phase can be solved by using the finite difference with an explicit integral method:

$$\frac{\partial C_f(x,t)}{\partial t} = \frac{C_f(x,t+\Delta t) - C_f(x,t)}{\Delta t} \quad (\text{A.1})$$

$$\mathcal{D}_f \cdot \frac{\partial^2 C_f(x,t)}{\partial x^2} = \mathcal{D}_f \cdot \left(\frac{C_f(x+\Delta x,t) - 2C_f(x,t) + C_f(x-\Delta x,t)}{(\Delta x)^2} \right) \quad (\text{A.2})$$

$$\frac{q_f}{A_f} \frac{\partial C_f(x,t)}{\partial x} = \frac{q_f}{A_f} \left(\frac{C_f(x,t) - C_f(x-\Delta x,t)}{\Delta x} \right) \quad (\text{A.3})$$

Substituting Eq. (A.1) – (A.3) into Eq. (3.11) gives:

$$\begin{aligned} \frac{C_f(x, t + \Delta t) - C_f(x, t)}{\Delta t} = \mathcal{D}_f \cdot \left(\frac{C_f(x + \Delta x, t) - 2C_f(x, t) + C_f(x - \Delta x, t)}{(\Delta x)^2} \right) \\ - \frac{q_f}{A_f} \left(\frac{C_f(x, t) - C_f(x - \Delta x, t)}{\Delta x} \right) + \varepsilon \cdot \frac{A_p}{A_f} k_f (C_f(x, t))^n \end{aligned} \quad (\text{A.4})$$

Rearranging Eq. (A.4) as in Eq. (A.5) provides an answer to the concentration profile of mercury (II) in the outlet feed solution. This is a solution to a time-dependent convection–diffusion–reaction system in this modeling study:

$$\begin{aligned} C_f(x, t + \Delta t) = C_f(x, t) + \mathcal{D}_f \cdot \Delta t \left(\frac{C_f(x + \Delta x, t) - 2C_f(x, t) + C_f(x - \Delta x, t)}{(\Delta x)^2} \right) \\ - \frac{q_f}{A_f} \cdot \Delta t \cdot \left(\frac{C_f(x, t) - C_f(x - \Delta x, t)}{\Delta x} \right) + \varepsilon \cdot \frac{A_p}{A_f} \cdot k_f \cdot \Delta t (C_f(x, t))^n \end{aligned} \quad (\text{A.5})$$

where

$$\text{Initial condition: } C_f(0, 0) = 0 \text{ initial feed concentration} \quad (\text{A.6})$$

$$C_f(x, 0) = 0 \quad (\text{A.7})$$

At time > 0 :

$$C_f(0, t + \Delta t) = \frac{q_f \Delta t}{V_F} (C_f(L, t) - C_f(0, t)) + C_f(0, t) \quad (\text{A.8})$$

Eq. (A.6) and Eq. (A.7) stands for HFSLM condition at the initial stage where the initial feed to HFSLM is the known feed solution concentration and nil mercury (II) inside the fiber tubes.

Eq. (A.8) is the feed concentration for HFSLM at any time. This varies according to the single-pass of feed solution and circulating of stripping solution whereby the HFSLM product stream returns to the feed reservoir tank and then back to the entrance of HFSLM by means of a pump at identical rate. The equation is derived from the concentration profile around the feed reservoir tank.

Based on Eq. (3.18) the conservation of mass for stripping phase can be solved by using the finite difference with an explicit integral method:

$$\frac{\partial C_s(\bar{x}, t)}{\partial t} = \frac{C_s(\bar{x}, t + \Delta t) - C_s(\bar{x}, t)}{\Delta t} \quad (\text{A.9})$$

$$\mathcal{D}_s \cdot \frac{\partial^2 C_s(\bar{x}, t)}{\partial x^2} = \mathcal{D}_s \cdot \left(\frac{C_s(\bar{x} + \Delta x, t) - 2C_s(\bar{x}, t) + C_s(\bar{x} - \Delta x, t)}{(\Delta x)^2} \right) \quad (\text{A.10})$$

$$\frac{q_s}{A_s} \frac{\partial C_s(\bar{x}, t)}{\partial x} = \frac{q_s}{A_s} \left(\frac{C_s(\bar{x}, t) - C_s(\bar{x} - \Delta x, t)}{\Delta x} \right) \quad (\text{A.11})$$

Substituting Eq. (A.9) – (A.11) into Eq. (3.18) gives:

$$\begin{aligned} \frac{C_s(\bar{x}, t + \Delta t) - C_s(\bar{x}, t)}{\Delta t} = & \mathcal{D}_s \cdot \left(\frac{C_s(\bar{x} + \Delta x, t) - 2C_s(\bar{x}, t) + C_s(\bar{x} - \Delta x, t)}{(\Delta x)^2} \right) \\ & - \frac{q_s}{A_s} \left(\frac{C_s(\bar{x}, t) - C_s(\bar{x} - \Delta x, t)}{\Delta x} \right) + \varepsilon \cdot \frac{A_p}{A_s} k_s (C_s(\bar{x}, t))^m \end{aligned} \quad (\text{A.12})$$

Rearranging Eq. (A.12) as in Eq. (A.13) provides an answer to the concentration profile of mercury (II) in the outlet stripping solution. This is a solution to a time-dependent convection–diffusion–reaction system in this modeling study:

$$\begin{aligned}
C_s(\bar{x}, t + \Delta t) = & C_s(\bar{x}, t) + \mathcal{D}_s \cdot \Delta t \left(\frac{C_s(\bar{x} + \Delta x, t) - 2C_s(\bar{x}, t) + C_s(\bar{x} - \Delta x, t)}{(\Delta x)^2} \right) \\
& - \frac{q_s}{A_s} \cdot \Delta t \cdot \left(\frac{C_s(\bar{x}, t) - C_s(\bar{x} - \Delta x, t)}{\Delta x} \right) + \varepsilon \cdot \frac{A_p}{A_s} \cdot k_s \cdot \Delta t (C_s(\bar{x}, t))^m
\end{aligned}
\tag{A.13}$$

The diffusion coefficient was estimated using Wilke–Chang correlation in Eq. (A.14). The correlation is considered applicable to this study system where the solution system is in dilution. It links diffusivity to solute metal ions and bulk solvent i.e. feed and stripping phase such as molar volume (v), molecular weight (M_B), liquid viscosity (μ) and association parameter (ϕ).

$$\mathcal{D}_{AB} = 4.44 \times 10^{-10} \frac{(\sqrt{\phi M_B})T}{\mu_B v_A^{0.6}}
\tag{A.14}$$

The above correlation equation demonstrates the diffusion coefficient of solute A in solvent B. It contains the term of solute molar volume which could be converted to a more common term by solute concentration. Accordingly, Eq. (A.15) and Eq. (A.16) were derived to represent a relevant correlation between the diffusion coefficient and metal ions concentration. It is assumed that water predominated

both feed and stripping solutions. Hence, the solvent properties in Eq. (A.14) used the water properties.

$$\mathcal{Q}_f = 1.228 \times 10^{-13} C_f^{0.6} \quad (\text{A.15})$$

$$\mathcal{Q}_s = 1.211 \times 10^{-13} C_s^{0.6} \quad (\text{A.16})$$

where

ϕ = Association parameter of solvent (equals 2.6 for water)

M_B = Molecular weight of liquid medium (equals 18 g/mol for water)

T = 28°C or 301 K (controlled experiment temperature)

μ_B = Solvent viscosity (0.894 centipoise at 28°C)

3.9 References

- [1] D.L. Gallup, J.B. Strong, Removal of Mercury and Arsenic from Produced Water, Chevron Corporation Chevron Corporation, 2007.
- [2] F.T. Minhas, S. Memon, M.I. Bhangar, Transport of Hg(II) through bulk liquid membrane containing calix[4]arene thioalkyl derivative as a carrier, Desalination 262 (2010) 215-220.
- [3] S.F. CH. Ngim, K.W. Boey, J. Keyaratnam, Chronic neurobehavioral effects of elemental mercury in dentists, Br. J. Ind. Med. 49 (1992) 782–790.
- [4] Y.X. Liang, R.K. Sun, Y. Sun, Z.Q. Chen, L.H. Li, Psychological Effects of Low Exposure to Mercury Vapor: Application of a Computer-Administered Neurobehavioral Evaluation System, Environmental Research 60 (1993) 320-327.
- [5] S. Gupta, M. Chakraborty, Z.V.P. Murthy, Optimization of process parameters for mercury extraction through pseudo-emulsion hollow fiber strip dispersion system, Sep. Purif. Technol. 114 (2013) 43-52.
- [6] S. Díez, Human health effects of methylmercury exposure, 2009, pp. 111-132.
- [7] S. Chiarle, M. Ratto, M. Rovatti, Mercury removal from water by ion exchange resins adsorption, Water Research 34 (2000) 2971-2978.

- [8] J.A. Ritter, J.P. Bibler, Removal of mercury from waste water: Large-scale performance of an ion exchange process, *Water Science and Technology* 25 (1992) 165-172.
- [9] W.R. Knocke, L.H. Hemphill, Mercury(II) sorption by waste rubber, *Water Research* 15 (1981) 275-282.
- [10] J.Y. Lu, W.H. Schroeder, Comparison of conventional filtration and a denuder-based methodology for sampling of particulate-phase mercury in ambient air, *Talanta* 49 (1999) 15-24.
- [11] Q. Wang, X. Chang, D. Li, Z. Hu, R. Li, Q. He, Adsorption of chromium(III), mercury(II) and lead(II) ions onto 4-aminoantipyrine immobilized bentonite, *J. Hazard. Mater.* 186 (2011) 1076-1081.
- [12] B.S. Inbaraj, J.S. Wang, J.F. Lu, F.Y. Siao, B.H. Chen, Adsorption of toxic mercury(II) by an extracellular biopolymer poly(γ -glutamic acid), *Bioresource Technology* 100 (2009) 200-207.
- [13] C. Jeon, H.P. Kwang, Adsorption and desorption characteristics of mercury(II) ions using aminated chitosan bead, *Water Research* 39 (2005) 3938-3944.
- [14] V.K. Gupta, P. Singh, N. Rahman, Adsorption behavior of Hg(II), Pb(II), and Cd(II) from aqueous solution on Duolite C-433: A synthetic resin, *J. Colloid Interface Sci.* 275 (2004) 398-402.

- [15] X. Chai, X. Chang, Z. Hu, Q. He, Z. Tu, Z. Li, Solid phase extraction of trace Hg(II) on silica gel modified with 2-(2-oxoethyl)hydrazine carbothioamide and determination by ICP-AES, *Talanta* 82 (2010) 1791-1796.
- [16] D.C. Nambiar, N.N. Patil, V.M. Shinde, Liquid-liquid extraction of mercury(II) with triphenylphosphine sulphide: Application to medicinal and environmental samples, *Fresenius J. Anal. Chem.* 360 (1998) 205-207.
- [17] S. Sangtumrong, P. Ramakul, C. Satayaprasert, U. Pancharoen, A.W. Lothongkum, Purely Separation of Mixture of Mercury and Arsenic via Hollow Fiber Supported Liquid Membrane, *J. Ind. Eng. Chem.* 13 (2007) 751-756.
- [18] K. Tang, C. Zhou, X. Jiang, Racemic ofloxacin separation by supported-liquid membrane extraction with two organic phases, *Sc. China Ser. B-Chem.* 46 (2003) 96-103.
- [19] M. Takht Ravanchi, T. Kaghazchi, A. Kargari, Application of membrane separation processes in petrochemical industry: a review, *Desalination* 235 (2009) 199-244.
- [20] A.W. Lothongkum, U. Pancharoen, T. Prapasawat, in: J. Markos (Ed.), *Mass transfer in Chemical Engineering Process*, Intech, 2011, pp. 177-204.
- [21] U. Pancharoen, W. Poonkum, A.W. Lothongkum, Treatment of arsenic ions from produced water through hollow fiber supported liquid membrane, *J. Alloys Comp.* 482 (2009) 328-334.

- [22] I.M. Coelho, M.M. Cardoso, R.M.C. Viegas, J.P.S.G. Crespo, Transport mechanisms and modelling in liquid membrane contactors, *Sep. Purif. Technol.* 19 (2000) 183-197.
- [23] S.A. Ansari, D.R. Prabhu, R.B. Gujar, A.S. Kanekar, B. Rajeswari, M.J. Kulkarni, M.S. Murali, Y. Babu, V. Natarajan, S. Rajeswari, A. Suresh, R. Manivannan, M.P. Antony, T.G. Srinivasan, V.K. Manchanda, Counter-current extraction of uranium and lanthanides from simulated high-level waste using N,N,N',N'-tetraoctyl diglycolamide, *Sep. Purif. Technol.* 66 (2009) 118-124.
- [24] S.A. Ansari, P.K. Mohapatra, V.K. Manchanda, Recovery of Actinides and Lanthanides from High-Level Waste Using Hollow-Fiber Supported Liquid Membrane with TODGA as the Carrier, *Ind. Eng. Chem. Res.* 48 (2009) 8605-8612.
- [25] S.C. Roy, J.V. Sonawane, N.S. Rathore, A.K. Pabby, P. Janardan, R.D. Changrani, P.K. Dey, S.R. Bharadwaj, Pseudo-Emulsion Based Hollow Fiber Strip Dispersion Technique (PEHFSD): Optimization, Modelling and Application of PEHFSD for Recovery of U(VI) from Process Effluent, *Sep. Sci. Technol.* 43 (2008) 3305-3332.
- [26] A.M. Donia, A.A. Atia, A.M. Heniesh, Efficient removal of Hg(II) using magnetic chelating resin derived from copolymerization of bistiourea/thiourea/ glutaraldehyde, *Sep. Purif. Technol.* 60 (2008) 46-53.

- [27] S.A. Ansari, P.K. Mohapatra, D.R. Raut, M. Kumar, B. Rajeswari, V.K. Manchanda, Performance of some extractants used for 'actinide partitioning' in a comparative hollow fibre supported liquid membrane transport study using simulated high level nuclear waste, *J. Membr. Sci.* 337 (2009) 304-309.
- [28] D. Huang, K. Huang, S. Chen, S. Liu, J. Yu, Rapid Reaction Diffusion Model for the Enantioseparation of Phenylalanine across Hollow Fiber Supported Liquid Membrane, *Sep. Sci. Technol.* 43 (2008) 259-272.
- [29] K.F. Lam, X. Chen, G. McKay, K.L. Yeung, Anion Effect on Cu^{2+} Adsorption on $\text{NH}_2\text{-MCM-41}$, *Ind. Eng. Chem. Res.* 47 (2008) 9376-9383.
- [30] S. Heng, K.L. Yeung, A. Julbe, A. Ayral, J.-C. Schrotter, Preparation of composite zeolite membrane separator/contactor for ozone water treatment, *Microporous Mesoporous Mater.* 115 (2008) 137-146.
- [31] W.K. Chan, J. Jouet, S. Heng, K.L. Yeung, J.C. Schrotter, Membrane contactor/separator for an advanced ozone membrane reactor for treatment of recalcitrant organic pollutants in water, *J. Solid State Chem.* 189 (2012) 96-100.
- [32] K.F. Lam, H. Kassab, M. Pera-Titus, K.L. Yeung, B. Albel, L. Bonneviot, MCM-41 "LUS": Alumina Tubular Membranes for Metal Separation in Aqueous Solution, *J. Phys. Chem. C* 115 (2010) 176-187.

- [33] R. Guell, E. Antico, V. Salvado, C. Fontas, Efficient hollow fiber supported liquid membrane system for the removal and preconcentration of Cr(VI) at trace levels, *Sep. Purif. Technol.* 62 (2008) 389-393.
- [34] T. Wannachod, N. Leepipatpiboon, U. Pancharoen, K. Nootong, Synergistic effect of various neutral donors in D2EHPA for selective neodymium separation from lanthanide series via HFSLM, *J. Ind. Eng. Chem.* 20(2014) 4152-4162.
- [35] L.D. Mafu, T.A.M. Msagati, B.B. Mamba, The enrichment and removal of arsenic (III) from water samples using HFSLM, *Phys. Chem. Earth.* 50-52 (2012) 121-126.
- [36] A. Mtibe, T.A.M. Msagati, A.K. Mishra, B.B. Mamba, Determination of phthalate ester plasticizers in the aquatic environment using hollow fibre supported liquid membranes, *Phys. Chem. Earth.* 50-52 (2012) 239-242.
- [37] C. Fontàs, M. Hidalgo, V. Salvadó, E. Anticó, Selective recovery and preconcentration of mercury with a benzoylthiourea-solid supported liquid membrane system, *Analytica Chimica Acta* 547 (2005) 255-261.
- [38] Thailand Regulatory Discharge Standards 2, Ministry of Industry, Thailand. 1996.
- [39] F.d.M. Fábrega, M.B. Mansur, Liquid-liquid extraction of mercury (II) from hydrochloric acid solutions by Aliquat 336, *Hydrometallurgy* 87 (2007) 83-90.

- [40] U. Pancharoen, T. Wongsawa, A.W. Lothongkum, A reaction flux model for extraction of Cu(II) with LIX84I in HFSLM, *Sep. Sci. Technol.* 46 (2011) 2183-2190.
- [41] Q.W. Li, Quanmin Liu, Xianjun, Separation study of mercury through an emulsion liquid membrane, *Talanta* 43 (1996) 1837-1842.
- [42] A. Jabbari, M. Esmaeili, M. Shamsipur, Selective transport of mercury as HgCl through a bulk liquid membrane using K^+ -dicyclohexyl-18-crown-6 as carrier, *J. Sep. Purif. Technol.* 24 (2001) 139-145.
- [43] R. Meera, T. Francis, M.L.P. Reddy, Studies on the liquid-liquid extraction of mercury(II) from acidic chloride solutions using Cyanex 923, *Hydrometallurgy* 61 (2001) 97-103.
- [44] M. Huebra, M.P. Elizalde, A. Almela, Hg(II) extraction by LIX 34. Mercury removal from sludge, *Hydrometallurgy* 68 (2003) 33-42.
- [45] T. Francis, T. Prasada Rao, M.L.P. Reddy, Cyanex 471X as extractant for the recovery of Hg(II) from industrial wastes, *Hydrometallurgy* 57 (2000) 263-268.
- [46] K. Chakrabarty, P. Saha, A.K. Ghoshal, Simultaneous separation of mercury and lignosulfonate from aqueous solution using supported liquid membrane, *J. Membr. Sci.* 346 (2010) 37-44.

- [47] P.V. Vernekar, Y.D. Jagdale, A.W. Patwardhan, A.V. Patwardhan, S.A. Ansari, P.K. Mohapatra, V.K. Manchanda, Transport of cobalt(II) through a hollow fiber supported liquid membrane containing di-(2-ethylhexyl) phosphoric acid (D2EHPA) as the carrier, *Chem. Eng. Res. Des.* 91 (2013) 141-157.
- [48] P. Kandwal, S. Dixit, S. Mukhopadhyay, P.K. Mohapatra, Mass transport modeling of Cs(I) through hollow fiber supported liquid membrane containing calix-[4]-bis(2,3-naphtho)-crown-6 as the mobile carrier, *Chem. Eng. J.* 174 (2011) 110-116.
- [49] Q. Yang, N.M. Kocherginsky, Copper removal from ammoniacal wastewater through a hollow fiber supported liquid membrane system: modeling and experimental verification, *J. Membr. Sci.* 297 (2007) 121-129.
- [50] S. Suren, U. Pancharoen, N. Thamphiphit, N. Leepipatpiboon, A Generating Function applied on a reaction model for the selective separation of Pb(II) and Hg(II) via HFSLM, *J. Membr. Sci.* 448 (2013) 23-33.
- [51] S. Chaturabul, K. Wongkaew, U. Pancharoen, Selective Transport of Palladium through a Hollow Fiber Supported Liquid Membrane and Prediction Model Based on Reaction Flux, *Separation Science and Technology* 48 (2012) 93-104.
- [52] J.D. Miller, M.C. Fuerstenau, Hydration effects in quaternary amine extraction systems, *Metallurgical Transactions* 1 (1970) 2531-2535.

- [53] C.W. McDonald, T.-S. Lin, Solvent Extraction Studies of Zinc and Cadmium with Aliquat 336-S in Aqueous Chloride Solutions, *Separation Science* 10 (1975) 499-505.
- [54] T. Sato, T. Shimomura, S. Murakami, T. Maeda, T. Nakamura, Liquid-liquid extraction of divalent manganese, cobalt, copper, zinc and cadmium from aqueous chloride solutions by tricaprilmethylammonium chloride, *Hydrometallurgy* 12 (1984) 245-254.
- [55] X. Sun, Y. Ji, L. Zhang, J. Chen, D. Li, Separation of cobalt and nickel using inner synergistic extraction from bifunctional ionic liquid extractant (Bif-ILE), *J. Hazard. Mater.* 182 (2010) 447-452.
- [56] A.W. Lothongkum, S. Suren, S. Chaturabul, N. Thamphiphit, U. Pancharoen, Simultaneous removal of arsenic and mercury from natural-gas-co-produced water from the Gulf of Thailand using synergistic extractant via HFSLM, *J. Membr. Sci.* 369 (2011) 350-358.
- [57] T. Prapasawat, P. Ramakul, C. Satayaprasert, U. Pancharoen, A. Lothongkum, Separation of As(III) and As(V) by hollow fiber supported liquid membrane based on the mass transfer theory, *Korean J. Chem. Eng.* 25 (2008) 158-163.

CHAPTER 4

MASS TRANSFER RESISTANCE OF SIMULTANEOUS EXTRACTION AND STRIPPING OF MERCURY (II) FROM PETROLEUM PRODUCED WATER VIA HFSLM

Srestha Chaturabul^a, Thanaporn Wannachod^a, Natchanun Leepipatpiboon^b, Ura
Pancharoen^{a, †} and Soorathep Kheawhom^{a, ††}

^a*Department of Chemical Engineering, Faculty of Engineering, Chulalongkorn
University, Bangkok 10330, Thailand*

^b*Chromatography and Separation Research Unit, Department of Chemistry, Faculty
of Science, Chulalongkorn University, Patumwan, Bangkok 10330, Thailand*

This article has been published in Journal: Journal of Industrial and Engineering
Chemistry.

Page: 1020–1028. Volume: 21. Year: 2015.

4.1. Abstract

The simultaneous extraction and stripping of mercury (II) from petroleum produced water via hollow fiber supported liquid membrane (HFSLM) was examined. Optimum conditions for extraction and stripping were pH 1 in feed solution, 5% (v/v) Aliquat 336 in the liquid membrane and 0.05 M thiourea in the stripping solution. Percentages obtained for extraction and stripping of mercury (II) were 96.8% and 92.5% which were below the legislation limit of 5 ppb. The overall mass transfer resistance (R) was 7.286×10^2 s/cm. Results showed that the mass transfer model fitted in well with the experimental data.

4.2. Introduction

Mercury is one of the most hazardous metals because of its ability to evaporate in soil or water. It is extremely dangerous. Short-term exposure to mercury in water can result in kidney damage while a lifetime of exposure can lead to impairment in neurological functioning. Though the most common source of mercury in water is natural erosion of soil and ore deposits, runoff from factories and refineries can leak mercury into surface water sources [73]. In the production of

offshore oil and gas, water becomes contaminated with organic and inorganic compounds, salts, hydrocarbons, radioactive elements, trace heavy and toxic metals as well as chemical additives [74]. The amount of components that are exposed to the environment increases with the volume of produced water due to high petroleum demand and maturity of oil and gas wells. The produced water shall be treated before being discharged to the environment or re-injected into the original reservoir depending on its quality and environmental constraints. In the Gulf of Thailand, a trace heavy and toxic metal in produced water is mercury with a reported range between 30–800 ppb [3]. Mercury appears predominantly in elemental form with the rest being inorganic (such as HgCl_2), organic (such as CH_3HgCH_3 and $\text{C}_2\text{H}_5\text{HgC}_2\text{H}_5$) and organo-ionic compounds (such as ClHgCH_3) [75, 76]. Mercury toxicity can cause both acute and chronic poisoning in human beings [62, 77].

According to the permissible discharge limits by both the Ministry of Industry and the Ministry of Natural Resources and Environment, Thailand, it is essential for operators to remove mercury from offshore waste discharges to a limit no greater than 5 ppb [78]. Many researchers apply a chemical treatment process to remove mercury from the produced water prior to overboard discharge. Continuous on-line Hg monitors that determine mercury concentration have been problematic but are

needed to allow adjustment of chemical treatment rates in order to achieve the desired metal discharge concentration. Multidisciplinary research and technology have been increasingly working out how to reduce and control the environmental effects of drilling waste discharges, particularly produced water. It is noted that a combination of different technologies can reduce and regulate undesired components in produced water to almost undetectable levels which comply with the legislation discharge [75]. Typically, a mercury removal unit based on chemical production aids precipitation [79], ultra filtration [12], adsorption [13] or solid phase extraction [17] and can deal excellently with elementary mercury at bulk concentration. Ionic mercury is left as residue in the produced water stream. Subsequently, it becomes a predominantly mercury species in the produced water [19]. According to this fact, a secondary or fine treatment is deemed necessary for removal of this ionic mercury residue. However, it is ineffective at a very low concentration of the contaminated metal ions [14]. The removal threshold for this study was targeted to be less than 5 ppb which is the permissible discharge limit of industrial wastewater imposed by the government regulator in the Kingdom of Thailand [25, 79].

Accordingly, a hollow fiber supported liquid membrane (HFSLM) was used to separate trace metal ions from various solutions. HFSLM is an effective method for

separating diluted concentrations of metal ions. This system has specific characteristics that allow the simultaneous extraction and stripping processes of target ions in a single-step operation, with high selectivity [24]. HFSLM has many advantages over conventional methods. For example, it has lower energy consumption, lower capital and operating costs and less solvent is used [80]. The high surface area of the HFSLM system attains high separation rates [81]. Hollow fiber modules can be connected in series or in parallel for a larger capacity [82]. Several studies have used the hollow fiber supported liquid membrane process to remove trace metal ions from industrial wastewater [83] and coproduced waters [23]. HFSLM, therefore, is most suitable to use as a secondary method in order to manage a very low concentration of metal ions. Examples of methods for mercury (II) treatment are shown in Table 4.1.

Sangtumrong et al. [19] simultaneously separated Hg(II) and As(III) ions from chloride media via HFSLM by means of TOA dissolved in toluene as the extractant and NaOH as the stripping solution; about 95% Hg(II) was recovered but none of As(III). Uedee et al. [84] attained 100% extraction and 97% recovery of Hg(II) ions from chloride media via HFSLM using TOA dissolved in kerosene as the extractant and NaOH as the stripping solution.

Recently, Pancharoen et al. [85] separated mercury (II) from co-produced water. Mercury was highly extracted by TOA dissolved in toluene with NaOH as the stripping solution. The amount of mercury ions that complied with the regulatory limit was obtained in 6-cycle separations at pH 2.5 of feed solution using 2% (v/v) TOA and 0.5M NaOH.

Table 4.1 summary of previous research on mercury (II) separation

Authors	Feed solution	Hg (II) (ppm)	Extractants	Flow pattern	Method	% Ex
Sangtumrong et al. [19]	Synthetic water	20	TOA	SFS	HFSLM	100
Pancharoen et al. [22]	Produced water	1.25	TOA	SFS	HFSLM	100
Chakabarty et al. [23]	Synthetic water	4.5	TOA	NF	FSLM	95
Shamsipur et al. [61]	Synthetic water	2.7	PhenS ₂ O + TT12C4	NF	FSLM	95
Jabbari et al. [86]	Synthetic water	10	DC18C6	NF	BLM	95
Shaik et al. [87]	Synthetic water	1	TOA	NF	BLM	95
Fontas et al. [55]	Synthetic water	10	N-benzoyl	CFS	HFSLM	100
This work	Petroleum produced water	0.5	Aliquat 336	SFCS	HFSLM	97

Note: BLM: bulk liquid membrane; FSLM: flat sheet supported liquid membrane; HFSLM: hollow fiber supported liquid membrane; NF: non-flow; CFS: circulating of feed and stripping solutions; SFCS: single-pass of feed solution and circulating of stripping solution and SFS: single-pass of feed and stripping solutions.

This work studies the extraction and stripping of mercury (II) from petroleum produced water. The properties of feed solutions are as shown in Table 4.2. The pH feed solution, the concentration of extractant Aliquat 336 (trioctyl methyl ammonium chloride, $(R_3N^+CH_3Cl^-)$), the types of diluents, the concentration of stripping solution, the flow rates of both feed and stripping solutions and flow patterns of the HFSLM process were investigated. The selection of extractant, organic diluent and stripping solution proved vital for the success of the separation of mercury (II) as in previous work [33]. The separation of mercury (II) from petroleum produced water and the investigation concerning the related mass transfer is the objective of this study.

Table 4.2 Composition of petroleum produced water (initial pH of feed solution= 6)

Metal ions	Concentration (ppm)
As	0.2
Ca	16
Fe	0.17
Hg	0.5
Mg	2
Na	1820

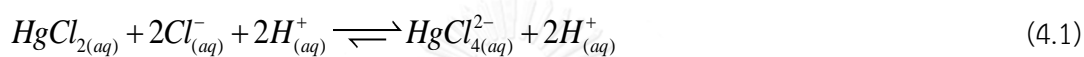
4.3. Theory

4.3.1 Transport of mercury (II) across the liquid membrane phase

In the HFSLM operation, both feed and stripping solutions are fed into the tube and shell sides of the hollow fibers, respectively. Both solutions are separated by an organic extractant embedded in the supported liquid membrane. The transport schematic mechanism of mercury (II) across the liquid membrane is shown in Fig. 4.1. The transference of mercury (II) through HFSLM was carried out via the following steps.

Step I: Mercury chloride compound in produced water is deprotonated to $HgCl_4^{2-}$ in the presence of excess chloride ions, as described in Eq. (4.1) [29]. Subsequently,

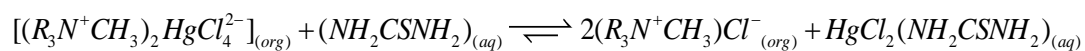
$HgCl_4^{2-}$ in the feed solution is transported to a contact interface between the feed phase and the liquid membrane phase. Subsequently, mercury (II) reacted with Aliquat 336 at the feed–liquid membrane interface resulting in the formation of a metal–extractant complex, $[(R_3N^+CH_3)_2HgCl_4^{2-}]$, as described in Eq. (4.2) [28].



where (aq) is the aqueous phase and (org) is the species in the liquid membrane phase.

Step II: The mercury (II) complex species diffuses across the liquid membrane phase to the liquid membrane stripping interface phase by the concentration gradient.

Step III: The metal–extractant complex, at the liquid membrane stripping interface, reacts continuously with thiourea (NH_2CSNH_2) from the stripping solution and releases mercury (II) into the stripping phase. The reaction is shown below [33].



(4.3)

Step IV: Mercury (II) transfers into the stripping phase while the extractant diffuses back to the liquid membrane phase by the concentration gradient and reacts again with the target ions.

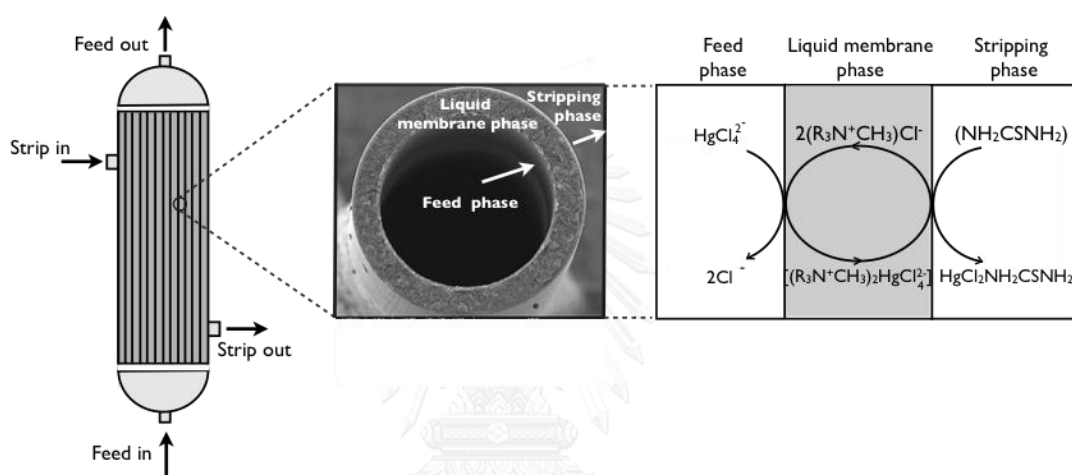


Figure 4.1 Schematic of mass transport of mercury (II) across the liquid membrane phase using Aliquat 336 ($\text{R}_3\text{N}^+\text{CH}_3\text{Cl}^-$) as the extractant and thiourea (NH_2CSNH_2) as the stripping solution

4.3.2 Mass transfer resistance of mercury (II) in HFSLM

Mercury (II) diffuses through the layer of the feed phase towards the feed-liquid membrane interface where it instantly reacts with Aliquat 336 to form a complex. Then, the complex diffuses across the membrane phase and reaches the

liquid membrane–stripping interface where de–complexing occurs by reacting with the stripping solution. Finally, *mercury (II)* diffuses through the layer of the stripping phase to the stripping solution. The diffusion process is explained by Fick’s law.

For the feed solution flowing through the tube side of the hollow fiber, mercury (II) transport from the feed to the liquid membrane phase is given by [88]:

$$d \frac{[HgCl_4^{2-}]_f}{dt} = -\frac{A}{V_a} J \quad (4.4)$$

The flux through the supported liquid membrane can be described by:

$$J = K[HgCl_4^{2-}]_f \quad (4.5)$$

where A is the membrane area (cm^2), V_a is the volume of the feed solution (cm^3), J is the flux of mercury (II) through the supported liquid membrane phase ($\text{mg}/\text{cm}^2 \cdot \text{s}$) and K is the overall mass transfer coefficient (cm/s).

Therefore

$$\ln \frac{[HgCl_4^{2-}]_f}{[HgCl_4^{2-}]_{fo}} = -\frac{KA}{V_a} t \quad (4.6)$$

where $[HgCl_4^{2-}]_{fo}$ is the initial concentration of mercury (II) in the feed solution and $[HgCl_4^{2-}]_f$ is the outlet concentration of mercury (II) in the feed solution. Then, the overall mass transfer coefficient can be calculated from Eq. (4.8).

The overall mass transfer resistance through HFSLM is equal to the sum of all the individual mass-transfer resistances consisting of (1) the feed-side resistance (R_{af}) (2) the interfacial resistance of extraction reaction (R_e) (3) the liquid membrane phase resistance (R_m) (4) the shell-side resistance (R_o) (5) the interfacial resistance of stripping reaction (R_s) and (6) the strip-side resistance (R_{as}). The overall mass transfer resistance (R) or the overall mass transfer coefficient can be described as [89]:

$$R = R_{af} + R_e + R_m + R_o + R_s + R_{as} \quad (4.7)$$

Or

$$\frac{1}{K} = \frac{1}{k_{af}} + \frac{1}{k_e} + \frac{1}{m_f k_m} + \frac{1}{m_s k_o} + \frac{1}{m_s k_s} + \frac{1}{(m_s / k_s) k_{as}}$$

where k_{of} is the mass transfer coefficient in the feed phase; k_e is the mass transfer due to extraction reaction rate whereas k_s is the mass transfer due to stripping reaction rate; k_m is the mass transfer coefficient of the complex species in the liquid membrane phase; k_o is the mass transfer coefficient in the shell side between the hollow fibers; and k_{as} is the mass transfer coefficient for the stripping solution.

Eq. (4.7) can be simplified by neglecting the transport resistances involving the stripping reaction which were negligible because the stripping reaction was completed almost instantaneously during the HFSLM process:

$$\frac{1}{K} = \frac{1}{k_{af}} + \frac{1}{k_e} + \frac{1}{m_f k_m} + \frac{1}{m_s k_o} \quad (4.8)$$

The partition coefficient (m_f) of mercury (II) between the feed phase and the liquid membrane phase can be calculated by [89]:

$$m_f = \frac{[(R_3N^+CH_3)_2HgCl_4^{2-}]_o}{[HgCl_4^{2-}]_f} \quad (4.9)$$

where m_f is the partition coefficient between the liquid membrane phase and the feed solution (-) and $[(R_3N^+CH_3)_2HgCl_4^{2-}]_o$ is calculated by Eq. (4.10) which describes the partition equilibrium between the feed and the liquid membrane solution.

$$[(R_3N^+CH_3)_2HgCl_4^{2-}]_o = \frac{V_a}{V_o} ([HgCl_4^{2-}]_{fo} - [HgCl_4^{2-}]_f) \quad (4.10)$$

where V_a is the volume of the feed solution (cm^3), V_o is the volume of the liquid membrane solution (cm^3).

The mass transfer coefficients of mercury (II) in the aqueous feed phase with laminar flow of feed solution be calculated using the L ev eque equation [90]:

$$k_{af} = 1.62 \frac{D_f}{d_i} \left(\frac{d_i^2 v_f}{LD_f} \right)^{0.33} \quad (4.11)$$

where D_f is the diffusivity of mercury (II) in the aqueous feed solution (cm^2/s), v_f is the linear velocity of feed solution in the tube side (cm/s) and d_i is the inner diameter of the feed side (cm).

The mass transfer due to extraction reaction rate (k_e) can be calculated by [34]:

$$k_e = \frac{1}{k_{Ex} [HgCl_4^{2-}] [R_3N^+ CH_3Cl^-]^2 - k_{St} [(R_3N^+ CH_3)_2 HgCl_4^{2-}] [Cl^-]^2} \quad (4.12)$$

where k_{Ex} and k_{St} are the reaction rate constants of extraction and stripping.

The mass transfer coefficient in the membrane phase can be approximated as follows:

$$k_m = \frac{D_m \varepsilon d_{lm}}{\delta \tau d_o} \quad (4.13)$$

where D_m is the diffusivity of mercury (II) in the membrane solution (cm^2/s), d_{lm} is the log-mean diameter of the membrane (cm), d_o is the outer diameter of the membrane (cm), ε is the porosity of the hollow fiber, τ is the tortuosity of the hollow fiber and δ is the membrane thickness (cm).

The mass transfer coefficient on the shell side of the two hollow fibers can be calculated by [91]:

$$k_o = 1.25 \frac{D_m}{d_h^{0.07}} \left(\frac{d_h v_s}{\nu L} \right)^{0.93} \left(\frac{\nu}{D_m} \right)^{0.33} \quad (4.14)$$

where

$$Sh = \frac{k_o d_h}{D_m} = 0.56 Re^{0.62} Sc^{0.33}$$

$$Re = \frac{d_h v_s}{\nu}$$

$$Sc = \frac{\nu}{D_m}$$

จุฬาลงกรณ์มหาวิทยาลัย
CHULALONGKORN UNIVERSITY

where v_s is the linear velocity of stripping solution in the shell side (cm/s), ν is the kinematic viscosity (cm²/s), D_m is the diffusivity of mercury (II) extractant complex in the liquid membrane phase (cm²/s), Re is the Reynolds number (-), Sh is the Sherwood number (-) and Sc is the Schmidt number (-).

The hydraulic diameter (d_h) of the hollow fibers is calculated again by [91]:

$$d_h = \frac{d_a^2 - d_i^2 - nd_0^2}{nd_0} \quad (4.15)$$

4.4. Experimental

4.4.1 The reagents and the feed

The feed solution was petroleum produced water from one of the oil and gas operators in the Gulf of Thailand. The composition of the petroleum produced water, as shown in Table 4.2, was analysed by an inductively coupled plasma spectroscopy (ICP). The liquid membrane was composed of Aliquat 336 and a toluene. The stripping solution was thiourea dissolved in dilute hydrochloric acid solution. The source and mass fraction purity of materials are listed in Table 4.3. All materials were used without further purification. All the chemicals were of GR grade.

Table 4.3 Source and mass fraction purity of materials

Material name	Source	Purity/ % mass	Analysis method
Aliquat 336	Sigma-Aldrich	97.99	HPLC
Toluene	Sigma-Aldrich	99.99	HPLC
Thiourea	Merck Ltd.	99.99	HPLC
Hydrochloric acid	Merck Ltd.	99.80	GC

Note: HPLC: High performance liquid chromatography and GC: Gas chromatography

4.4.2 Apparatus

The HFSLM (Liqui-Cel Extra-Flow membrane contactor) was manufactured by Hoechst Celanese, USA. The module uses Celgard microporous polypropylene fibers that are woven into a fabric. The properties of the hollow fiber module are shown in Table 4.4. The concentration of mercury (II) in both feed and stripping solutions were analysed by an inductively coupled plasma spectrometry (ICP).

Table 4.4 Properties of the hollow fiber module

Material	Polypropylene
Inside diameter of hollow fiber (cm)	0.024
Outside diameter of hollow fiber (cm)	0.03
Effective length of hollow fiber (cm)	15
Number of hollow fibers	35,000
Average pore size (cm)	3×10^{-6}
Porosity (%)	30
Effective surface area (cm ²)	1.4×10^4
Area per unit volume (cm ² .cm ⁻³)	29.3
Module diameter (cm)	6.3
Module length (cm)	20.3
Tortuosity factor	2.6
Operating temperature (K)	273–333

4.4.3 Procedures

A single module HFSLM operation is shown in Fig. 4.2. At first, the extractant Aliquat 336 was dissolved in toluene (500 mL). Then, the extractant was simultaneously pumped into the tube and shell sides of the hollow fiber module for 40 min. to ensure that the extractant was entirely embedded in the micropores of the hollow fibers. Subsequently, 10 L of both feed and stripping solution were fed counter-currently into the tube and shell sides of the hollow fiber. The operating

mode was single-pass of feed solution and circulating of stripping solutions, which was the best flow patterns observed from previous work [36]. Mercury (II) in the hydrochloric acid solution moved across the liquid membrane to the stripping phase and was collected in the stripping reservoir. The concentration of mercury (II) in the sample from the feed and stripping solution was analyzed by ICP to determine the percentages of extraction and stripping. In this research, the extractability of mercury (II) can be determined by the extraction percentage;

$$\% \textit{Extraction} = \frac{[C]_{f,in} - [C]_{f,out}}{[C]_{f,in}} \cdot 100 \quad (4.16)$$

and the stripping percentage was calculated by:

$$\% \textit{Stripping} = \frac{[C]_{s,out} - [C]_{s,in}}{[C]_{f,in}} \cdot 100 \quad (4.17)$$

where $[C]_{f,in}$, $[C]_{f,out}$ denote the inlet and outlet feed concentration of metal ions (ppm) and stripping phases and $[C]_{s,in}$, $[C]_{s,out}$ denote the inlet and outlet stripping concentration of metal ions (ppm).

The mathematical model was validated by the percentage of standard deviation (% S.D.) obtained from the model and experimental results. The standard deviation is as follows:

$$\% \text{ S.D.} = 100 \times \sqrt{\frac{\sum_{i=1}^n \left\{ \left(\frac{D_{\text{Exp.}}}{D_{\text{Model}}} - 1 \right)^2 \right\}}{N-1}} \quad (4.18)$$

where $D_{\text{Exp.}}$ is the experimental data, D_{Model} is the calculated value from the mathematical model and N is the number of experimental points.

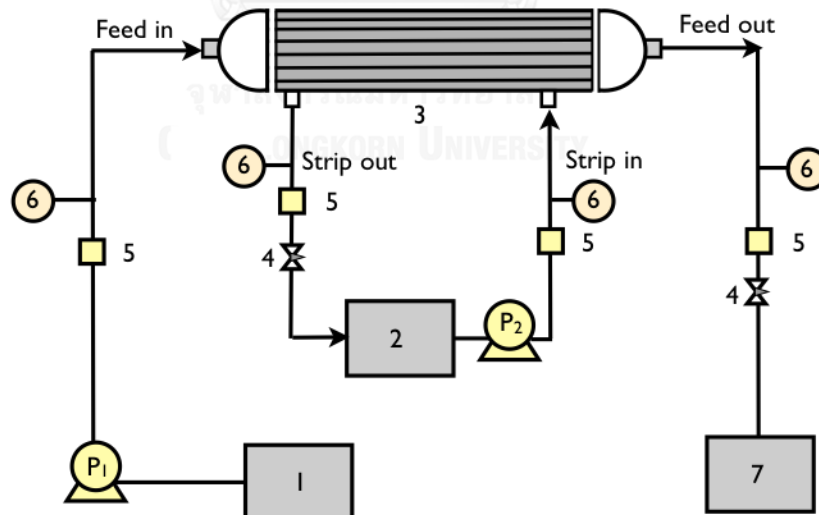


Figure 4.2 Schematic representation of the counter-current flow diagram for single-pass of feed solution and circulating of stripping solution operation in HFSLM: (1)

Inlet Feed reservoir (2) Stripping reservoir (3) HFSLM (4) Flow regulator valve (5) Flow indicator and (6) Pressure indicator (8) Outlet Feed reservoir.

4.5. Results and discussion

4.5.1 Effect of pH of feed solution

pH is an important factor for consideration in extracting mercury (II) from petroleum produced water. As previously mentioned, the extraction of metals by amines as well as by cationic extractants is affected by the pH of the aqueous phase [33]. The effect of pH feed solution was studied by varying pH in the range of 0.5 – 3.5 as recommended by Breembroek et al. [37].

In Fig. 4.3, percentages of extraction and stripping increased rapidly at pH 1 of feed solution. When pH was higher than 1, percentages of extraction and stripping were not improved due to the equilibrium reaction at the feed–liquid membrane interface [92]. It would rather tend to decline since less chloride ions were generated with an incremental pH. These free chloride ions play an essential role in this system. It facilitates the forwards transport by ionising Hg in the petroleum produced water feed to Hg (II) prior it can bridge with extractant solution to form a complex in

the liquid membrane phase. The facilitated mechanism is described by earlier presented reactions in Eq. (4.1) and Eq. (4.2).

In order to ensure the maximum performance of this Hg extraction system, pH = 1 of the produced water feed was chosen to study further the variables. This chosen is in line with an earlier report by Fábrega et al. [33]. Moreover it is within tolerance that its acidity.

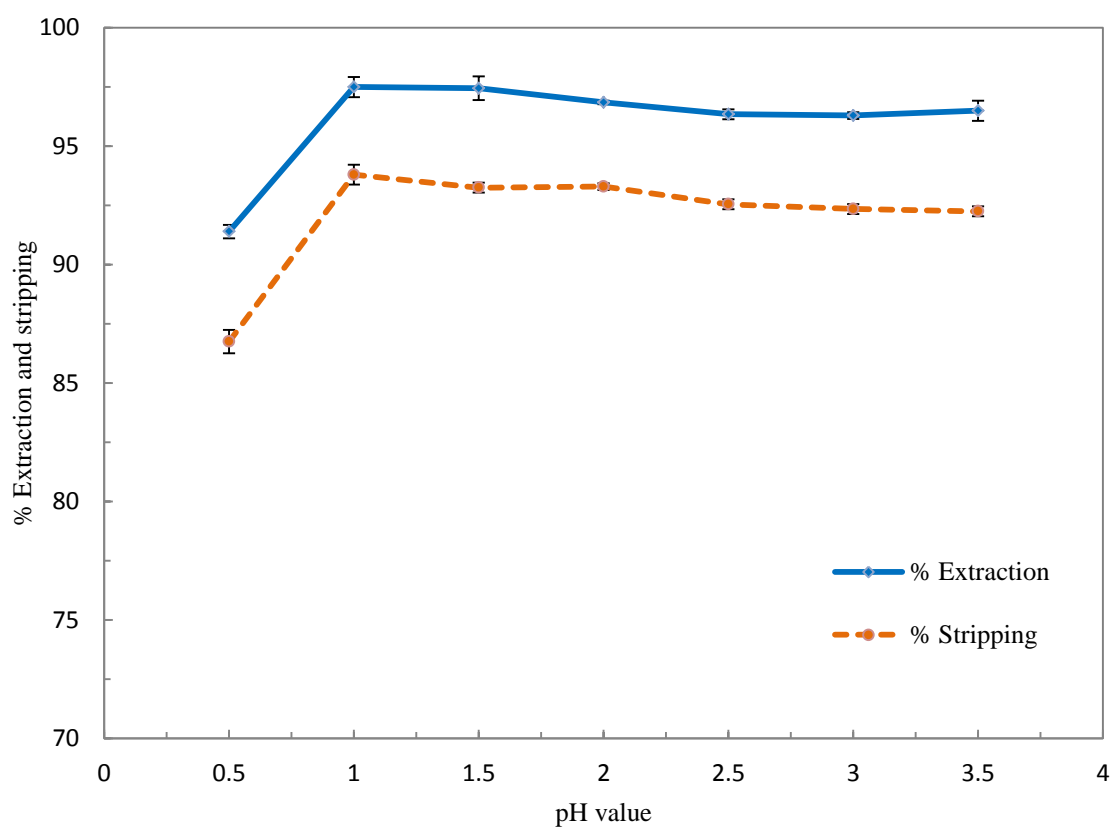


Figure 4.3 Percentages of mercury (II) vs pH value (extractant = 5% (v/v) Aliquat 336 = stripping = 0.05 M thiourea + 1% (v/v) HCl; flow rate = 100 mL/min for both feed and stripping solutions; 30°C).

4.5.2 Effect of concentration of Aliquat 336

The concentration of Aliquat 336 was studied in the range of 1 – 7 % (v/v). Consequently, the increase in mercury (II) extraction corresponded to an increase in the extractant concentration, as shown in Fig. 4.4. The overall mass transfer coefficient of mercury (II) across HFSLM is shown in Table 4.5. The highest percentage of mercury (II) extraction was obtained at a concentration of 5 % (v/v). Consequently, the highest extraction of mercury (II) obtained by the Aliquat 336 extractant was 96.8% and the stripping percentage obtained was 92.5%. When the extractant concentration increased more than 5 % (v/v), no significant change in mercury (II) extraction was observed. In fact, due to excessive viscosity from the high concentration, the percentage of mercury (II) extraction decreased. According to the molecular kinetic interpretation by Stokes and Einstein, an increase in high viscosity leads to a lower diffusion coefficient, resulting in lower extraction. Chakrabarty et al.

[93] also observed that the viscosity of the membrane phase increases when extractant concentration is increased, resulting in a decrease of flux.

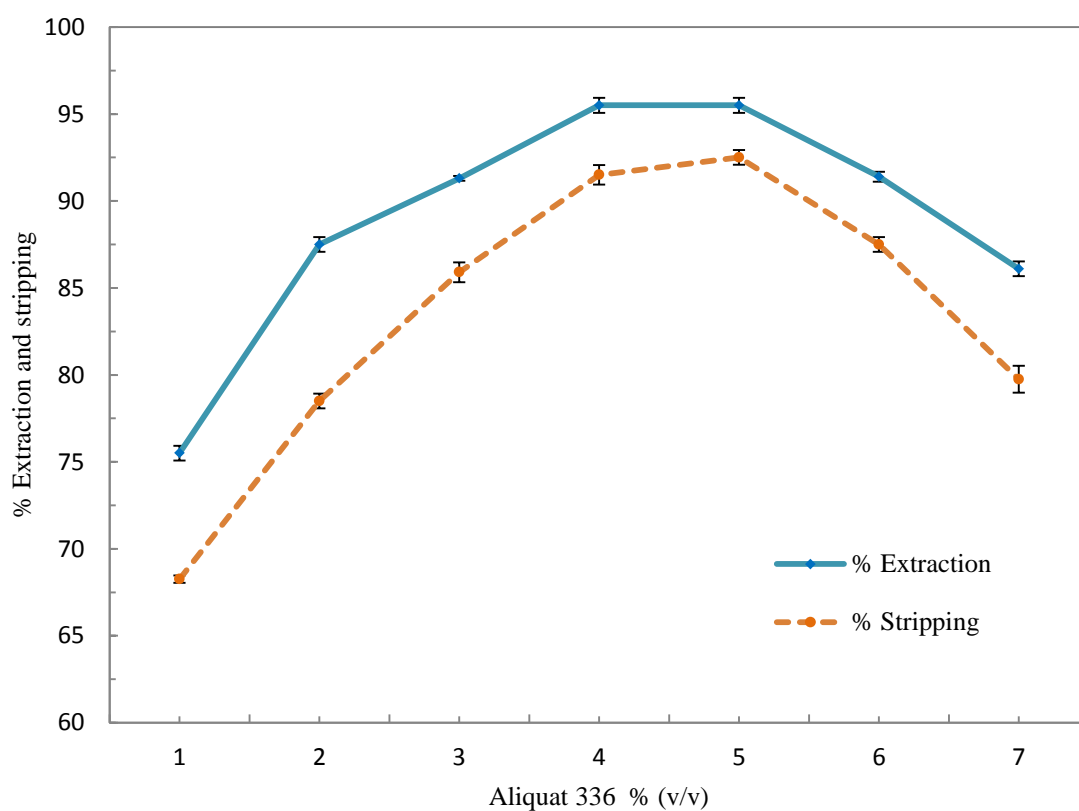


Figure 4.4 Percentages of mercury (II) vs concentration of Aliquat 336 (feed = pH 1; stripping = 0.05 M thiourea + 1% (v/v) HCl; flow rate = 100 mL/min for both feed and stripping solutions; 30°C).

Table 4.5 Validation of overall mass transfer coefficient (K) of mercury (II) across HFSLM

[Aliquat 336] % (v/v)	K (10^4 cm/s)
1	6.421
2	8.295
3	10.018
4	12.354
5	13.725
6	12.415
7	9.917

Note: Feed = pH 1; extractant = 5% (v/v) Aliquat 336; stripping = 0.05 M thiourea + 1% (v/v) HCl; flow rate = 100 mL/min for both feed and stripping solutions; 30°C.

4.5.3 Effect of concentration of stripping solution

Stripping investigations were carried out with regards to the organic solution consisting of 5 % (v/v) Aliquat 336 as the extractant and thiourea as the stripping agent. Thiourea was selected following the result from the study by Lothongkum et al. [40], which identified thiourea as the best performance among the other potential

candidates such as NaOH, deionized water, HNO₃ and H₂SO₄. Thiourea has large anion capable of stripping mercury complex ion from Aliquat 336 [28].

This study varied the concentration of thiourea to observe the effect. The results given in Fig. 4.5 show that when the concentration of stripping solution increased up to 0.05 M, then the percentage of stripping decreased. This was confirmed by Wannachod et al. [41] who found that the stripping of metal ions was obstructed by concentration polarization when the concentration of stripping increased to 0.05 M. Thus optimum percentage of mercury (II) stripping was obtained at 0.05 M thiourea. Similar trends were reported previously where stripping percentage reduced significantly [33]. Thus, 0.05 M thiourea was chosen to study further variables.

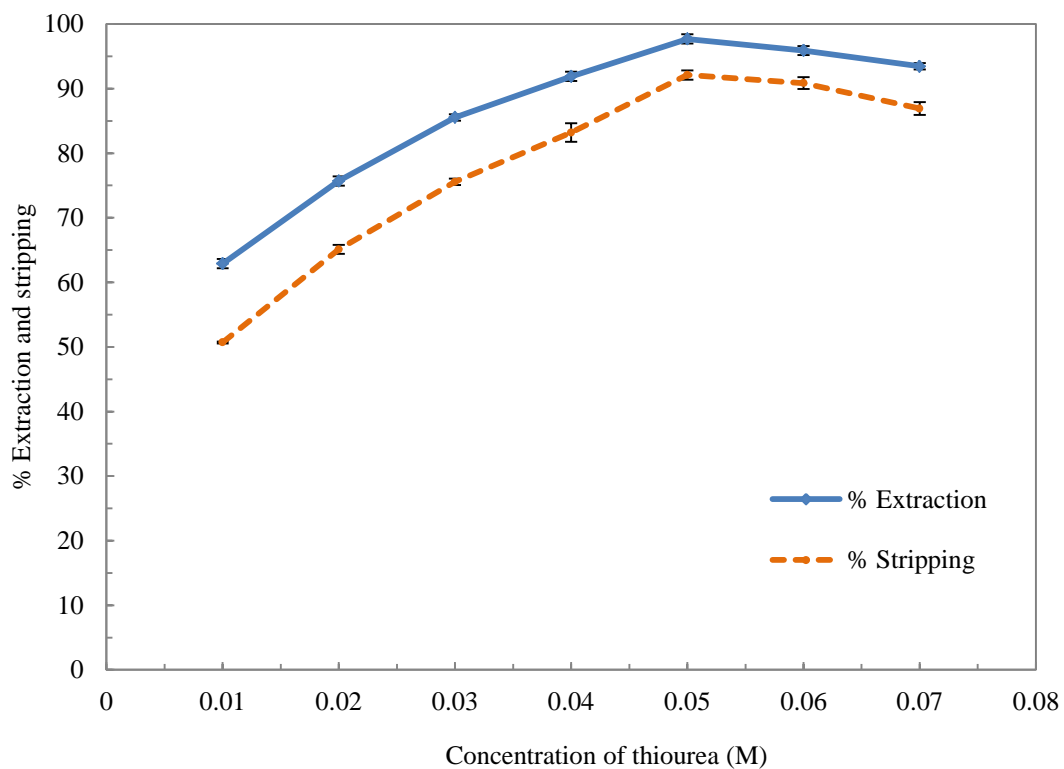


Figure 4.5 Percentage of mercury (II) vs concentration of thiourea (feed = pH 1, extractant = 5% (v/v) Aliquat 336; flow rate = 100 mL/min for both feed and stripping solutions; 30°C).

4.5.4 Effect of types of diluents

In this study, several diluents with different polarity indexes were chosen i.e. nitrobenzene, dichloromethane, chloroform, xylene and toluene [36]. The polarity indexes of the diluents are shown in Table 4.6. Results show that the percentage of

extraction of mercury (II) varies with the nature of the diluents. Generally, when the dielectric constant and the dipole moment of diluents decrease, extraction increases. This can be explained by the fact that the interaction of diluents, having high dielectric constant with the extractant, are generally stronger than those of low dielectric constant e.g. toluene. Strong interaction of diluents with an extractant can result in a lower extraction of metal ions. Therefore, toluene was used in further studies.

Table 4.6 Effect of dielectric constant and dipole moment of diluents on the extraction and overall mass transfer coefficient (K)

Diluents	Nitrobenzene	Dichloromethane	Chloroform	Xylene	Toluene
Dielectric constant	34.82	10.42	4.81	2.54	2.39
Dipole moment	4.22	1.20	1.01	0.62	0
Extraction (%)	71	78	85	90	97
K (10^4 cm/s)	9.82	10.95	11.21	11.72	13.73

Note: Feed = pH 1; extractant = 5% (v/v) Aliquat 336; stripping = 0.05 M thiourea + 1% (v/v) HCl; flow rate = 100 mL/min for both feed and stripping solutions; 30°C.

4.5.5 Effect of the flow rate of feed and stripping solution

The effect of flow rates was investigated using mercury (II) in hydrochloric solution as feed solution. Flow rates of feed and stripping solutions varied from 50 to 500 mL/min as shown in Fig. 4.6. In this experiment, optimum percentages of mercury (II) extraction and stripping were obtained at flow rates for both feed and stripping solutions of 100 mL/min using a single-module operation for a period of 40 min. Percentages of mercury (II) extraction and stripping obtained were 97% and 93%, respectively. However, percentages of mercury (II) extraction and stripping decreased when the flow rates of feed and stripping solutions increased due to the resident time of the solution in the hollow fiber module. This was in agreement with an earlier report by Yang et al. [94].

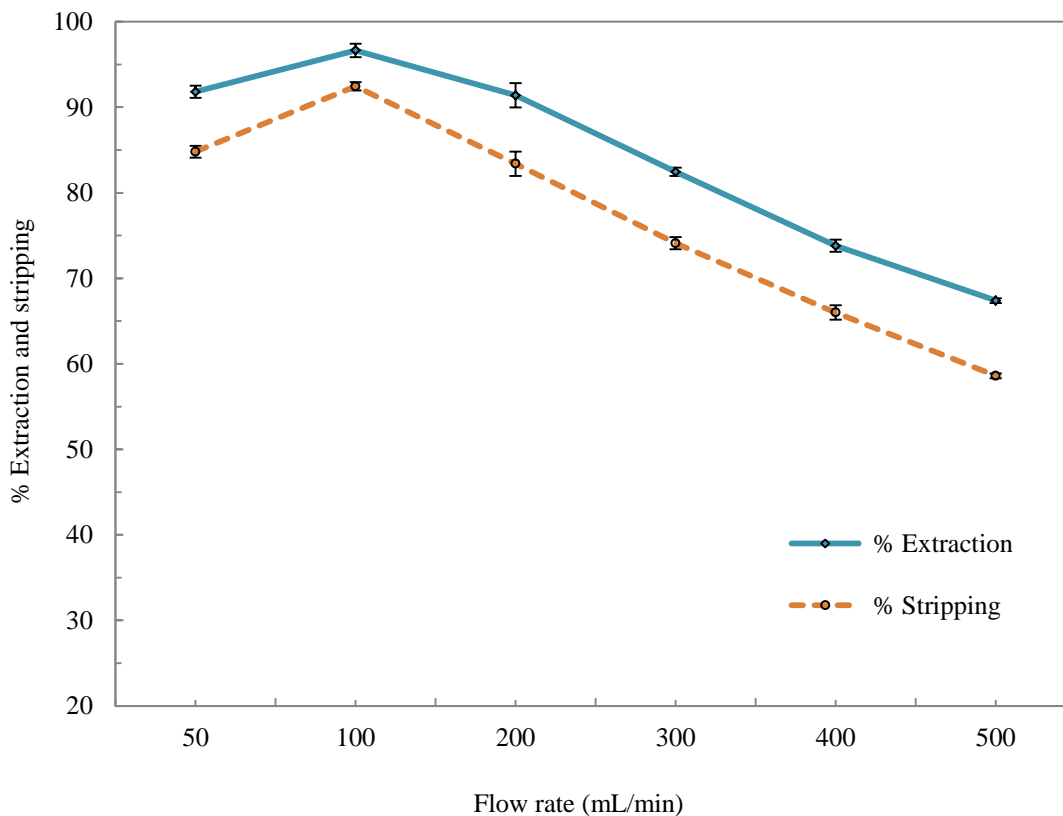


Figure 4.6 Percentage of mercury (II) vs flow rate of feed and stripping solutions (feed = pH 1, extractant = 5% (v/v) Aliquat 336; stripping = 0.05 M thiourea + 1% (v/v) HCl; flow rate = 100 mL/min for both feed and stripping solutions; 30°C).

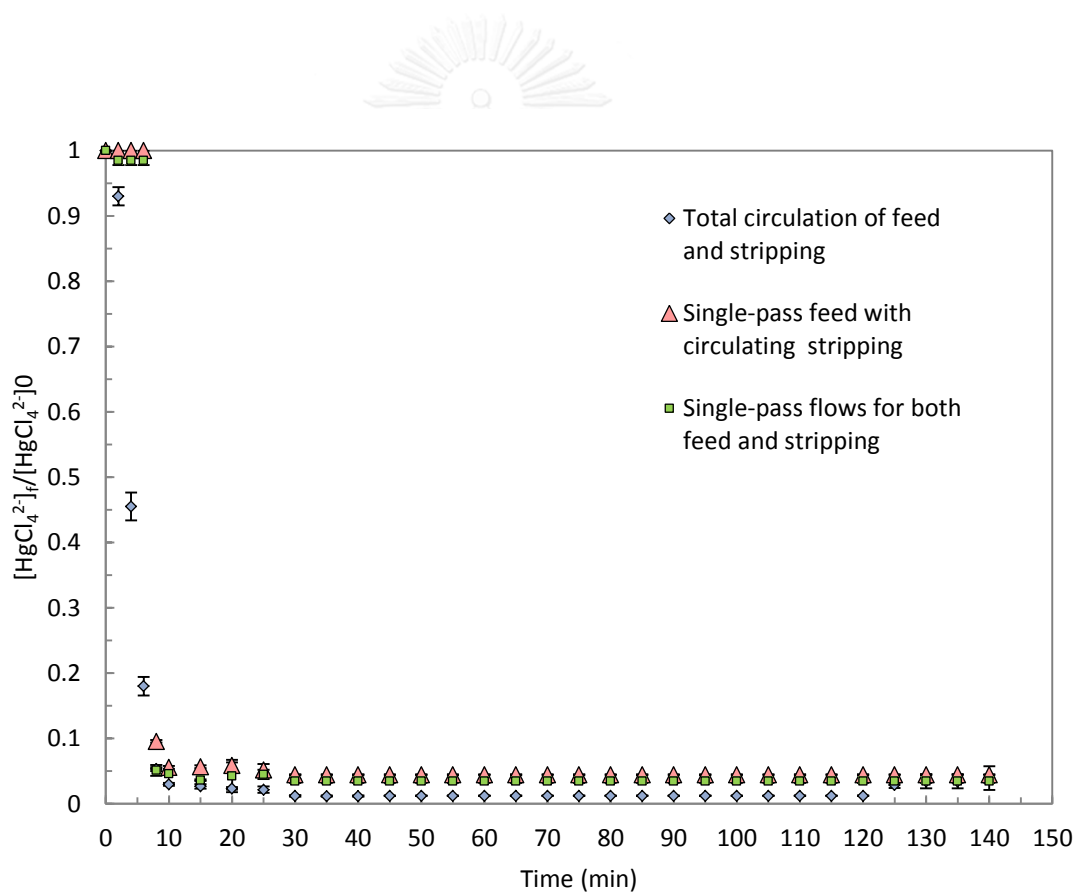
4.5.6 Effect of flow patterns of feed and stripping solutions

The effects of different flow patterns were investigated. The experiments ran with total circulation of feed and strip (Pattern #1), single-pass feed with circulating

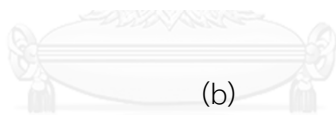
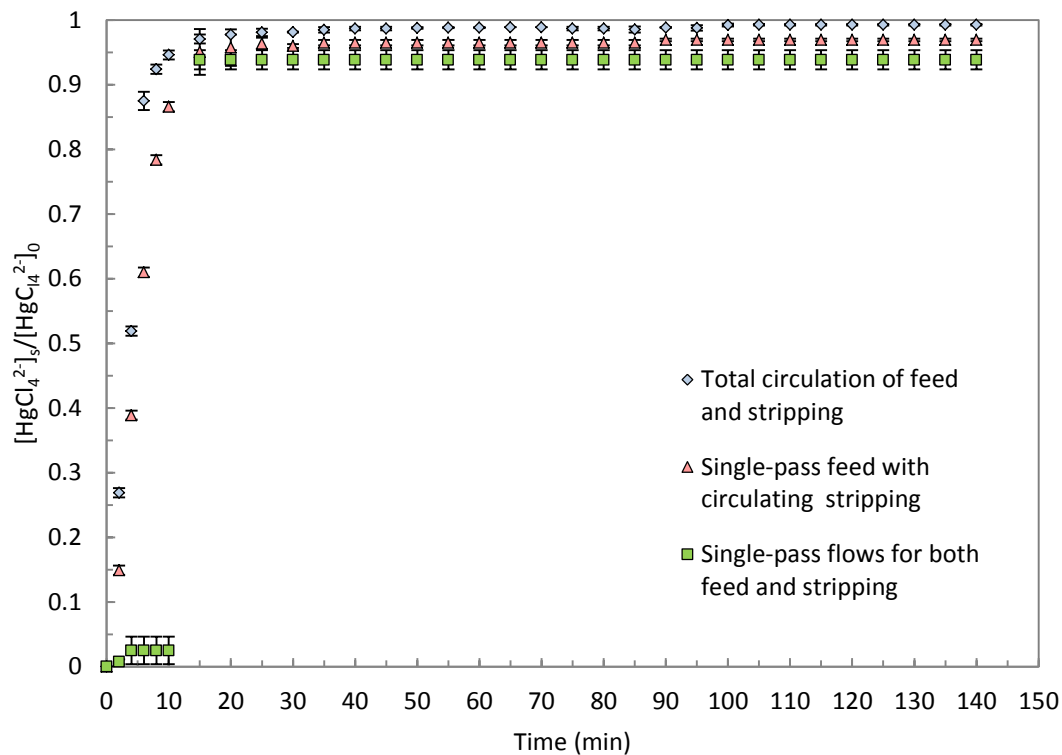
strip (Pattern #2) and single-pass flows for both feed and strip (Pattern #3). The results are presented with the plots in Fig. 4.7: (a) the effects in the feed phase (b) the effects in the stripping phase.

According to the results, the highest extraction and recovery was obtained from the total circulation where both feed and strip are circulated. The Hg concentration in the feed was decreasing due to the numbers of circulation. Vice versa, the Hg concentration in the stripping was correspondingly increasing. Although it is the best result, this total circulation pattern is considered impractical for use in industrial applications since the amount of produced water is tremendous while also being generated continuously. For some marginal oil production field, the produced water is reported with the range up to 50,000 barrels of water per day [3]. It required the huge hold-up vessels for the treatment in this case. Unfortunately, it is uncommon for offshore structure to offer space and weight spare to accommodate such the big hold-up vessels. As an alternative to the total circulation flow, the single-pass feed for Pattern #2 & #3 was studied and compared. This single-pass feed will allow continuous treatment of produced water, from which the reasonable size of hold-up vessel can be acquired. From the result, the performance by Pattern #2 & #3 was very close and in the same league as the total circulation. It is a good

result since it demonstrates a promising solution for mercury treatment by a single-pass flow. Pattern #2 where the limited-volume stripping solution is on circulation is of high interest. By the stripping solution in limited volume, it is noteworthy that any disposal or further treatment of the Hg saturated stripping solution can be achievable in the limited volume as well.



(a)



(b)

จุฬาลงกรณ์มหาวิทยาลัย

Figure 4.7 Concentration of mercury (II) plotted as a function of time (a) in the feed solution (b) in the stripping (feed = pH 1, extractant = 5% (v/v) Aliquat 336; stripping = 0.05 M thiourea + 1% (v/v) HCl; flow rate = 100 mL/min for both feed and stripping solutions; 30°C)

4.5.7 Mass transport resistance

The values of the mass transfer resistances were calculated employing optimum conditions. The values of the four individual transfer resistances are shown in Table 4.7. The overall mass transfer resistance was determined experimentally. This was found to be $R = 7.286 \times 10^2$ s/cm. The mass transfer resistances from the extraction reaction, the shell side mass transfer resistances and the mass transfer resistances from the feed side proved to be much higher than that from the membrane phase. This indicated that the mass transfer resistance in the membrane phase had little effect on the overall mass transfer process.

Table 4.7 Mass transfer resistances under optimum conditions

Individual mass transfer resistances (10^{-2} s/cm)	
R_{af}	0.742
R_e	5.182
R_m	0.521
R_o	0.841

Note: Feed = pH 1; extractant = 5% (v/v) Aliquat 336; stripping = 0.05 M thiourea + 1% (v/v) HCl; flow rate = 100 mL/min for both feed and stripping solutions; 30°C.

4.5.8 Model for mass transfer of mercury (II)

Fig. 4.8 illustrates the comparison of concentrations of mercury (II) from the experimental data and theoretical values estimated using Eq. (6) which employs K from Eq. (4.8).

The results indicated that when the concentration of Aliquat 336 was $\leq 5\%$ (v/v), the mass transfer model proved satisfactory, as demonstrated in Fig. 4.8. However, when the concentration of Aliquat 336 was more than 5% (v/v), the mass transfer model was poor. So, when the concentration of Aliquat 336 was higher than 5% (v/v), the viscosity of the liquid membrane was very high. This resulted in the obstruction of the mass transfer while the metal-complex accumulated in the liquid membrane. Moreover, the free Aliquat 336 molecule was difficult to transport. Therefore, higher than 5%(v/v) concentration of Aliquat 336 did not match the experimental results. The average deviation in feed side is shown in Table 4.8.

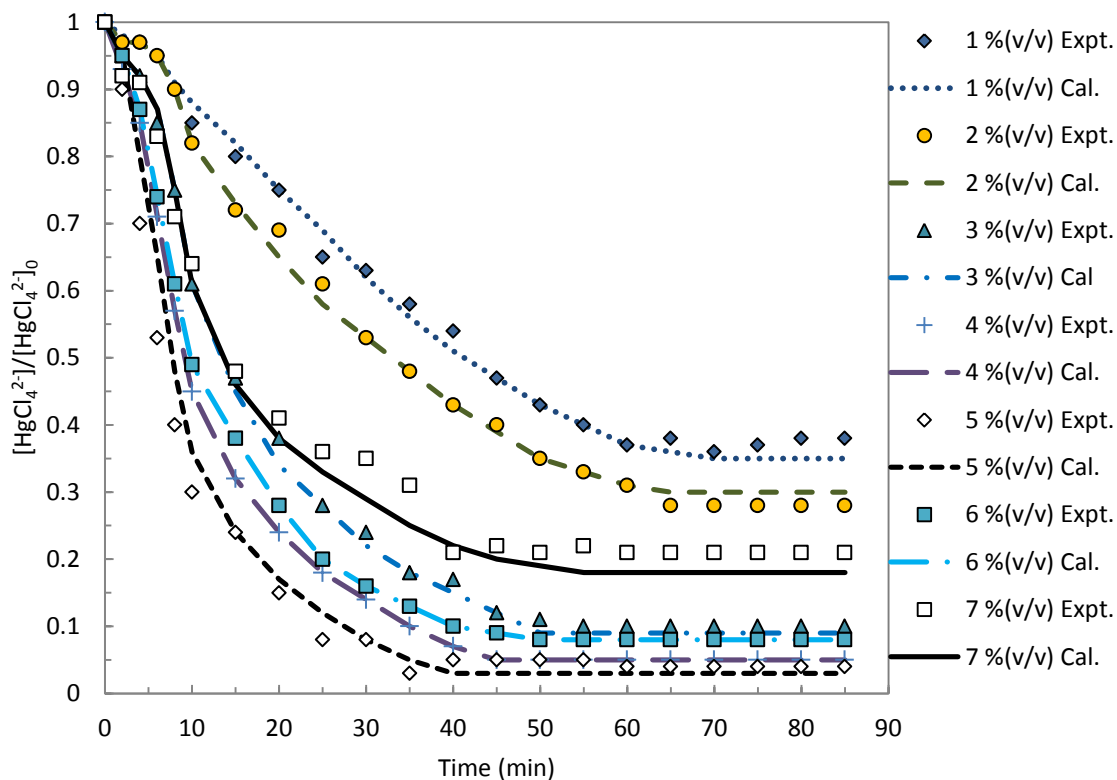


Figure 4.8 Concentration of mercury (II) in the feed solution, plotted as a function of time at different concentrations of Aliquat 336 (feed = pH 1; stripping = 0.05 M thiourea + 1% (v/v) HCl; flow rate = 100 mL/min for both feed and stripping solutions; 30°C).

Table 4.8 The average deviation in feed side

[Aliquat 336] % (v/v)	1	2	3	4	5	6	7
% S.D.	2.41	2.45	2.55	2.58	2.69	8.54	10.9

Note: Feed = pH 1; stripping = 0.05 M thiourea + 1% (v/v) HCl; flow rate = 100 mL/min for both feed and stripping solutions; 30°C.

4.6. Conclusions

The commercial extractant Aliquat 336 was investigated in order to extract mercury (II) from petroleum produced water via HFSLM. Results showed that HFSLM can extract mercury (II). Optimum conditions were found at 5 % (v/v) Aliquat 336 in the liquid membrane, 0.05 M thiourea + 1% (v/v) HCl in the stripping solution. The flow rates of both feed and stripping solutions were 100 mL/min. The extraction and stripping of mercury (II) were found to be 96.8% and 92.5%, respectively. Under optimal operating conditions, the overall transfer resistance, the extraction reaction resistance, the feed phase resistance, the organic phase shell-side resistance, and the membrane resistance were $R = 7.286 \times 10^2$, $R_e = 5.182 \times 10^2$, $R_{of} = 0.742 \times 10^2$, $R_o = 0.841 \times 10^2$ and $R_m = 0.521 \times 10^2$ s/cm, respectively. The overall transfer resistance therefore proved to be the superior influence. Thus, the experimental data and theoretical values were found to be in good agreement when the concentration of mercury (II) in the membrane phase was $\leq 5\%$ (v/v) of Aliquat 336.

4.7. Nomenclature


A	membrane area (cm^2)
d_h	hydraulic diameter of the hollow fiber (cm)
d_i	inner diameter of the hollow fiber (cm)
d_{lm}	log-mean diameter of the hollow fiber (cm)
d_o	outer diameter of the of the hollow fiber (cm)
D_f	diffusivity of mercury (II) in the feed solution (cm^2/s)
D_m	diffusivity of mercury (II) in the liquid membrane solution (cm^2/s)
J	flux of mercury (II) through the supported liquid membrane phase ($\text{mg}/\text{cm}^2 \cdot \text{s}$)
k_{af}	mass transfer coefficient in the feed solution (cm/s)
k_{as}	mass transfer coefficient in the stripping solution (cm/s)
k_e	mass transfer coefficient due to the extraction reaction (cm/s)
k_{Ex}	reaction rate constants of extraction ($\text{cm}^3/\text{mg} \cdot \text{s}$)
k_m	mass transfer coefficient of the membrane phase (cm/s)
k_o	mass transfer coefficient in the shell side between of the hollow fibers (cm/s)
k_s	mass transfer coefficient due to the stripping reaction (cm/s)
k_{St}	reaction rate constants of extraction and stripping ($\text{cm}^3/\text{mg} \cdot \text{s}$)
K	overall mass transfer coefficient (cm/s)

L	fiber module length (cm)
m_f	partition coefficient between the membrane phase and the feed phase (-)
m_s	partition coefficient between the membrane phase and the stripping phase (-)
r	inner radius of the hollow fiber (cm)
R	overall mass transfer resistance (s/cm)
Re	Reynolds number (-)
Sc	Schmidt number (-)
Sh	Sherwood number (-)
t	time (s)
v_f	linear velocity of feed solution in the tube side (cm/s)
v_s	linear velocity of stripping solution in the shell side (cm/s)
V_a	volume of the feed solution (cm ³)
V_o	volume of the liquid membrane solution (cm ³)
\mathcal{E}	porosity of hollow fiber (%)
τ	tortuosity factor membrane (-)
δ	membrane thickness (cm)
ν	kinematic viscosity (cm ² /s)

4.8. Acknowledgments

The author would like to express sincere gratitude towards the Rachadapisek-somphot Endowment Fund of Chulalongkorn University (Grant No. RES560530215-EN), as well as the joint supported from the Thailand Research Fund and Chulalongkorn University under the Royal Golden Jubilee Ph. D Program (Grant No. PHD/0372/2552) and also the Separation Laboratory, Department of Chemical Engineering, Faculty of Engineering, Chulalongkorn University who support this work.

4.9. References

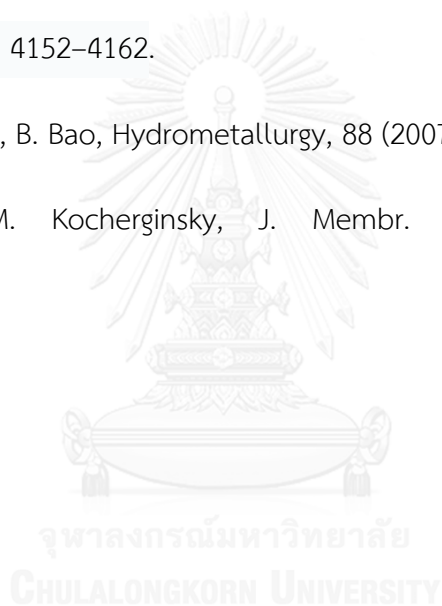
- 
- [1] D.R. Chester, Groundwater Contamination, Volume 1: Contamination Sources and Hydrology, Technomic Publishing Company, Inc. Lancaster, Pennsylvania, 2000.
- [2] J.M. Neff, N.N. Rabalais, D.F. Boesch, Offshore oil and gas development activities potentially causing long-term environmental effects, in: D.F. Boesch, N.N. Rabalais (Eds.), Long-Term Environmental Effects of Offshore Oil and Gas Development, Elsevier Applied Science Publishers, London, 1987, pp. 149-170.

- [3] S. Pairoj-Boriboon, N. Kositrat, Y. In-na, P. Chongprasith, W. Utoomprurkporn, E. Praekulvanich and P. Sangwichit, United Nations Environment Programme (UNEP) Chemicals, 2001.
- [4] D.L. Gallup, J.B. Strong, Removal of mercury and arsenic from produced water, Chevron Corporation, (2007) pp.1-9.
- [5] G. Corvini, J. Stiltner, K. Clark, UOP LLC, Keith Clark, (2007) pp. 3.
- [6] K. Chakrabarty, P. Saha, A.K. Ghoshal, J. Membr. Sci. 346 (2010) 37-44.
- [7] R. van der Vaart, J. Akkerhuis, P. Feron, B. Jansen, J. Membr. Sci. 187 (2001) 151-157.
- [8] Thailand Regulatory Discharge Standards 2, Ministry of Industry, Thailand. 1996.
- [9] G.V. Ramanaiah, Talanta, 46 (1998) 533-540.
- [10] J.Y. Lu, W.H. Schroeder, Talanta, 49 (1999) 15-24.
- [11] Q. Wang, X. Chang, D. Li, Z. Hu, R. Li, Q. He, J. Hazard. Mater. 186 (2011) 1076-1081.
- [12] X. Chai, X. Chang, Z. Hu, Q. He, Z. Tu, Z. Li, Talanta, 82 (2010) 1791-1796.
- [13] S. Sangtumrong, P. Ramakul, C. Satayaprasert, U. Pancharoen, A.W. Lothongkum, J. Ind. Eng. Chem. 13 (2007) 751-756.
- [14] B.S. Inbaraj, J.S. Wang, J.F. Lu, F.Y. Siao, B.H. Chen, Bioresource Technology, 100 (2009) 200-207.

- [15] I.M. Coelho, M.M. Cardoso, R.M.C. Viegas, J.P.S.G. Crespo, *Sep. Puri. Technol.* 19 (2000) 183-197.
- [16] M.F. San Román, E. Bringas, R. Ibañez, I. Ortiz, *J. Chem. Tech. Biotechnol.* 85 (2010) 2-10.
- [17] N.M. Kocherginsky, Q. Yang, L. Seelam, *Sep. Puri. Technol.* 53 (2007) 171-177.
- [18] U. Pancharoen, A.W. Lothongkum, S. Chaturabul, in: Mohamed El-Amin, *Roles of Facilitated Transport through HFSLM in Engineering Applications, Mass Transfer in Multiphase Systems and Its Applications*, InTech, India, 2011, pp. 499-524.
- [19] T. Francis, T. Prasada Rao, M.L.P. Reddy, *Hydrometallurgy*, 57 (2000) 263-268.
- [20] U. Pancharoen, W. Poonkum, A.W. Lothongkum, *J. Alloys Comp.* 482 (2009) 328-334.
- [21] E. Uedee, P. Ramakul, U. Pancharoen, A. Lothongkum, *Korean J. Chem. Eng.* 25 (2008) 1486-1494.
- [22] U. Pancharoen, S. Somboonpanya, S. Chaturabul, A.W. Lothongkum, *J. Alloys Comp.* 489 (2010) 72-79.
- [23] K. Chakrabarty, P. Saha, A.K. Ghoshal, *J. Membr. Sci.* 350 (2010) 395-401
- [24] M. Shamsipur, O. R. Hashemi, V. Lippolis', *J. Membr. Sci.* 282 (2006) 322-327.
- [25] A. Jabbari, M. Esmaili, M. Shamsipur, *Sep. Purif. Technol.* (2001) 139-145.

- [26] A.B. Shaik, K. Chakrabarty, P. Saha, A.K. Ghoshal, *Ind. Eng. Chem. Res.* 49 (2010) 2889-2894.
- [27] C. Fontàs, M. Hidalgo, V. Salvadó, E. Anticó, *Anal Chim Acta*, 547 (2005) 255-261.
- [28] F.M. Fàbrega, M.B. Mansur, *Hydrometallurgy*, 87 (2007) 83-90.
- [29] J. D. Miller, M.C. Fuerstenau, *Metall. Trans. B*, 1(1970)2531-2535.
- [30] W.S.W. Ho, B. Wang, *Ind. Eng. Chem. Res.* 41 (2002) 381-388.
- [31] Y. Tang, W. Liu, J. Wan, Y. Wang, X. Yang, *Process Biochemistry*, 48 (2013) 1980-1991.
- [32] S.R. Wickramasinghe, M.J. Semmens, E.L. Cussler, *J. Membr. Sci.* 69 (1992) 235-250.
- [33] M.C. Yang, E.L. Cussler, *AIChE Journal*, 32 (1986) 1910-1916.
- [34] Q. Yang, N.M. Kocherginsky, *J. Memb. Sci.* 297 (2007) 121-129.
- [35] J. Baudot, H.E. Flourey, Smorenburg, *AIChE Journal*, 47 (2001) 1780-1793.
- [36] S. Suren, U. Pancharoen, N. Thamphiphit, N. Leepipatpiboon, *J. Membr. Sci.* 448 (2013) 23-33.
- [37] G.R.M. Breembroek, A. van Straalen, G.J. Witkamp, G.M. van Rosmalen, *J. Memb. Sci.* 146 (1998) 185-195.
- [38] S. Suren, U. Pancharoen, S. Kheawhom, *J. Ind. Eng. Chem.* 20 (2014) 2584-2593.

- [39] K. Chakrabarty, K.V. Krishna, P. Saha, A.K. Ghoshal, J. Memb. Sci. 330 (2009) 135-144.
- [40] A.W. Lothongkum, S. Suren, S. Chaturabul, N. Tamphiphit and U. Pancharoen, J. Membr. Sci. 369 (2011) 350-358.
- [41] T. Wannachod, N. Leepipatpiboon, U. Pancharoen, K. Nootong, J. Ind. Eng. Chem. 20 (2014) 4152-4162.
- [42] D. Wu, Q. Zhang, B. Bao, Hydrometallurgy, 88 (2007) 210-215.
- [43] Q. Yang, N.M. Kocherginsky, J. Membr. Sci. 286 (2006) 301-309.



CHAPTER 5

AN INVESTIGATION OF CALIX[4] ARENE NITRILE FOR MERCURY TREATMENT IN HFSLM APPLICATION

Srestha Chaturabul, Thanaporn Wannachod, Vanee Mohdee, Ura Pancharoen,[†] and
Suphot Phatanasri,^{††}

*Department of Chemical Engineering, Faculty of Engineering, Chulalongkorn
University, Bangkok 10330, Thailand*

มหาวิทยาลัย
CHULALONGKORN UNIVERSITY

This article has been published in Journal: Chemical Engineering and Processing:

Process Intensification.

Page: 35–40. Volume: 89. Year: 2015

5.1. Abstract

The transport of mercury ions (Hg^{2+}) through hollow fiber supported liquid membrane was examined using the extractant Calix[4]arene nitrile. Optimum condition was achieved using 4.5 pH of feed solution, 0.004 M of Calix[4]arene nitrile as extractant, de-ionized water as stripping solution and an operating temperature of 313 K. Percentages of extraction and stripping of mercury (II) ions obtained reached 99.5% and 97.5%, respectively. The stability of the liquid membrane was investigated and showed stable performance over 24 hours. After treatment, mercury (II) ions from petroleum produced water in feed solution was found to be below the legislation limit of 5 ppb.

จุฬาลงกรณ์มหาวิทยาลัย
CHULALONGKORN UNIVERSITY

Keywords: Calix[4]arene nitrile; Treatment; Mercury (II); HFSLM; Liquid membrane.

*Corresponding author. Tel.: +66 2 218 6891; Fax: +66 2 218 6877.

**Corresponding author. Tel.: +66 2 218 6890; Fax: +66 2 218 6877.

E-mail address: ura.p@chula.ac.th (U. Pancharoen), s.phatanasri@yahoo.com (S. Phatanasri).

5.2. Introduction

Mercury (Hg) and its compounds, especially methyl mercury, are toxic components that can harm the environment and bio-living even in small quantities. Mercury can be absorbed through skin, respiratory and gastro-intestinal tissues [1, 2] and poses a tendency to concentrate within the living bodies [3].

Membrane technology has attracted the attention of many researchers for metal removal and wastewater treatment [4]. Several studies have shown that hollow fiber supported liquid membrane (HFSLM) is an effective method for separating a very low concentration of metal ions from various aqueous solutions. This method allows for both simultaneous extraction and stripping processes of target ions in one single-step operation, with high selectivity [5, 6]. Many advantages of HFSLM over traditional methods include lower energy consumption, lower capital and operating costs and less solvent used [7]. HFSLM has a high surface area per unit volume that contributes to the adequate rates of separation for industrial purposes [8, 9]. It has many applications in industries, such as in chemical, food and pharmaceutical processing [8, 10-12]. Hollow fiber modules can be connected in

parallel or in series for a larger capacity [13]. Therefore, HFSLM can be suitably used as a secondary method in order to effectively manage trace metal ions.

Recent studies have investigated the use of HFSLM for separating various trace metal ions from aqueous solutions [14] or wastewater [15]. Fontàs et al. [16] for example, separated Hg(II) from Cd(II) and Pb(II) in nitrate media at 2 pH. *N*-benzoyl-*N*,*N*-diheptadecylthiourea was used as an extractant and 0.3 M thiourea was used as the stripping solution and resulted in high separation of mercury. Mafu et al. [15] studied the extraction of arsenic(III) from wastewater via HFSLM. The results showed that 50% of arsenic (III) was removed using *n*-undecane and di-*n*-hexyl ether mixtures (3:1 %v/v) as the liquid membrane. The stripping solution used was H₂SO₄. Güell et al. [14] separated Cr(VI) at a low concentration from different aqueous matrices via HFSLM using Aliquat 336 as the extractant. 0.5 M HNO₃ was used as the stripping solution. The results demonstrated high efficiency in removing Cr(VI) from different aqueous samples. Previous success in the separation of mercury ions are summarized in Table 5.1.

Table 5.1 Summary of previous research on mercury (II) ions separation

Authors	Feed	Extractants	Diluents	Stripping	pattern	Method	%Ex
Fontàs et al. [16]	Synthetic water	N-benzoyl- N',N'- diheptadecyl thiourea	Cumene	Thiourea	CFS	HFSLM	100
Gubbuk et al. [17]	Synthetic water	Calix[4]arene nitrile	Chloro- form	DI-water	NF	BLM	N/A
Alpoguz et al. [18]	Synthetic water	Calix[4]arene dinitrile	CH ₂ Cl ₂	DI-water	NF	FBLM	N/A
Alpoguz et al. [19]	Synthetic water	Calix[4]arene ketone derivative	CH ₂ Cl ₂	DI-water	NF	FSLM	N/A
Jabbari et al. [20]	Synthetic water	DC18C6	Chloro- form	DI-water	NF	BLM	95
Shaik et al. [21]	Synthetic water	TOA	Dichloro ethane	NaOH	NF	BLM	95
Chakabarty et al. [22]	Synthetic water	TOA	Dichloro ethane	NaOH	NF	FSLM	95
Sangtumrong et al. [23]	Synthetic water	TOA	Toluene	NaOH	SFS	HFSLM	100
Pancharoen et al. [24]	Produced water	TOA	Toluene	NaOH	SFS	HFSLM	100
Lothongkum et al. [25]	Produced water	Aliquat 336 + Cyanex471	Toluene	Thiourea	SFS	HFSLM	100
This work	Produced water	Calix[4]arene nitrile	NPOE	DI-water	SFCS	HFSLM	99.5

Note: BLM: bulk liquid membrane; CFS: circulating of feed and stripping solutions;

FSLM: flat sheet supported liquid membrane; HFSLM: hollow fiber supported liquid

membrane; L-L: liquid-liquid extraction; NF: non-flow; SFCS: single-pass of feed

solution and circulating of stripping solution and SFS: single-pass of feed and stripping solutions.

In this work, Calix[4]arene nitrile was deployed as mercury (II) ions extractant. Calix[4]arenes is used in various applications such as purification, chromatography, catalysis, enzyme mimics, ion selective electrodes, phase transfer and transport across the liquid membranes. A variety of Calix[n]arene derivatives is known for its effective use in the selective removal of metal ions from wastewater [26, 27]. Calix[4]arene nitrile has the capacity to capture Hg^{2+} in weak acid condition and thereby can form mercury complex ions. The complex ions are in co-ordination bond which is reasonably strong but not too hard for a neutral-based stripping solution to break the bond.

This study was set up to identify key parameters that influence the performance of extraction and recovery of Hg^{2+} from petroleum produced water. The effects of experimental parameters such as pH in feed solution, compositions of feed solution, concentration of extractant, flow rate of both feed and stripping solutions and temperature were investigated. The removal threshold for this study was targeted to be less than 5 ppb which is the permissible discharge limit of industrial wastewater imposed by the government regulator in the Kingdom of Thailand [28].

5.3. Theory

5.3.1 Transport of mercury (II) ions across the liquid membrane phase

In the HFSLM system, both feed and stripping solutions are fed into the tube and shell sides of the hollow fibers, respectively. Both solutions are separated by an organic extractant embedded in the supported liquid membrane. The schematic representation of the chemical reaction of mercury (II) ions with Calix[4]arene nitrile (*L*) to form complex species is shown in Fig. 5.1. The reactions involved are as follows in Eqs (5.1) and (5.2). The extraction of Hg^{2+} from the feed phase is as described in Eq. (5.1) [29]:

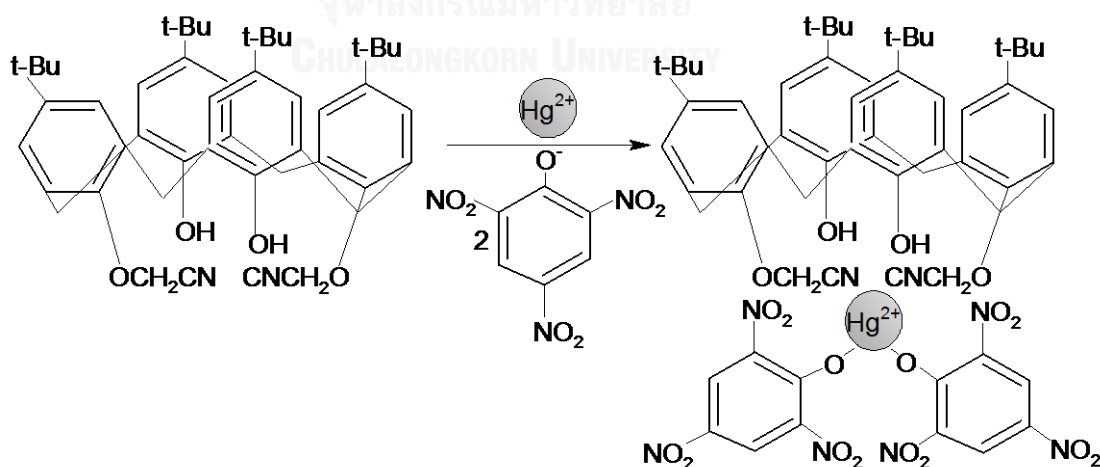
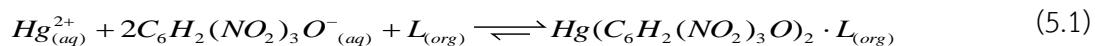
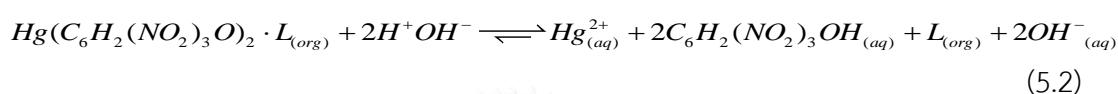


Figure 5.1 Schematic representation of the chemical reaction of mercury (II) ions with Calix[4]arene nitrile (*L*) to form the complex species $[Hg(C_6H_2(NO_2)_3O)_2 \cdot L]$



The stripping reaction is shown below in Eq. (5.2) [29]:



where the subscript (*aq*) designate aqueous species and the subscript (*org*) is the organic species in the liquid membrane phase.

5.4. Experiment

5.4.1 Feed solution and reagent

Feed solution was petroleum produced water from one of the oil and gas operators in the Gulf of Thailand. The composition of the petroleum produced water, as shown in Table 5.2, was analysed by an inductively coupled plasma optical emission spectrometer (ICP-OES). The liquid membrane was composed of Calix[4]arene nitrile (5,11,17,23-Tetra-tert-butyl-25,27-dicyano-methoxy-26,28-dihydroxycalix[4]arene) and NOPE (2-nitrophenyl octyl ether). The stripping solution was de-ionized water (H_2O). The source and mass fraction purity of materials are

listed in Table 5.3. All materials were used without further purification. All the chemicals were of GR grade.

Table 5.2 The composition of petroleum produced water

Compositions in feed	(ppm)
Ca	0.152
Fe	0.002
Hg	0.5
Mg	0.201
Na	1.811

Table 5.3 Source and mass fraction purity of materials

Material name	Source	Purity/ % mass	Analysis method
Calix[4]arene nitrile	Merck Ltd.	97.99	HPLC
NPOE	Sigma–Aldrich	99.99	HPLC
Picric acid	Merck Ltd.	99.99	GC
Hydrochloric acid	Merck Ltd.	99.80	GC

Note: GC: Gas chromatography and HPLC: high performance liquid chromatography

5.4.2 Apparatus

The HFSLM was manufactured by Hoechst Celanese, USA. The module was Celgard micro-porous polypropylene fibers that were woven into a fabric. The properties of the hollow fiber module are shown in Table 5.4. An inductively coupled plasma optical emission spectrometer (ICP-OES) was used to determine the concentration of metal ions whereby the minimum detection limit for Hg^{2+} is 5 ppb [30].

Table 5.4 Properties of the hollow fiber module

Property	Description
Material	Polypropylene
Module diameter (cm)	6.3
Module length (cm)	20.3
Number of hollow fibers	35,000
Inside diameter (cm)	0.024
Outside diameter (cm)	0.03
Effective length (cm)	15
Average pore size (cm)	3×10^{-6}
Porosity (%)	25
Effective surface area (cm^2)	1.4×10^4
Area per unit volume (cm^2/cm^3)	29.3
Tortuosity factor	2.6
Operating temperature (K)	273–333

5.4.3 Procedure

A single module HFSLM operation is shown in Fig. 5.3. At first, the liquid membrane was prepared by dissolving the extractant Calix[4]arene nitrile in NPOE. Then, the extractant was simultaneously pumped into the tube and shell sides of the hollow fiber module for 40 min. to ensure that the liquid membrane was entirely embedded in the micro-pores of the hollow fibers. Subsequently, both feed and stripping solution was fed counter-currently into the tube and shell sides of the hollow fiber. The pattern flow is single-pass of feed solution and circulating of stripping solution. Mercury (II) ions moved across the liquid membrane to the stripping phase and were collected in the stripping reservoir. Operating time for one cycle for each operation was 40 min. The concentration of Hg^{2+} in the sample from the feed and stripping solution was analyzed by ICP-OES in order to determine the percentages of extraction and stripping. In this research, the extractability of Hg^{2+} can be determined by the extraction percentage as shown in Eq. (5.9):

$$\% \text{Extraction} = \frac{[C]_{f,in} - [C]_{f,out}}{[C]_{f,in}} \cdot 100 \quad (5.9)$$

and the stripping percentage was calculated as in Eq. (10):

$$\%Stripping = \frac{[C]_{s,out}}{[C]_{f,in}} \cdot 100 \quad (5.10)$$

where $[C]_{f,in}$, $[C]_{f,out}$ denote the inlet and outlet feed concentration of metal ions (ppm) and $[C]_{s,in}$, $[C]_{s,out}$ denote the inlet and outlet stripping concentration of metal ions (ppm).

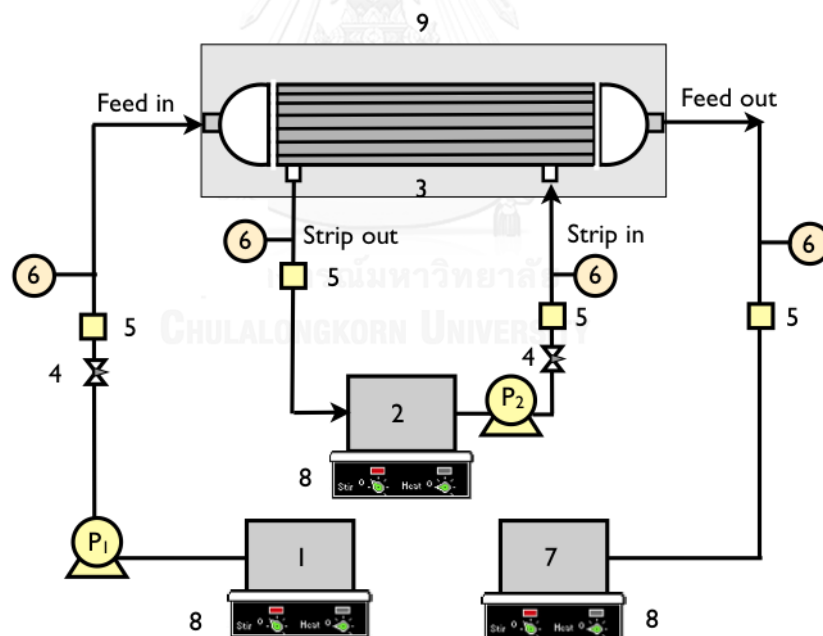


Figure 5.2 HFSLM in counter-current flow diagram of a single-pass of feed solution and circulating of stripping solution operation in HFSLM: (1) inlet feed reservoir (2)

stripping reservoir (3) HFSLM (4) flow regulator valve (5) flow indicator (6) pressure indicator (7) outlet feed reservoir (8) heating plate and (9) temperature control box

5.5. Result and discussion

5.5.1 Effect of pH of feed solution



The transference of Hg^{2+} through HFSLM was carried out in the following sequence. Mercury (II) ions in the feed solution are transported to a contact interface between the feed phase and the liquid membrane phase. Subsequently, Hg^{2+} react with Calix[4]arene nitrile resulting in the mercury–extractant complex. Then, the mercury–extractant complex diffuses across the liquid membrane phase to the liquid membrane stripping interface phase by the concentration gradient. The mercury–extractant complex, at the liquid membrane stripping interface, reacts continuously with de-ionized water from the stripping solution and is decomposed back to Hg^{2+} and the extractant. Hg^{2+} are released into the stripping phase while the extractant diffuses back to the liquid membrane phase by the concentration gradient and reacts again with the target ions at the feed–liquid membrane interface.

Based on the transport mechanism of Hg^{2+} across HFSLM, the concentration gradient of hydrogen ions between feed and stripping solutions proved to be a prominent driving force. In this work, the pH of feed solution in the ranges of 3–6 was studied, as shown in Fig. 5.3. The highest percentages of extraction and stripping of Hg^{2+} obtained were 98% and 96%, respectively. Results indicated that when the pH value increased up to 4.5, the percentages of extraction and stripping increased. Thereafter, the percentages of extraction and stripping decreased. This was in an agreement with an earlier report by Alpoquz et al. [18]. This phenomenon can be explained by the HSAB principle whereby $-\text{C} \equiv \text{N}$ group which is a soft base showing a stronger affinity towards soft acidic cation like Hg^{2+} [29]. Moreover, Hg^{2+} in feed solution at pH greater than 3 started to form $\text{Hg}(\text{OH})_2$ and became saturated at pH 5 [31]. The precipitate from $\text{Hg}(\text{OH})_2$ may foul the interfacial layer between feed and liquid membrane and impede overall ions transport. Therefore, the percentages of extraction and stripping decreased. Thus, the feed solution pH of 4.5 was considered as the optimum pH condition in the feed phase and is used in further experiments.

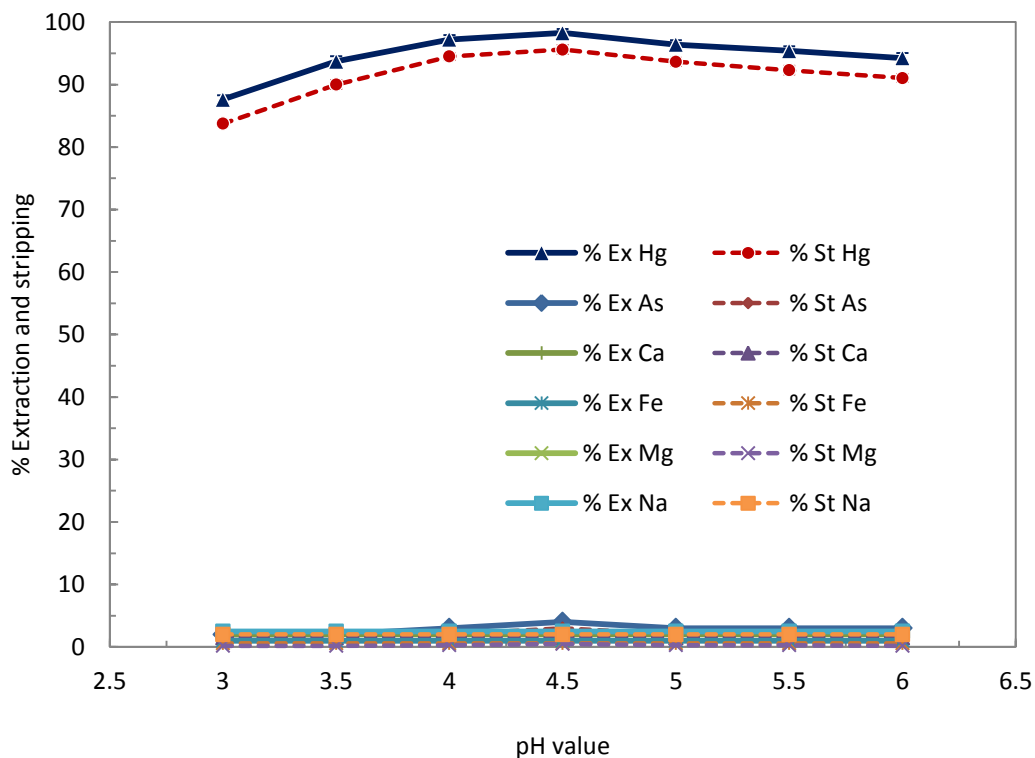


Figure 5.3 Percentages of mercury (II) ions vs pH value (extractant = 0.004 M Calix[4]arene nitrile; stripping = deionized water; flow rates = 100 mL/min. for both feed and stripping solutions; 303 K).

5.5.2 Effect of compositions of feed solution

The effect of compositions of feed solution was investigated using 0.004 M Calix[4]arene nitrile as the extractant. The results are shown in Fig. 5.4. Mercury (II) ions were found to be quantitatively extracted (98%) under the present experimental

conditions. Those above-mentioned ions will not form the complex [32]. Thus, mercury (II) ions can be selectively separated from the above metal ions using Calix[4]arene nitrile as extractant.

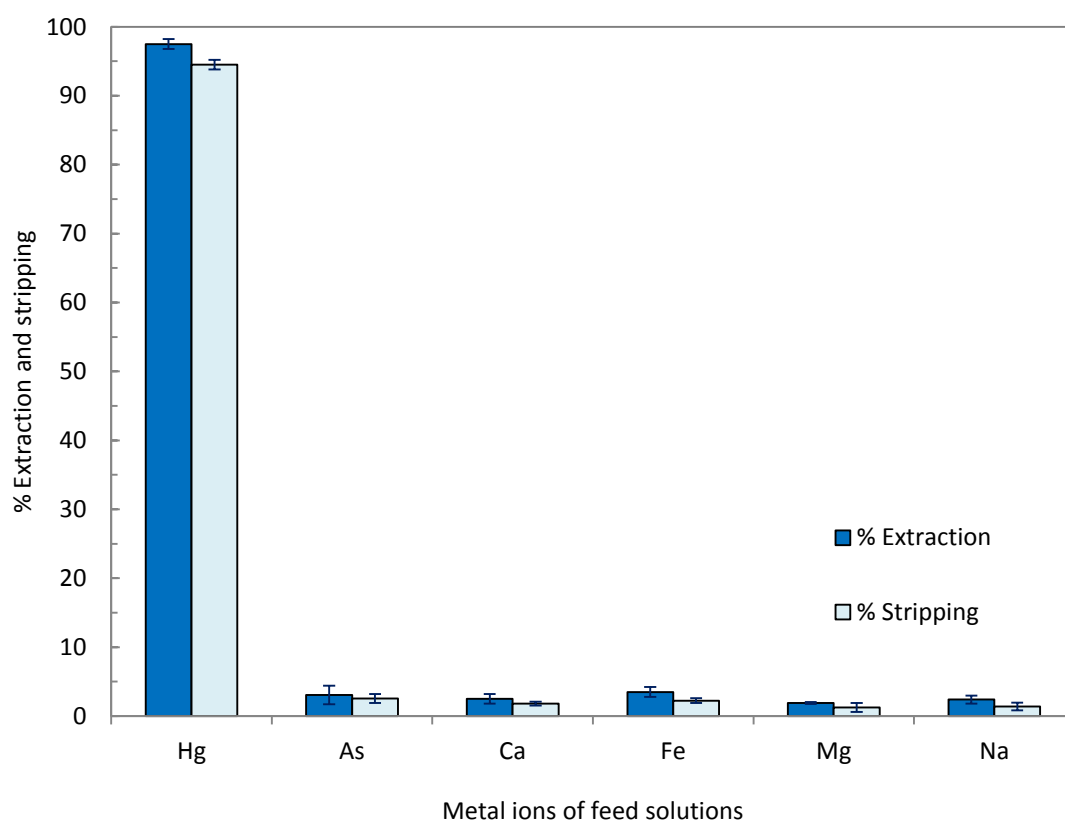


Figure 5.4 Percentages of mercury (II) ions vs metal ions of feed solutions (pH feed = 4.5; extractant = 0.004 M Calix[4]arene nitrile; stripping = de-ionized water; flow rate = 100 mL/min. for both feed and stripping solutions; 303 K).

5.5.3 Effect of concentration of extractant

The concentration of Calix[4]arene nitrile was investigated in the range of 1×10^{-3} – 6×10^{-3} M, as shown in Fig. 5.5. Percentages of extraction and stripping of Hg^{2+} increased when the concentration of Calix[4]arene nitrile increased in accordance with chemical kinetics. Maximum percentages of Hg^{2+} extraction and stripping of about 98% and 96% were achieved at 4×10^{-3} M Calix[4]arene nitrile. However, percentages of extraction and stripping of Hg^{2+} decreased when extractant concentration was higher than 4×10^{-3} M. This was due to an increase in viscosity in the liquid membrane that obstructed the mass transfer in the liquid membrane phase, corresponding to previous works [18]. Thus, 4×10^{-3} M Calix[4]arene nitrile was chosen to study further variables.

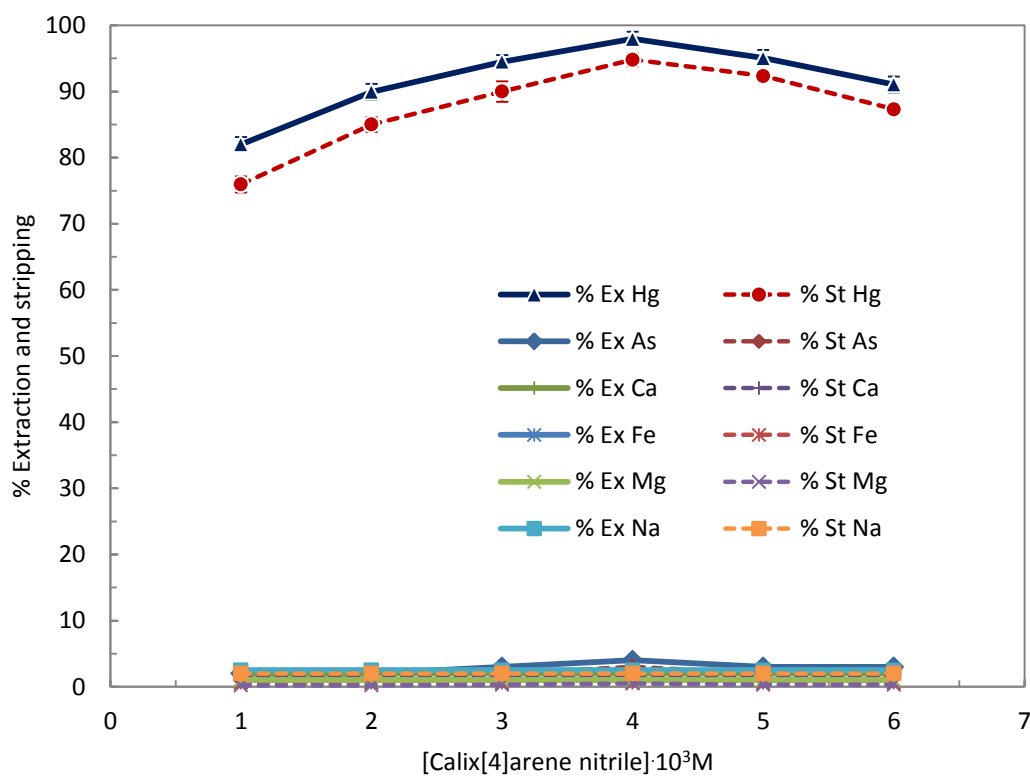


Figure 5.5 Percentages of mercury (II) ions vs concentration of Calix[4]arene nitrile (pH feed = 4.5; stripping = de-ionized water; flow rates = 100 mL/min. for both feed and stripping solutions; 303 K).

5.5.4 Effect of flow rates of both feed and stripping solutions

The effect of flow rates of both feed and stripping solutions was investigated using Hg^{2+} in petroleum produced water as feed solution. Flow rates of feed and stripping solutions were varied from 50 to 300 mL/min as shown in Fig. 5.6. Optimum

Figure 5.6 Percentage of mercury (II) ions vs flow rate of both feed and stripping solutions (pH feed = 4.5; extractant = 0.004 M Calix[4]arene nitrile; stripping = de-ionized water; 303 K).

5.5.5 Effect of temperature

The effect of temperature on the extraction of Hg^{2+} was investigated at 293-313 K. For Calix[4]arene nitrile, as shown in Fig. 5.7, the percentages of extraction and stripping of Hg^{2+} increased as temperature increased. This was in agreement with an earlier report by Alpoguz et al. [19] whereby extraction by Calix[4]arene nitrile is an endothermic reaction since the process is driven by heat input. From a starting temperature of 293 K, a step increment in temperature yielded a notable effect. When the temperature was raised above 303 K, the effect became less but still active. When operating at 313 K, the highest extraction and stripping was reported at 99.5 and 97.5 % respectively.

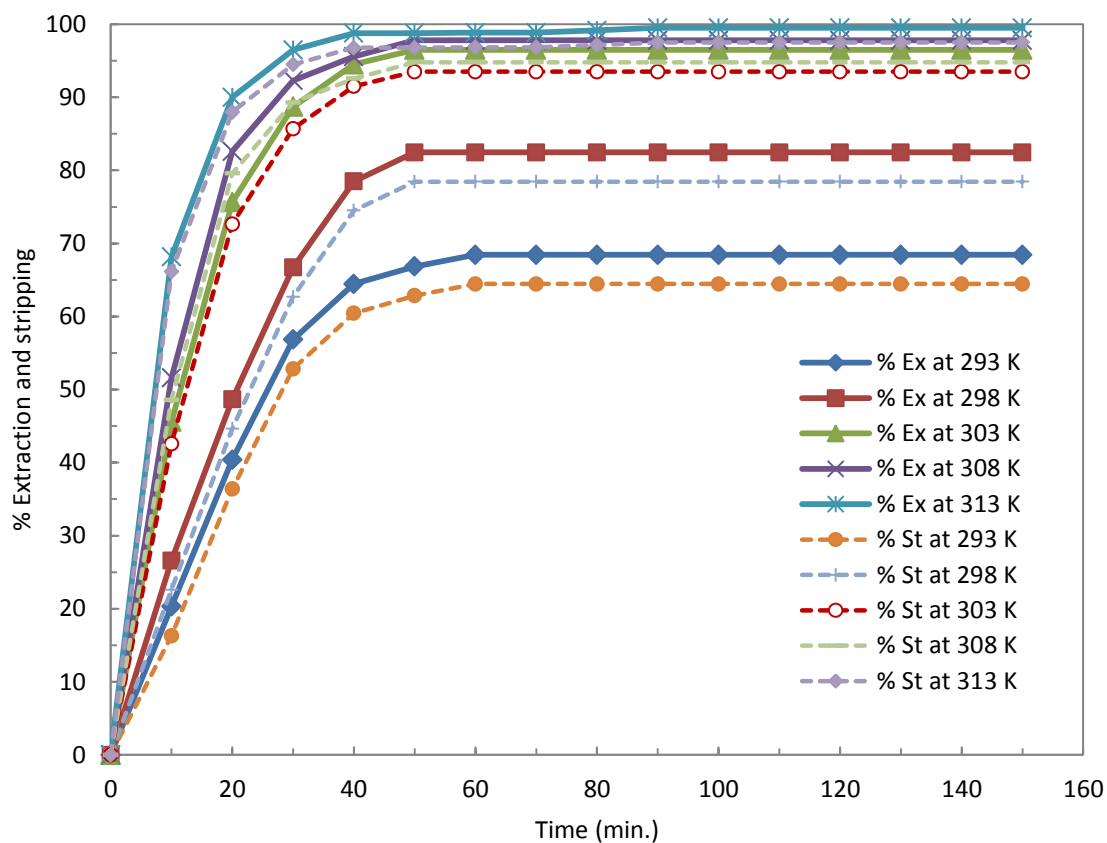
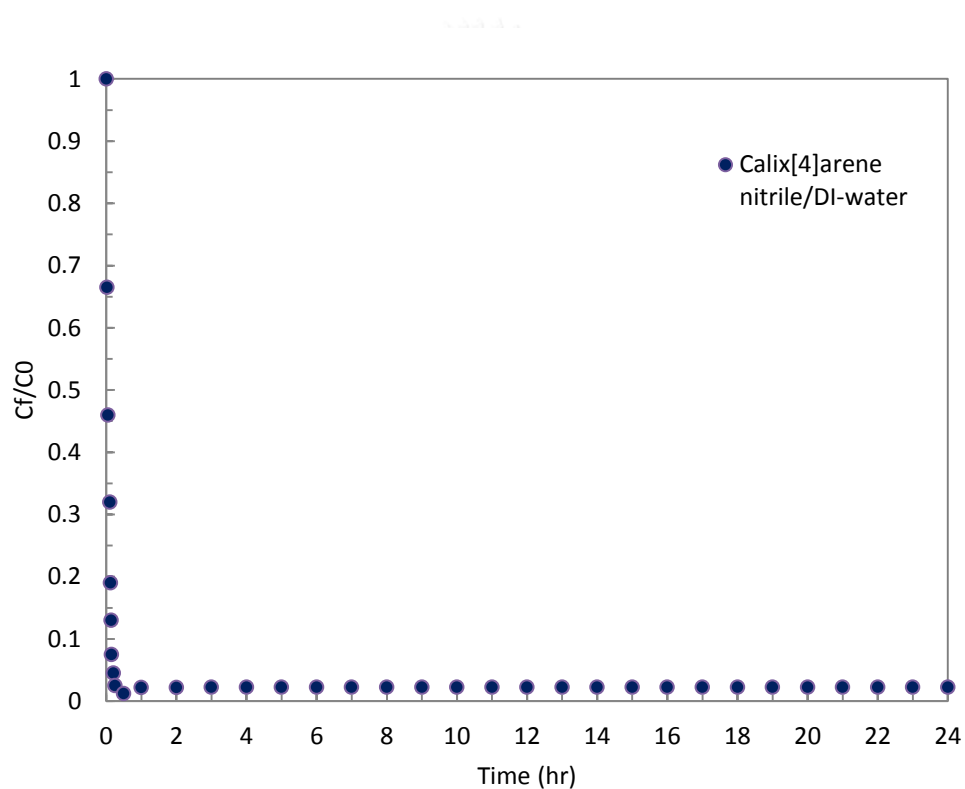


Figure 5.7 Effect of temperature feed = pH 1, extractant = 0.1M Aliquat 336; stripping = 0.05 M thiourea + 1% (v/v) HCl; flow rate = 100 mL/min. for both feed and stripping solutions

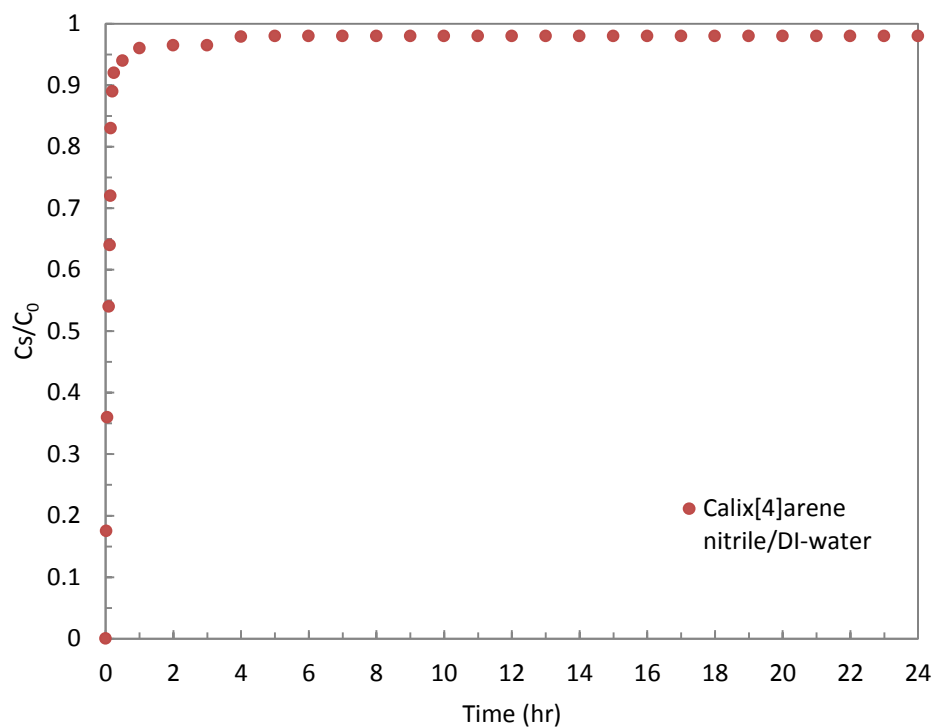
5.5.6 Stability

It is noteworthy that, despite its well-known advantages, the HFLSM system suffers from instability with time. This is mainly due to the loss of carrier and/or

membrane solvent from the membrane support which has an influence on both the flux and selectivity of the membrane [34]. The results are shown in Fig. 5.8. In this study, the liquid membrane was used for 24 hours. When Calix[4] arene nitrile was the extractant, the liquid membrane was found to be stable for at least 24 hours.



(a)



(b)

Figure 5.8 Comparison of stability of extractant (a) extraction (b) stripping

5.6. Conclusion

The investigation of the transport of Hg^{2+} impregnated with Calix[4]arene nitrile via HFSLM revealed that the best percentage of mercury (II) ions extraction from petroleum produced water was obtained at 99.5%. Further, the best percentage of stripping was obtained at 97.5%. Operating temperature was 313 K, feed solution was pH = 4.5 and 0.004 M Calix[4]arene nitrile was dissolved in NPOE.

This process offers the advantage of treatment in weak acid condition and stripping solution can simply be de-ionized water. It does not require strong pH in the feed solution and toxic stripping solution. On stability, the results showed that Calix[4]arene nitrile performed over 24 hours of continuous treatment. After treatment, Hg^{2+} from petroleum produced water in feed solution was found to be below the permissible discharge limit of 5 ppb.

5.7. Nomenclatures

r_i inner radius of the hollow fiber (cm)

r_o outer radius of the hollow fiber (cm)

t time (s)

T temperature (K)

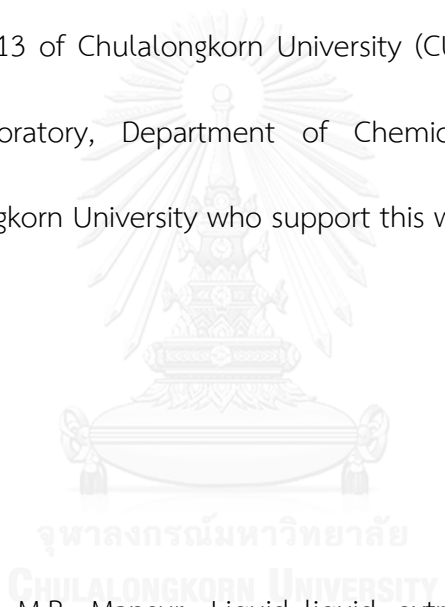
\mathcal{E} porosity of hollow fiber (%)

τ tortuosity factor membrane (-)

5.8. Acknowledgments

The author would like to express sincere gratitude towards the Thailand Research Fund and Chulalongkorn University under the Royal Golden Jubilee Ph. D Program (Grant No. PHD/0372/2552) as well as the Ratchadaphiseksomphot Endowment Fund 2013 of Chulalongkorn University (CU-56-387-CC). Thanks also to the Separation Laboratory, Department of Chemical Engineering, Faculty of Engineering, Chulalongkorn University who support this work

5.9. References

- 
- [1] F.D.M. Fábrega, M.B. Mansur, Liquid-liquid extraction of mercury (II) from hydrochloric acid solutions by Aliquat 336, *Hydrometallurgy* 87 (2007) 83-90.
- [2] D.K. Mondal, B.K. Nandi, M.K. Purkait, Removal of mercury (II) from aqueous solution using bamboo leaf powder: Equilibrium, thermodynamic and kinetic studies, *J. Environ. Chem. Eng.* 1 (2013) 891-898.
- [3] M. Kılıç, M.E. Keskin, S. Mazlum, N. Mazlum, Effect of conditioning for Pb(II) and Hg(II) biosorption on waste activated sludge, *Chem. Eng. Proc.: Process Intensification*, 47 (2008) 31-40.

- [4] K.F. Lam, H. Kassab, M. Pera-Titus, K.L. Yeung, B. Albela, L. Bonneviot, MCM-41 “LUS”: Alumina Tubular Membranes for Metal Separation in Aqueous Solution, *J. Phys. Chem. C* 115 (2010) 176-187.
- [5] I.M. Coelho, M.M. Cardoso, R.M.C. Viegas, J.P.S.G. Crespo, Transport mechanisms and modelling in liquid membrane contactors, *Sep. Purif. Technol.* 19 (2000) 183-197.
- [6] P.C. Rout, K. Sarangi, A comparative study on extraction of Mo(VI) using both solvent extraction and hollow fiber membrane technique, *Hydrometallurgy*. 133 (2013) 149-155.
- [7] M.F. San Roman, E. Bringas, R. Ibanez, I. Ortiz, Liquid membrane technology: fundamentals and review of its applications, *J. Chem. Technol. Biotechnol.* 85 (2010) 2-10.
- [8] N.M. Kocherginsky, Q. Yang, L. Seelam, Recent advances in supported liquid membrane technology, *Sep. Purif. Technol.* 53 (2007) 171-177.
- [9] P.K. Mohapatra, V.K. Manchanda, Liquid membrane-based separations of actinides. In: Pabby, A.K., Rizvi, S.S.H., Sastre, A.M. (Eds.), *Handbook of Membrane Separations: Chemical, Pharmaceutical, Food and Biotechnological Applications*. CRC Press, pp. 883–918., (2009).

- [10] B.F. Jirjis, S. Luque, Chapter 9 - Practical aspects of membrane system design in food and bioprocessing applications, in: Z.F. Cui, H.S. Muralidhara (Eds.) Membrane Technology, Butterworth-Heinemann, Oxford, 2010, pp. 179-212.
- [11] Z. Lazarova, B. Syska, K. Schügerl, Application of large-scale hollow fiber membrane contactors for simultaneous extractive removal and stripping of penicillin G, *J. Membr. Sci.* 202 (2002) 151-164.
- [12] K. Tang, C. Zhou, X. Jiang, Racemic ofloxacin separation by supported-liquid membrane extraction with two organic phases, *Sc. China Ser. B-Chem.* 46 (2003) 96-103.
- [13] U. Pancharoen, A.W. Lothongkum, S. Chaturabul, in: M. El-Amin. (Ed.), Mass Transfer in Multiphase Systems and its Applications, InTech, India, 2011, pp. 499-524.
- [14] R. Guell, E. Antico, V. Salvado, C. Fontas, Efficient hollow fiber supported liquid membrane system for the removal and preconcentration of Cr(VI) at trace levels, *Sep. Purif. Technol.* 62 (2008) 389-393.
- [15] L.D. Mafu, T.A.M. Msagati, B.B. Mamba, The enrichment and removal of arsenic (III) from water samples using HFSLM, *Phys. Chem. Earth.* 50-52 (2012) 121-126.

- [16] C. Fontàs, M. Hidalgo, V. Salvadó, E. Anticó, Selective recovery and preconcentration of mercury with a benzoylthiourea-solid supported liquid membrane system, *Anal. Chim. Acta.* 547 (2005) 255-261.
- [17] I.H. Gubbuk, O. Gungor, H.K. Alpoguz, M. Ersoz, M. Yilmaz, Kinetic study of mercury (II) transport through a liquid membrane containing calix[4]arene nitrile derivatives as a carrier in chloroform, *Desalination* 261 (2010) 157-161.
- [18] H. Korkmaz Alpoguz, A. Kaya, S. Memon, M. Yilmaz, Kinetic Study of Hg²⁺ Transport Through a Liquid Membrane Containing Calix[4]arene Dinitrile Oligomer as Carrier, *J. Macrom. Sci. Part A* 42 (2005) 1159-1168.
- [19] H.K. Alpoguz, S. Memon, M. Ersoz, M. Yilmaz, Transport of Hg²⁺ Ions across a Supported Liquid Membrane Containing Calix[4]arene Nitrile Derivatives as a Specific Ion Carrier, *Sep. Sci. Technol.* 40 (2005) 2365-2372.
- [20] A. Jabbari, M. Esmaili, M. Shamsipur, Selective transport of mercury as HgCl₄²⁻ through a bulk liquid membrane using K⁺-dicyclohexyl-18-crown-6 as carrier, *Sep. Purif. Technol* (2001) 139–145.
- [21] A.B. Shaik, K. Chakrabarty, P. Saha, A.K. Ghoshal, Separation of Hg(II) from Its Aqueous Solution Using Bulk Liquid Membrane, *Ind. Eng. Chem. Res.* 49 (2010) 2889-2894.

- [22] K. Chakrabarty, P. Saha, A.K. Ghoshal, Simultaneous separation of mercury and lignosulfonate from aqueous solution using supported liquid membrane, *J. Membr. Sci.* 346 (2010) 37-44



CHAPTER 6

6.1. Conclusions

In this study, HFSLM can effectively separate mercury ions in ppb (by weight) level from petroleum produced water. The concentrations of discharged mercury ions comply with the regulatory discharge limits, of which the concentration is not higher than 5 ppb, by the extraction and stripping of mercury (II) ions in a single-step operation via HFSLM application. As stated earlier in the previous Chapters, treatment at this stringent level is hardly achievable by conventional techniques.

6.1.1 Effects to the performance

To investigate and learn various variables that influence the system performance, we have first to set up the experiment properly. In this work, the experiment was set up with a single-pass feed and circulating stripping solution through HFSLM. This setup offers continuous treatment of the produced water effluent. The stripping solution, which was circulating in limited volume, offers a manageable volume for waste disposal after the stripping solution becomes

saturated. Although, the best performance, as investigated in Chapter IV, was reported from the batch treatment, i.e. feed and strip in full circulation, it is considered impractical for industrial applications where the feed is large and continuous. For some marginal oil production field, the produced water is reported with the range up to 50,000 barrels of water per day. It required the huge hold-up vessels for the treatment in this case. Unfortunately, it is uncommon for offshore structure to offer space and weight spare to accommodate such the big hold-up vessels. On the contrary, the reasonable size of hold-up vessel can be acquired from the single-pass feed and circulating stripping solution through HFLSM, which demonstrates a promising solution for mercury treatment by a single-pass flow.

For the produced water that was adopted as the feed in this study, it has ions contaminations ranging from arsenic, calcium, ferric, sodium and etc. The study revealed to no or very little interference to the separation performance. The mercury (II) ions can be selectively extracted up to 98%.

Pretreatment to the feed solution is necessary in this system. HCl solution was used to deprotonate mercury chloride compound in the feed and to adjust pH in order to maintain driving force throughout the separation. For the latter, the concentration gradient of hydrogen ions from HCl was revealed to be a prominent driving force between feed and stripping solutions. In the early stages, with an

increase of HCl concentration, we observed an increase in the extraction and recovery of mercury (II). This was in accordance with Le Chatelier's Principle whereby increasing the concentration of the reactants drives the reaction forwards. However, in later stages with further increase, mercury (II) extraction became decreased. This was simply because the system turned out to be highly acidic, which is unsuitable condition for the extraction.

In this study, several diluents with different polarity indexes were chosen i.e. nitrobenzene, dichloromethane, chloroform, xylene and toluene. The polarity indexes of the diluents are shown in Table 4.6. Results show that the percentage of extraction of mercury (II) varies with the nature of the diluents. Generally, when the dielectric constant and the dipole moment of diluents decrease, extraction increases. This can be explained by the fact that the interaction of diluents, having high dielectric constant with the extractant, are generally stronger than those of low dielectric constant e.g. toluene. Strong interaction of diluents with an extractant can result in a lower extraction of metal ions.

From the reagent perspectives, it exhibited highly important role in this separation system. Two different reagent hybrids were investigated in this study as follows:

Aliquat 336 (extractant) – Thiourea (stripping)

The mechanism began with mercury (II) exchanging chloride ions with Aliquat 336 and subsequently generating mercury complex in the extraction reaction. The complex, once formed, would selectively diffuse to the opposite side of the liquid membrane and reacted with Thiourea for decomposition. Thiourea was selected since it had been reported as having outstanding performance for use as a stripping solution for mercury (II) recovery. It has large anions in the structure, which is strong enough to strip mercury complex ions from Aliquat 336, which is a large organic cation associated with chloride ions. Other advantage of using thiourea, it generates no trace of precipitates unlike NaOH which produced precipitates with mercury (II) resulting in membrane fouling and poor transport performance in the membrane phase.

In this study, we established optimum condition at 0.2M HCl, 4% (v/v) Aliquat 336 for extractant and 0.1 M thiourea for stripping solution. The best percentage obtained for extraction was 99.73% and for recovery 90.11%, respectively. The optimum concentration above was identified by varying concentration. From the result with Aliquat 336 extractant, it showed that when Aliquat 336 concentration increased in the range of 0.5 – 4 % (v/v), extraction and recovery percentage of mercury (II) was of a higher tendency. This was because Aliquat 336 as a reactant

pushed the reaction further forwards generating more mercury complex ions in the liquid membrane. Therefore, the extraction rate was higher. Likewise, when more mercury complex ions formed in the liquid membrane, more mercury (II) could be recovered at the stripping phase. In contrast, the percentage of extraction and recovery declined when concentration was more than 4% (v/v). This decline was due to the viscosity effect from higher extractant concentration. This hindered effective diffusion of the metal complex through the liquid membrane phase resulting in the drop in performance.

With Thiourea, the concentration was varied between 0.05 – 0.5 M. The result showed that the percentage of mercury ions recovery increased until Thiourea concentration reached 0.1 M. Subsequently, the percentage of recovery decreased due to concentration polarization. Thus, in this case, Thiourea concentration of 0.1 M yielded the best recovery.

The mass transfer resistance was also investigated. The overall system was described with the overall mass transfer resistance through HFSLM, which is equal to the sum of all the individual mass-transfer resistances consisting of (1) the feed-side resistance (R_{df}), (2) the interfacial resistance of extraction reaction (R_e), (3) the liquid membrane phase resistance (R_m), (4) the shell-side resistance (R_o), (5) the interfacial resistance of stripping reaction (R_s) and (6) the strip-side resistance (R_{os}). To simplify

the study, the resistance term from stripping reaction was negligible because the stripping reaction was completed almost instantaneously during the HFSLM process.

The overall mass transfer resistance was determined experimentally. This was found to be $R = 7.286 \times 10^2$ s/cm. The mass transfer resistances from the extraction reaction, the shell side mass transfer resistances and the mass transfer resistances from the feed side proved to be much higher than that from the membrane phase. This indicated that the mass transfer resistance in the membrane phase had little effect on the overall mass transfer process.

Applying the calculated mass transfer resistance in the model as the part of verification, the results indicated that when the concentration of Aliquat 336 was $\leq 5\%$ (v/v), the mass transfer model proved satisfactory. However, when the concentration of Aliquat 336 was more than 5% (v/v), the mass transfer model was poor. So, when the concentration of Aliquat 336 was higher than 5% (v/v), the viscosity of the liquid membrane was very high. This resulted in the obstruction of the mass transfer while the metal-complex accumulated in the liquid membrane. Moreover, the free Aliquat 336 molecule was difficult to transport. Therefore, higher than 5%(v/v) concentration of Aliquat 336 did not match the experimental results.

Calix (extractant) – Deionised water (stripping)

Alternative to the preceding system, Calix[4]arene nitrile was deployed as mercury (II) ions extractant. Calix[4]arene nitrile has the capacity to capture Hg^{2+} in weak acid condition and thereby can form mercury complex ions. The complex ions are in co-ordination bond which is reasonably strong but not too hard for a neutral-based stripping solution to break the bond. Mechanism describes the system with mercury (II) reacting with Calix[4]arene nitrile resulting in the mercury–extractant complex. Then, the mercury–extractant complex diffuses across the liquid membrane phase to the liquid membrane stripping interface phase by the concentration gradient. The mercury–extractant complex, at the liquid membrane stripping interface, reacts continuously with de-ionized water from the stripping solution and is decomposed back to Hg^{2+} and the extractant. Hg^{2+} are released into the stripping phase while the extractant diffuses back to the liquid membrane phase by the concentration gradient and reacts again with the target ions at the feed–liquid membrane interface.

This system offers the advantage of treatment in weak acid condition and stripping solution can simply be de-ionized water. The optimum pH value was registered at 4.5. Lower further the pH, the system performance declined. The acidic condition favored the reaction to generate $\text{Hg}(\text{OH})_2$ precipitate. The precipitate

caused fouling at the interfacial layer between feed and liquid membrane and impede overall ions transport.

The investigation of the transport of Hg^{2+} impregnated with Calix[4]arene nitrile via HFSLM revealed that the best percentage of mercury (II) ions extraction from petroleum produced water was obtained at 99.5%, whereas, the best percentage of stripping was obtained at 97.5%. It was obtained at optimum condition at 313 K, 4.5 pH in feed solution and 0.004 M Calix[4]arene nitrile.

The effect of temperature on the extraction of Hg^{2+} was investigated at 293-313 K. Extraction by Calix[4]arene nitrile was found to be endothermic reaction. Therefore, the percentages of extraction and stripping of Hg^{2+} increased as temperature increased. From a starting temperature of 293 K, a step increment in temperature yielded a notable effect. When the temperature was raised above 303 K, the effect became less but still active. When operating at 313 K, the highest extraction and stripping was reported at 99.5 and 97.5 % respectively.

System stability was observed. Despite its well-known advantages, the HFSLM system suffers from instability with time. This is mainly due to the loss of carrier and/or membrane solvent from the membrane support which has an influence on both the flux and selectivity of the membrane. However, in this system, the

performance was found to be stable for at least 24 hours. It appeared to be the promising solution for industrial application.

6.1.2 Prediction from mathematical model

Along with the experiments, a mathematical model was developed and presented. The model followed the schema taking combined fluxes i.e. convection–diffusion–kinetic into account. This is a significant feature posed by the proposed model in order to provide a more realistic unsteady time dependent. Prior to obtaining this model, we started it from Pancharoen U. et al. model that describes the metal ion transport in the feed and stripping phase with reaction flux influence.

Applying the above reaction flux principle to the Pd separation from aqua regia reagent, the full transport model from the feed to the stripping was developed. The key assumption for the model is that perfect mixing occurs within the sheer small cross sectional area of the inner hollow fiber tube. In consequence, there is no variation in ion concentration across the cross-sectional area but only in the axial direction, arising from reaction flux along the hollow fiber tube. The flow moves through the annulus as a series of infinitely thin coherent “plugs”. Following complete mixing, each plug has a uniform metal ion concentration. Each plug has a

slightly different ion concentration to the plugs immediately preceding and following it, due to the progressive conversion of metal ions into their complexes. For the transport within hollow fiber micropore for the mercury (II) complex to diffuse from feed to stripping phase, Fick's law is used.

The rate constant for mercury (II) extraction and recovery was determined and revealing that this system appears to obey a pseudo-second-order rate equation in which both extraction and stripping depends on the concentration of only one reactant. The rate constants of extraction reaction (k_f) and the stripping reaction (k_s) were 9.96×10^{-3} and $2.39 \times 10^{-3} \text{ cm}^3 \cdot \text{mg}^{-1} \cdot \text{min}^{-1}$ from the slopes of the respective plots. The k_f term was used to calculate the concentration profile of the feed phase in the tube. Similarly, the term k_s term was used to calculate the concentration profile in the stripping phase. For the membrane, the k_m term was applied in order to calculate the concentration profile following the transport of mercury (II) across the micro-pore sites of the membrane phase. The mass transfer coefficient in the membrane phase (k_m) was calculated as $7.02 \text{ cm} \cdot \text{min}^{-1}$.

With all inputs available, the model was computed. The outcome indicated that the hypothetical result for the recycling scenario showed good agreement with experiment data; the average percentage of deviation was 10.52% for the extraction

case and only 1.66 % for recovery. It was consistent although the third cycle elapsed.

The results from the varying flowrate scenario were less satisfactory. At 300 mL·min⁻¹ flowrate, the deviation was large (> 90%), i.e. 2.47 mg·L⁻¹ (Exp.) vs. 4.94 mg·L⁻¹ (Hypo.). A mismatch from the model parameter is likely to have been a contributory factor. The reaction rate constant was one of the parameters subsequently considered for review, given that the constant was from the reaction data running through HFSLM at 100 mL·min⁻¹. The use of the same constant may not be appropriate in cases of higher flowrate.

Advancing from above reaction flux model, a new mathematical model was developed from the basis of a combined flux principle i.e. convection–diffusion–kinetic and accumulation of mercury (II).

The result from new model was put in comparison which previous models including the works of Pancharoen et al. and Kandwal et al. Pancharoen et al. developed a model based on chemical reaction and conventional flux (neglecting diffusion); average standard deviations for extraction and recovery were 8.5% and 9.1%, respectively. Kandwal et al. developed their model based on the principle of a facilitated diffusional transport mechanism (neglecting conventional and chemical

reactions); average standard deviations for extraction and recovery were 9.8% and 8.4%, respectively. The model results from Pancharoen et al. and Kandwal et al. aligned with the experimental data to a great extent but still exhibited a high deviation. In contrast, the predicted results of the model, based on the combined convection–diffusion–kinetic flux in presence with mass accumulation term (non-steady), demonstrated very good agreement with the experimental results. For predictions in feed and recovery solutions, average percent deviations were low at 1.5% and 1.8%, respectively. This confirmed that the conservation of mass which consisted of convection, diffusion, reaction and accumulation were very important factors in controlling the rate of transport of mercury (II) along the hollow fibers. The results imply that the combination of convection, diffusion and reaction is crucial for accurate prediction in this unsteady state model. This robust model with its high accuracy provides a greater understanding of transport mechanism across the feed to the stripping solution; a design scale-up for industrial application could prove useful.

6.2. Recommendations for future studies

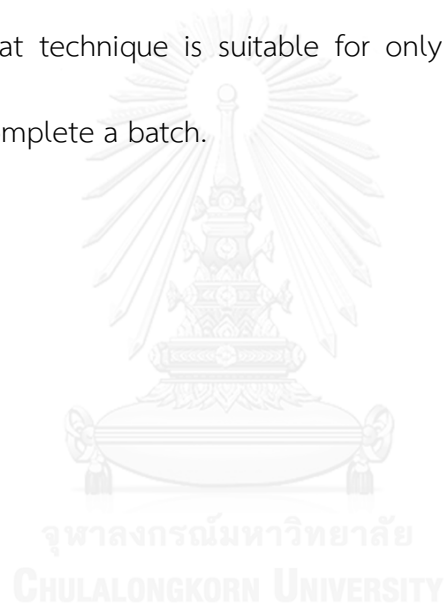
HFLSM have been widely studied for the separation and concentration of mercury (II) from petroleum produced water. It demonstrates the capability of neat

treatment to achieve an output level at stringent requirement of 5 ppb. However, there have been none at the pilot scale in actual field condition to prove the potential for deployment at full scale. Study at pilot scale treatment shall be the next Chapter after comprehensive studies of laboratory experiment. The parameters to be focused are suggested with the extraction & recovery performance in actual field operation, system stability and susceptibility to the contamination from which the feed is unlikely to be hydrocarbon free.

On the mathematical model, it is viewed that the model can be developed further to dimensionless form. With the dimensionless form, it should offer robust model for prediction at the universal flux spectrum. The dimensionless parameters can be adopted from presently defined dimensionless number. For instance, reaction flux with Damköhler number that relates the reaction timescale to the convection times scale, flow rate, through the HFSLM; diffusion flux with Schmidt number that relates viscosity and density to the diffusivity for mass transfer.

For the last but not the least important, HFSLM study can be extent to an application of hydrocarbon liquid treatment. It is not only petroleum produced water that suffers contamination from mercury. The petroleum hydrocarbon is, as well, suffering it. Excessive mercury in the hydrocarbon feed can poison process equipment in the plant facility by reacting with construction material of that

equipment to generate mercury amalgam product. Generally, the feed with 50 ppb wt. mercury is acceptable in most of the processing plant. HFSLM can be considered as a potential good choice for the treatment since it can handle continuous and large amount of industrial feed. It should overcome the deficiency from our previous work that applied Pulsed Sieve Plate Technique to treat arsenic in hydrocarbon liquid [appendix]. That technique is suitable for only batch treatment and poses lengthy process to complete a batch.



REFERENCES



REFERENCES

- [1] D.L. Gallup, J.B. Strong, Removal of Mercury and Arsenic from Produced Water, Chevron Corporation Chevron Corporation, 2007.
- [2] F.T. Minhas, S. Memon, M.I. Bhangar, Transport of Hg(II) through bulk liquid membrane containing calix[4]arene thioalkyl derivative as a carrier, *Desalination* 262 (2010) 215-220.
- [3] S.F. CH. Ngim, K.W. Boey, J. Keyaratnam, Chronic neurobehavioral effects of elemental mercury in dentists, *British J. of Industrial Medicine* 49 (1992) 782–790.
- [4] Y.X. Liang, R.K. Sun, Y. Sun, Z.Q. Chen, L.H. Li, Psychological Effects of Low Exposure to Mercury Vapor: Application of a Computer-Administered Neurobehavioral Evaluation System, *Environmental Research* 60 (1993) 320-327.
- [5] S. Gupta, M. Chakraborty, Z.V.P. Murthy, Optimization of process parameters for mercury extraction through pseudo-emulsion hollow fiber strip dispersion system, *Separation and Purification Technology* 114 (2013) 43-52.
- [6] S. Díez, Human health effects of methylmercury exposure, 2009, pp. 111-132.

- [7] <http://www.dmf.go.th/service/monthlyReport.php?m=2&y=2015&ln=en>, 27/3/2015.
- [8] <http://www.dmf.go.th/index.php?act=service&sec=map&ln=en>, 27/3/2015.
- [9] S. Chiarle, M. Ratto, M. Rovatti, Mercury removal from water by ion exchange resins adsorption, *Water Research* 34 (2000) 2971-2978.
- [10] J.A. Ritter, J.P. Bibler, Removal of mercury from waste water: Large-scale performance of an ion exchange process, *Water Science and Technology* 25 (1992) 165-172.
- [11] W.R. Knocke, L.H. Hemphill, Mercury(II) sorption by waste rubber, *Water Research* 15 (1981) 275-282.
- [12] J.Y. Lu, W.H. Schroeder, Comparison of conventional filtration and a denuder-based methodology for sampling of particulate-phase mercury in ambient air, *Talanta* 49 (1999) 15-24.
- [13] Q. Wang, X. Chang, D. Li, Z. Hu, R. Li, Q. He, Adsorption of chromium(III), mercury(II) and lead(II) ions onto 4-aminoantipyrine immobilized bentonite, *Journal of Hazardous Materials* 186 (2011) 1076-1081.
- [14] B.S. Inbaraj, J.S. Wang, J.F. Lu, F.Y. Siao, B.H. Chen, Adsorption of toxic mercury(II) by an extracellular biopolymer poly(γ -glutamic acid), *Bioresource Technology* 100 (2009) 200-207.

- [15] C. Jeon, H.P. Kwang, Adsorption and desorption characteristics of mercury(II) ions using aminated chitosan bead, *Water Research* 39 (2005) 3938-3944.
- [16] V.K. Gupta, P. Singh, N. Rahman, Adsorption behavior of Hg(II), Pb(II), and Cd(II) from aqueous solution on Duolite C-433: A synthetic resin, *Journal of Colloid and Interface Science* 275 (2004) 398-402.
- [17] X. Chai, X. Chang, Z. Hu, Q. He, Z. Tu, Z. Li, Solid phase extraction of trace Hg(II) on silica gel modified with 2-(2-oxoethyl)hydrazine carbothioamide and determination by ICP-AES, *Talanta* 82 (2010) 1791-1796.
- [18] D.C. Nambiar, N.N. Patil, V.M. Shinde, Liquid-liquid extraction of mercury(II) with triphenylphosphine sulphide: Application to medicinal and environmental samples, *Fresenius J Anal Chem* 360 (1998) 205-207.
- [19] S. Sangtumrong, P. Ramakul, C. Satayaprasert, U. Pancharoen, A.W. Lothongkum, Purely Separation of Mixture of Mercury and Arsenic via Hollow Fiber Supported Liquid Membrane, *Journal of Industrial and Engineering Chemistry* 13 (2007) 751-756.
- [20] K. Tang, C. Zhou, X. Jiang, Racemic ofloxacin separation by supported-liquid membrane extraction with two organic phases, *Sc. China Ser. B-Chem.* 46 (2003) 96-103.

- [21] M. Takht Ravanchi, T. Kaghazchi, A. Kargari, Application of membrane separation processes in petrochemical industry: a review, *Desalination* 235 (2009) 199-244.
- [22] A.W. Lothongkum, U. Pancharoen, T. Prapasawat, Roles of facilitated transport through HFSLM in engineering applications, 2011.
- [23] U. Pancharoen, W. Poonkum, A.W. Lothongkum, Treatment of arsenic ions from produced water through hollow fiber supported liquid membrane, *Journal of Alloys and Compounds* 482 (2009) 328-334.
- [24] I.M. Coelho, M.M. Cardoso, R.M.C. Viegas, J.P.S.G. Crespo, Transport mechanisms and modelling in liquid membrane contactors, *Separation and Purification Technology* 19 (2000) 183-197.
- [25] Thailand Regulatory Discharge Standards 2, Ministry of Industry, Thailand. 1996.
- [26] C. Ferens, U.S.E.P.A.O.o. Research, Development, A review of the physiological impact of mercurials, For sale by the Supt. of Docs., U.S. Govt. Print. Off.1974.
- [27] MCT, MCT Redbook: solvent extraction reagents and applications.
- [28] A. Manuel, L.C. Jose, Solvent extraction and membranes, fundamentals and applications in new materials, CRC Press, the United States of America, 2008.

- [29] T. Wannachod, N. Leepipatpiboon, U. Pancharoen, K. Nootong, Synergistic effect of various neutral donors in D2EHPA for selective neodymium separation from lanthanide series via HFSLM, *Journal of Industrial and Engineering Chemistry* 20 (2014) 4152-4162.
- [30] A.O. Adebayo, K. Sarangi, Separation of copper from chalcopyrite leach liquor containing copper, iron, zinc and magnesium by supported liquid membrane, *Separation and Purification Technology* 63 (2008) 392-399.
- [31] J.G. Malecki, A. Maron', I. Gryca, M. Serda, Characterization of a PdII complex with (E)-8-hydroxyquinoline-2-carbaldehyde O-benzyl oxime, *Mendeleev Communications* 24 (2014) 26-28.
- [32] T.W. Chapman, Chapter 8, Extraction – Metals Processing, in: R.W. Rousseau (Ed.) *Handbook of Separation Process Technology*, John Wiley & Sons, Inc., Canada, 1997, pp. 467–499.
- [33] F.d.M. Fábrega, M.B. Mansur, Liquid–liquid extraction of mercury (II) from hydrochloric acid solutions by Aliquat 336, *Hydrometallurgy* 87 (2007) 83-90.
- [34] E. Bringas, MF. San Román, JA. Irabien and I. Ortiz, An overview of the mathematical modelling of liquid membrane separation processes in hollow fiber contactors, In: *J. Chem Technol Biotechnol* 84 (2009) 1583-1614.

- [35] K.R. Chitra, A.G. Gaikwad, G.D. Surender, A.D. Damodaran, Studies on ion transport of some rare earth elements through solvating extractants immobilised on supported liquid membrane, *Journal of Membrane Science* 125 (1997) 257-268.
- [36] D. Wu, Q. Zhang, B. Bao, Solvent extraction of Pr and Nd (III) from chloride-acetate medium by 8-hydroquinoline with and without 2-ethylhexyl phosphoric acid mono-2-ethylhexyl ester as an added synergist in heptane diluent, *Hydrometallurgy* 88 (2007) 210-215.
- [37] S. Chaturabul, K. Wongkaew, U. Pancharoen, Selective Transport of Palladium through a Hollow Fiber Supported Liquid Membrane and Prediction Model Based on Reaction Flux, *Separation Science and Technology* 48 (2012) 93-104.
- [38] S. Chaturabul, W. Srirachat, T. Wannachod, P. Ramakul, U. Pancharoen, S. Kheawhom, Separation of mercury(II) from petroleum produced water via hollow fiber supported liquid membrane and mass transfer modeling, *Chemical Engineering Journal* 265 (2015) 34-46.
- [39] S. Chaturabul, T. Wannachod, N. Leepipatpiboon, U. Pancharoen, S. Kheawhom, Mass transfer resistance of simultaneous extraction and stripping of mercury(II) from petroleum produced water via HFSLM, *Journal of Industrial and Engineering Chemistry* 21 (2015) 1020-1028.

- [40] S. Chaturabul, T. Wannachod, V. Mohdee, U. Pancharoen, S. Phatanasri, An investigation of Calix[4]arene nitrile for mercury(II) treatment in HFSLM application, Chemical Engineering and Processing: Process Intensification 89 (2015) 35-40.



APPENDIX



APPENDIX A

Arsenic Removal from Natural-Gas Condensate using a Pulsed Sieve Plate

Column and Mass Transfer Efficiency

Srestha Chaturabul^a, Pharannalak Wannachod^a, Bongkotch Rojanasiraprapa^a, Supat Summakasipong^b, Anchaleeporn W. Lothongkum^c, Ura Pancharoen^{a,*}

a: Department of Chemical Engineering, Chulalongkorn University, Pathumwan Bangkok 10330, Thailand.

b: Department of Chemical Engineering Pathumwan Institute of Technology, Pathumwan Bangkok 10330, Thailand

c: Department of Chemical Engineering, Faculty of Engineering, King Mongkut's Institute of Technology Ladkrabang, Ladkrabang, Bangkok 10520, Thailand.

This article has been published in Journal: Separation Science and Technology.

Page: 432-439. Volume: 47. Year: 2012

A.1 Abstract

The aspect of using a pulsed sieve plate column for treatment of the arsenic contaminating natural-gas condensate is firstly introduced in this paper. The treatment involves the pulsed sieve plate column in conjunction with the liquid-liquid extraction technique. The pulsed sieve plate column is considered as the ideal unit of operation to cope with natural gas condensate because of its wet material invulnerable to hydrocarbon organic solvation. Moreover it utilises pulsation unit to enhance mass transfer without the need of rotating mechanical internals to deal with the viscous type liquid such as the natural gas condensate in this case. The several important parameters such as extractant type, extractant concentration, pulse velocity, volumetric-flow rate ratio, operating time and cycle were investigated. Mass-transfer efficiency in term of the overall height of transfer unit (HTU_{oy} , cm) and an interfacial area (m^2/m^3) were calculated. The highest percentage of arsenic removal from the study was 94% corresponding to the calculated HTU_{oy} of 26 cm and the calculated interfacial area of $118 m^2/m^3$ at the optimum conditions: the mixed extractant between 1M hydrochloric acid and 20% (v/v) methanol, the pulse velocity of 20 mm/s and the volumetric-flow rate ratio of the condensate to extractant at 1:4. With the continuous operation in cycle mode, the removal percentages were

observed at 94, 85 and 80 from the respective 1st – 3rd cycle, behaving in a linear decline trend. The operation was on the condition that the fresh feed (504 ppb arsenic) was introduced in each cycle while the extractant solvent was reused.

Keywords: arsenic; condensate; natural gas; extraction; pulsed sieve plate column

Corresponding author: Tel. +66-022186891; Fax. +66-022186877

E-mail address: ura.p@chula.ac.th



A.2 Introduction

Natural-gas condensate is the low density liquid hydrocarbon generally produced in association with natural gas. It presents as gas phase in subsurface reservoir condition and subsequently condenses to liquid phase upon isothermic depressurisation process at the surface [1]. The natural-gas condensate is known to contain a variety of metallic trace contamination whilst some are environmentally harmful, for example, arsenic, mercury and other radioactive substance. Arsenic is the one focused here. It generally stays in the natural-gas condensate as organic-metallic compound called the triphenylarsine $As(C_6H_5)_3$, trimethylarsine (*TMA*), triethylarsine (*TTA*), dimethylethylarsine (*DMEA*) or methyldiethylarsine (*MEDA*) [2]. It is usually found in the range of 40 to 514000 ppb [3].

Removal of arsenic from the natural-gas condensate is necessary. Industrial-wise, arsenic has considered economic impacts on the plant that utilise catalyst against the arsenic contaminating natural-gas condensate. The arsenic can be poisonous to certain catalyst, reducing the plant efficiency and accelerating the catalyst changeover. Environmental-wise, arsenic is toxic to living organism, including human [4].

The process for arsenic removal is viable from several techniques. De-arsenic catalyst [5] is the most well-known, followed by adsorptive media process, coagulation/filtration process, ion exchange chemical process [6] and extraction via hollow fiber supported liquid membrane [7, 8]. Each technique has its pros and cons that consideration shall be given when the process selection is to be made, for example, the catalyst is reasonably effective in removing inorganic arsenic but not the organic arsenic, the filtration is the most simple but low efficiency and high operating expenditure from frequent filter changeover.

Introduction of new arsenic removal technique is presented in this paper. A pulsed sieve plate column (PSPC) in conjunction with liquid-liquid extraction is employed. The PSPC has extensively applied in chemical, biochemical and petroleum industries besides nuclear-fuel reprocessing [9-10]. The PSPC contains several advantages: simple operation, low capital & operating cost, less footprint and reasonably high efficiency. Moreover, it has clear advantages over other mechanical contractors when processing with corrosive solution due to the wet parts made of highly corrosive resistant material such as stainless steel; or processing with radioactive solutions since the pulsing unit can be set in a remote area for safety considerations. It has no mechanical or rotating components inside the column,

obviating unnecessary repair and service [11] and more effective to deal with viscous liquid in this natural-gas condensate case.

The PSPC operation with an appropriate extraction solvent makes the doable removal of organic arsenic compound from the natural-gas condensate – while the de-arsenic catalyst process cannot overcome [5]. The operation consists of counter current flow between the natural-gas condensate and the extractant solvent. The arsenic transfers preferentially to the extractant phase in which the rate of mass transfer is enhanced by the degree of imparted turbulence from the pulsation motion.

Objective set by this study is to verify the application of PSPC in the arsenic removal from the natural-gas condensate and to investigate influence of operating parameters for achieving the high level of removal efficiency in term of mass transfer parameters.

A.3 Theory

The PSPC has a setup shown in Fig. A.1 (a) with an assembly of the fixed perforated plate inside the column as in Fig. A.1 (b). Pulsation unit is connecting at the bottom of the column to impart pulsing motion to the liquid by an external mechanical device [12]. The basic principle of operation is simple to understand with two immiscible phases within the column, i.e. the continuous phase and the dispersed phase. With respect to the arsenic removal study, the continuous phase is an extractant solvent feeding the column from the top; the dispersed phase is the natural-gas condensate feeding the column from the bottom. They flow in counter allowing transfer of arsenic from condensate (dispersed) phase to extractant (continuous) phase.

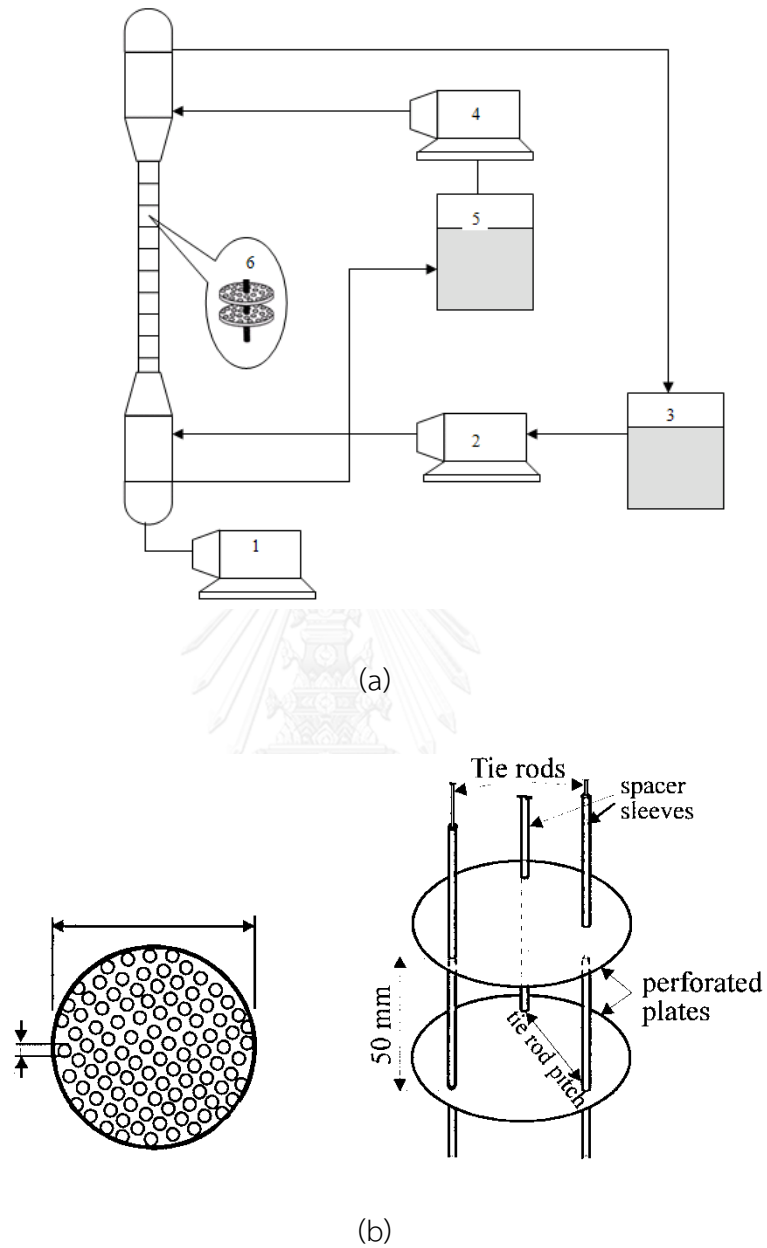


Figure A.1 (a) Schematic flow diagram of a pulsed sieve plate column: 1. Pulsation unit, 2. Feed pump, 3. Feed tank, 4. Extractant pump 5. Extractant tank, and 6. A perforated plate (b) Diagram of stainless steel perforated plates and spacers [13]

On the upstroke generated by the pulsation unit, the condensate phase is pushing through the holes of the upper perforated plate forming dispersion in the extractant phase on the next plate above. On the downstroke, the reverse takes place as the extractant phase is pushing through the holes of the bottom plates [9]. Following the upstroke and downstroke action, the mass transfer starts and enters in the regime behaving like a series of mixers and settlers as illustrated in Fig. A.2. At the proper pulse velocity, the dispersion becomes uniform; the solute concentration is perfectly mixed with respect to both phases and equal to emulsion leaving the column. The illustrative diagram for flow schematic of this operation in an emulsion regime is provided in Fig. A.3.

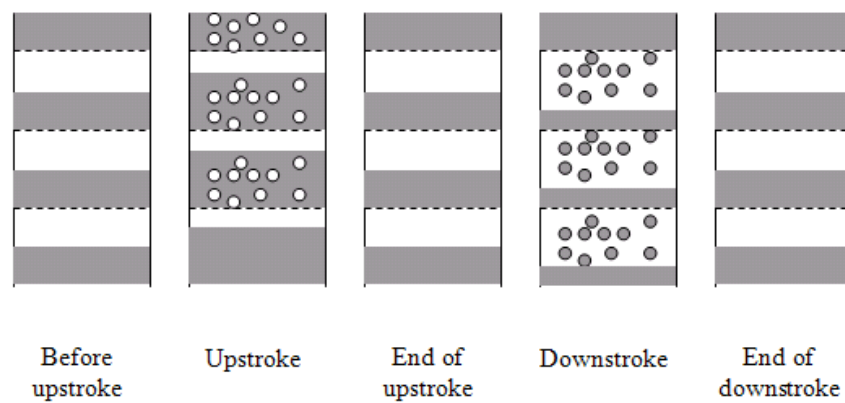


Figure A.2 Schematic flow patterns of continuous and dispersed phase in a pulsed sieve-plate column [10]

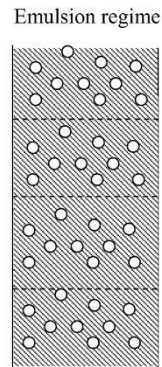


Figure A.3 Flow patterns of continuous and dispersed phase in emulsion regime [10]

Performance efficiency by this PSPC operation in mass transfer prospective for removal of arsenic from the condensate is classically reported in term of overall height of transfer unit (HTU_{oy}). Fig. A.4 shows the diagram describing a continuous countercurrent flow in the PSPC. Term L_c and L_d are the flowrate of the continuous phase and the dispersion phase; x and y are the fractions of solute concentration in the continuous phase and the dispersed phase [12]. The HTU_{oy} is considered, instead of using the mass-transfer coefficient, since it is only one dimensional length which does not account for the changes in compositions within the column but only the top and the bottom. It is also useful when the equilibrium line is straight and the curvature of operating line is negligible.

For the sake of simplicity, the term HTU_{oy} is used without correction to the axial backmixing effect which makes the system deviating from the ideal plug flow behavior.

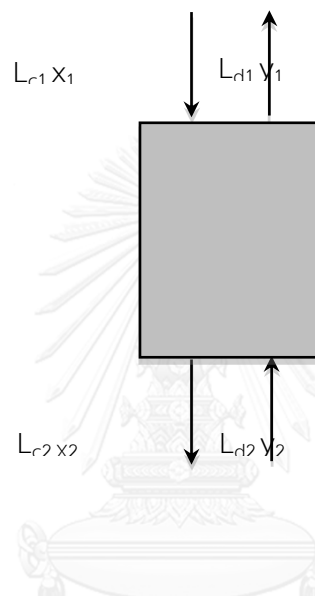


Figure A.4 The diagram for continuous countercurrent flow [12].

In order to calculate HTU_{oy} [11], the term to start with is the overall number of transfer units (NTU_{oy}) based on the dispersed phase. It is given by:

$$NTU_{oy} = \int_{y_1}^{y_2} \frac{dy}{y^* - y} = \frac{(y_1 - y_2)}{(y^* - y)_m} \quad (\text{A.1})$$

Where $(y^* - y)_m$ is the log-mean of $(mx_1 - y_1)$ and $(mx_2 - y_2)$, the potential concentration differences at the top and bottom of the column, and hence the log-mean value is given by:

$$(y^* - y)_m = \frac{(mx_1 - y_1) - (mx_2 - y_2)}{\ln \left(\frac{mx_1 - y_1}{mx_2 - y_2} \right)} \quad (\text{A.2})$$

Term “m” in Eq. (A.2) is the slope of the linear equilibrium curve provided that the system is taken as linear relationship of solute in ternary phase system. The overall height of transfer unit based on the dispersed phase is therefore calculated by

$$HTU_{oy} = \frac{Z}{NTU_{oy}} \quad (\text{A.3})$$

The other considered parameters to evaluate the column efficiency are fractional hold-up of dispersed phase (H_d) and interfacial area (a). The fractional hold-up is the volumetric dispersed phase corresponding to the total liquid volume in

the column. It is a factor not only determines mass transfer but also the onset of flooding [14]. It is defined by:

$$H_d = U_d / (U_c + U_d) \quad (\text{A.4})$$

Where H_d is the fractional hold-up of the dispersed phase; U_d is the volume of the dispersed phase and U_c is the total volume of the continuous phase [13].

Interfacial area of dispersion droplet (a) is a function of fractional hold up (H_d) and the surface mean diameter of dispersed drop size. It is the term which presents mass transfer area available from the means average dispersed drop. The larger the interfacial area has the greater mass transfer availability.

$$a = 6H_d / d_{vs} \quad (\text{A.5})$$

Surface mean diameter of dispersed drop size (d_{vs}) is originally proposed by J. Suater for a diameter of a sphere that has the same volume/surface area ratio as a particle of interest. Khemongkorn et al. proposed an empirical equation to determine d_{vs} as follows [10].

$$d_{vs} = 4.9 \times 10^{-5} A^{-1} f^{1.24} N^{-0.21} V_d^{-0.0002} \quad (\text{A.6})$$

A.4 Experimental

A.4.1 The Feed Condensate and the Reagents

The natural-gas condensate was obtained from Weerasuwan Co., Ltd., who owns the diesel oil production plant from natural-gas condensate throughput. The condensate contained initial arsenic concentration of 504 ppb determined by Inductively Coupled Plasma Spectrometry (ICP).

Candidate reagents in screening for a suitable extractant solvent were hydrochloric acid, methanol and ethanol. They are community chemicals, offering community price – which is in main favour due to economic aspect – and short time delivery.

Information in Table A.1 exhibits past successful researches on arsenic removal by liquid-liquid extraction.

Table A.1 Arsenic Removal from Past Researches

Extractant	Metal ion	Feed solution	Treatment	Strip solution	Solvent	Analysis
TBP [7]	Hg(II), As(III)	Produce water	SLM ^b	NaOH	Kerosene	ICP
TOA [7]	Hg(II), As(III)	Produce water	SLM ^b	H ₂ O	Kerosene	ICP
Cyanex 923 [8]	As	Synthetic water	SLM ^b	H ₂ O	Kerosene	ICP
Cyanex 301, Cyanex 923, TOA, Aliquat 336 [15]	As	Produced water	SLM ^b	NaOH	Kerosene	ICP
Aliquat 336, Cyanex 471 [16]	Hg(II) As(V)	Produced water	SLM ^b	Thiourea a	Kerosene	ICP
HCl, PCl ₃ [17]	As	Shale oil	Acidic chloride addition	N/A	N/A	ICP
H ₃ PO ₄ , CH ₃ OH [18]	As	Biological sample	Reactor	N/A	Water	ICP
CH ₃ OH C ₂ H ₅ OH [19]	As	rice straw	Ultrasonic Microwave assisted extraction	N/A	Water	ICP/HPLC -HG-AFS

Notes: SLM - Supported liquid membrane, a - Flat sheet, b - Hollow fiber

ICP - Inductively Coupled Plasma, UV - ultraviolet-visible spectroscopy

A.4.2 Apparatus

Pulsed Sieve Extraction Column

The configuration of the PSPC in the study was same as demonstration in Fig. A.1. Specification is summarized in Table A.2. The column was fitted with the regularly spaced horizontal sieve plates which help bringing the two immiscible phases into contact. A pulsation unit was located at the column base, imparting the pulse motion from the bottom to the top of the column.

Table A.2 Characteristics of the Pulsed Sieve-Plate Column in this Study

Specifications	Descriptions
Column diameter	50 mm
Effective height of each column section	1,000 mm
Number of sieve plates	19 per section
Plate spacing	50 mm
Plate diameter	50 mm
Hole size	2 mm
Average number of holes	140 per plate
Average free area	25%
Number of column sections	2

A.4.3 Procedures

The extractant solvent (continuous phase) was pumped from the tank to the top of the column. The condensate feed (dispersed phase) was pumped counter-currently to the bottom. The pulse velocity was varied to the desired values by a pulsation unit. The pump speed was manipulated for flowrate adjustment to meet the desired volumetric flowrate ratio between the condensate and the extractant. The condensate and the extractant left the column, returned to their original tank. The step repeated until desired operating time reached.

Measurement of fractional hold-up was performed according to Eq. (A.4). It was performed by the simultaneous interruption of the operation and of the inlet and outlet streams when steady state had reached. The column was emptied to measure volume of both phases [20].

A.4.4 Analytical Instrument

Inductively Coupled Plasma Spectrometry (ICP)

The concentration of the arsenic was measured by the inductively coupled plasma spectroscopy (ICP). The arsenic reading was then taken further to identify performance by the use of the percentage of removal term in Eq. (A.7).

$$\% \text{ Removal} = \frac{C_{As,out}}{C_{As,in}} \times 100 \quad (\text{A.7})$$

$C_{As,in}$ and $C_{As,out}$ represents the concentrations of arsenic in the inlet condensate and the outlet extractant.

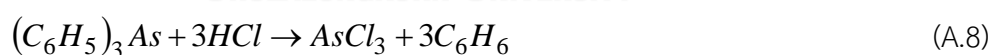
A.5 Results and Discussion

A.5.1 Extractant Effect

The experiment was set up to screen which reagent would provide good percentage of arsenic removal. The set up was taken on the background of the pulse velocity at 20 mm/s, volumetric-flowrate ratio of extractant to feed at 1:1.

Hydrochloric acid

The arsenic removal from using hydrochloric acid (*HCl*) as an extractant at various concentrations was presented in Fig. A.5. The highest arsenic removal was found at 18% from 1 M *HCl* before the performance declined. The extraction mechanism involves breaking of organometallic in arsenic hydrocarbon compound by chloride ion [4]. The mechanism is illustrated in Eq. (A.8).



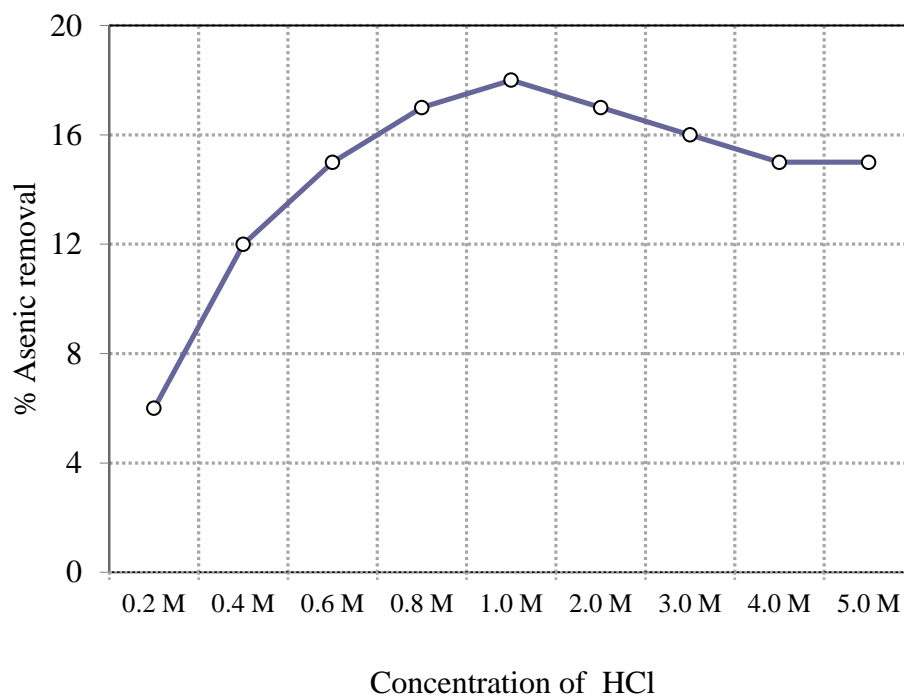


Figure A.5 The effects of *HCl* concentration on the percentage of arsenic removal:

pulse velocity 20 mm/s, volumetric-flowrate ratio of feed to *HCl* 1:1

Hydroxyl solvent

Hydroxyl group solvent such as methanol (CH_3OH) 5-35% (v/v) and ethanol (C_2H_5OH) 5-35% (v/v) for arsenic removal were examined with the results shown in Fig. A.6. The results revealed to the higher performance of methanol over the ethanol. This could be explained by the polarity aspect that the methanol contains

less polar hydroxyl [21-22], thus is easier to get in contact with the non-polar hydrocarbon than does the ethanol for the arsenic removal.

The reaction mechanisms by methanol and ethanol are presented in Eq. (A.9) and Eq. (A.10). The highest performance was found at the percentage of removal of 32% by 20% (v/v) methanol.

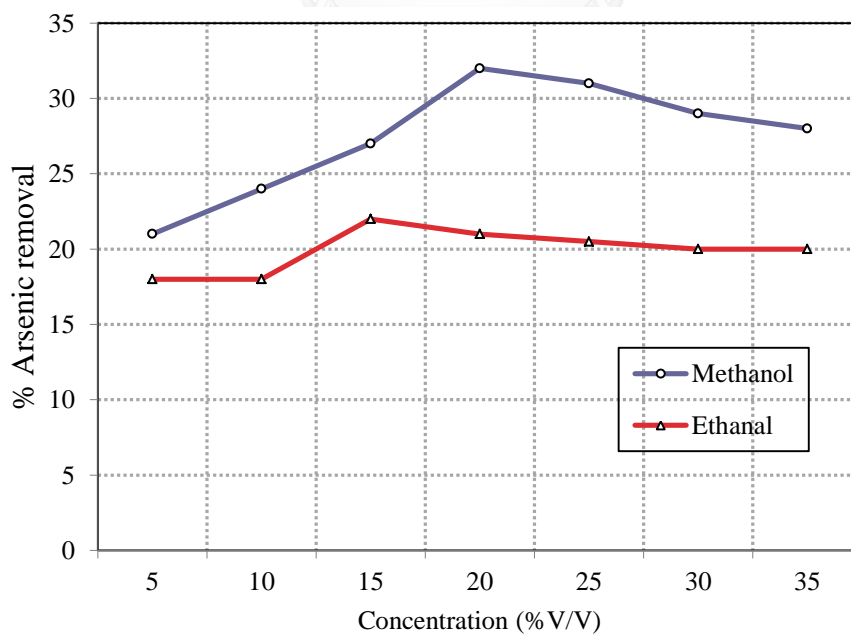
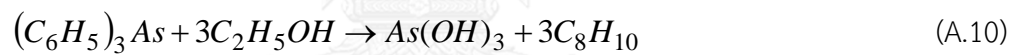
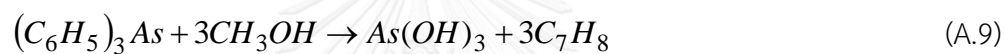


Figure A.6 The effects of methanol and ethanol concentration on the percentage of arsenic removal: pulse velocity 20 mm/s, volumetric-flowrate ratio of feed to methanol/ethanol 1:1

A.5.2 Synergistic Effect

An investigation was extended to a possible combined extractant from the previous successful reagents. The mixture of HCl and CH_3OH was evaluated at various concentrations with the results shown in Fig. A.7. The highest achievable arsenic removal was 45% by 1M HCl and 20% (v/v) CH_3OH mixture. It was higher than alone performed by HCl (18% highest) or CH_3OH (32% highest), obviously indicating the synergistic effect or performance enhancement from the use of the $HCl-CH_3OH$ mixture. Synergistic reaction is presented in Eq. (A.11) and Eq. (A.12) where CH_3Cl , a product of HCl and CH_3OH , is able to extract arsenic from the arsenic-hydrocarbon compound in addition to the reactions by HCl in Eq. (A.8) and the reaction by CH_3OH in Eq. (A.9).

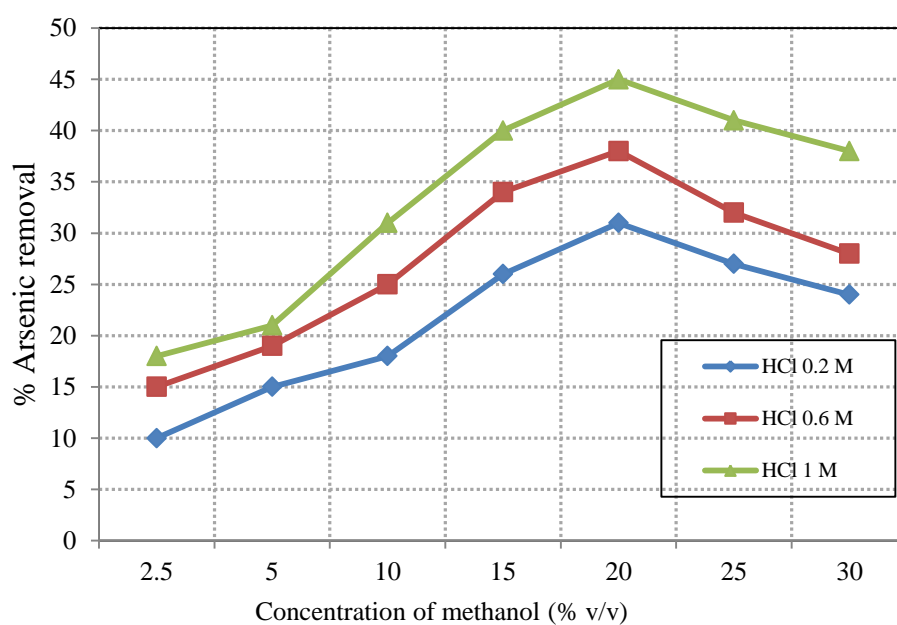
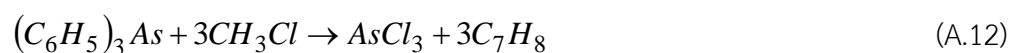
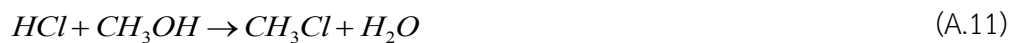


Figure A.7 The effects of the mixture of *HCl* solution and *CH*₃*OH* on the percentage of arsenic removal: pulse velocity 20 mm/s, volumetric flowrate ratio of the mixture of *HCl* and *CH*₃*OH* to feed solution 1:1

Table A.3 provides information on the physical properties of the natural-gas condensate and the selected extractant in the study.

Table A.3 Physical properties

Phase	Physical Properties (@ 25° C)		
	Density kg/m ³	Viscosity cP	Surface tension dyne/cm
Continuous (1M HCl and 20% v/v methanol)	955.6	0.70	65.74
Dispersed (Natural gas condensate)	844	8.86	25

A.5.3 Pulse Velocity Effect

The effect of pulse velocity was investigated with the result presented in Fig. A.8. It was found that increase in arsenic removal performance was corresponding to increasing of pulse velocity and operating time. Off 62% arsenic removal was obtained from the pulse velocity at 20 mm/s.

The pulsing velocity significantly improved the rate of mass transfer by reducing the size of dispersed drops thus increasing an interfacial area for more effective mass transfer.

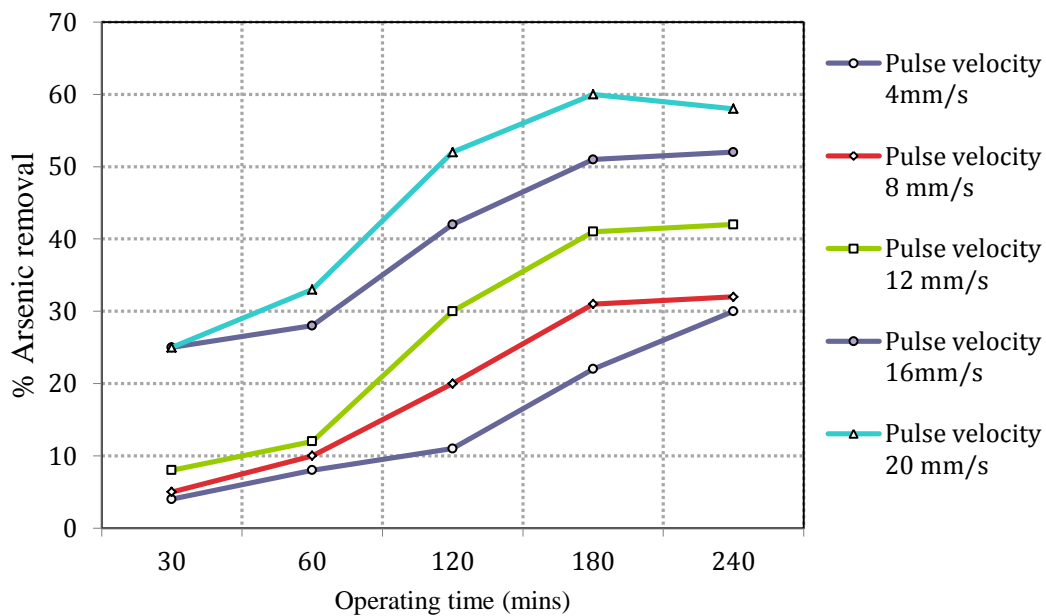


Figure A.8 The effects of pulse velocity and operating time on the percentage of arsenic removal using the mixture of 1M HCl and 20% (v/v) CH_3OH as the extractant at volumetric-flowrate ratio of the condensate to the extractant 1:1

To describe the performance following the effect of pulse velocity in term of classical overall height of transfer unit (HTU_{oy}), Eq. (A.1) and Eq. (A.3) are deployed to calculate NTU_{oy} and HTU_{oy} . An equilibrium diagram in Fig. A.9 was plotted to calculate slope “m” for Eq. (A.2) calculation. The mixture of condensate and extractant (the selected mixture of 1 M HCl and 20% (v/v) CH_3OH at volumetric-flowrate ratio of the condensate to the extractant 1:1) were stirred for 60 minutes, left approximately for one hour settlement when the layer became clear, then

sampled for concentration distribution analysis. The equilibrium curve was created with the slope (m) calculated to 0.8611.

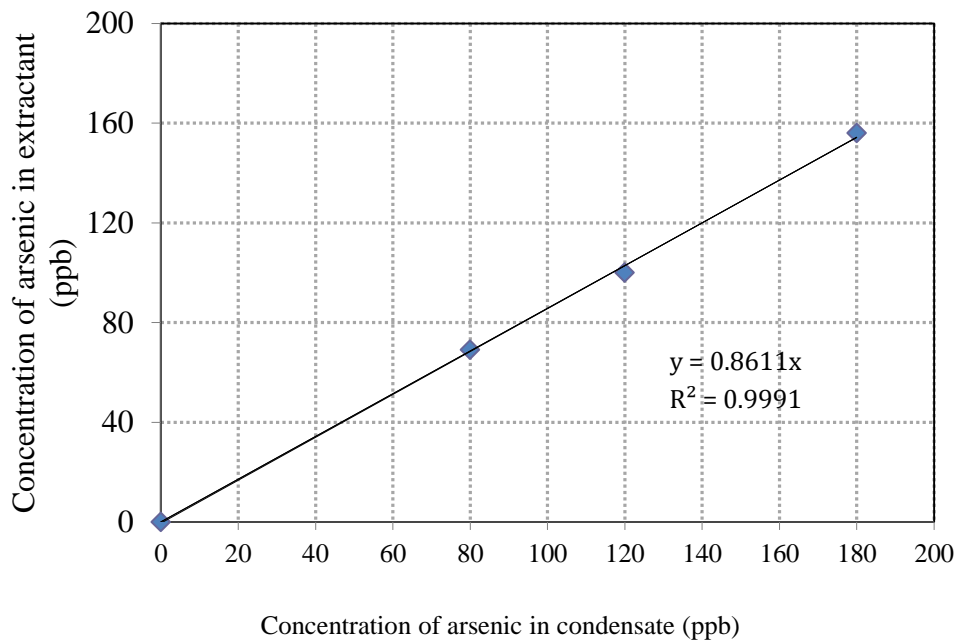


Figure A.9 The equilibrium diagram of the condensate and the extractant (the mixture of 1 M HCl and 20% (v/v) CH_3OH at volumetric-flowrate ratio of the condensate to the extractant 1:1)

Fig. A.10 presents the calculated HTU_{oy} with respect to the effect of pulse velocity by. At the pulse velocity of 20 mm/s where the removal efficiency is read highest, it corresponds to the smallest HTU_{oy} of 134 cm. The more efficient the mass transfer (i.e. larger mass transfer rate) corresponds to the smaller the value of HTU .

Hence it should be fair to make a statement that increase in arsenic removal performance markedly corresponds to an increasing pulse velocity that would as well shows in term of decreasing HTU_{oy} .

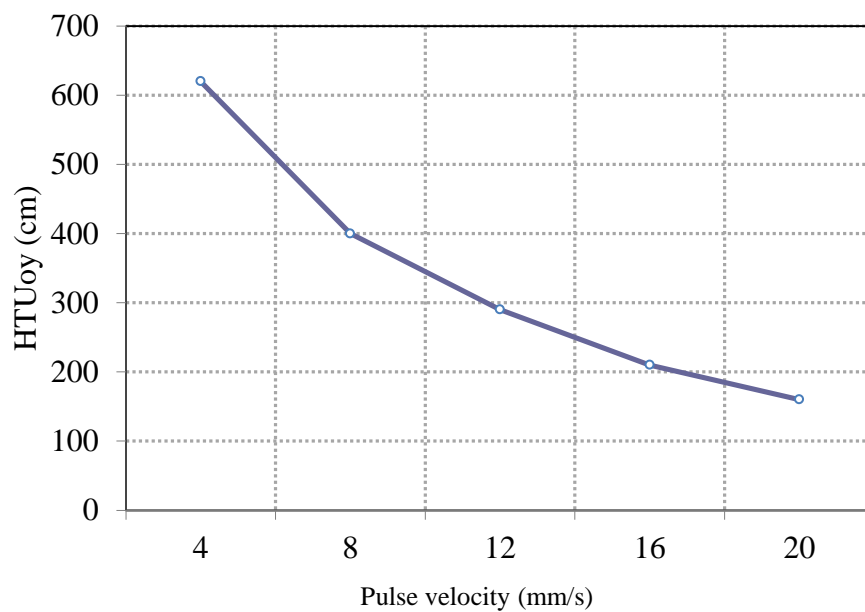


Figure A.10 The relation of the calculated HTU_{oy} from arsenic removal using the mixture of 1M HCl and 20% (v/v) CH_3OH as the extractant at the volumetric-flowrate ratio of the condensate to the extractant 1:1.

A.5.4 Feed-to-Extractant Flowrate Effect

The effect of the volumetric-flowrate ratio of the condensate-to-extractant phase was investigated with the results presented in Fig. A.11. The flowrate ratios

were varied to observe the effect. As the ratio progressed from high to low, the percentage of arsenic removal was found increasing. Until the ratio of 1:4 where the arsenic removal was found highest at 94%, the removal performance started to decline.

The increase in removal performance during the early part when the flowrate ratio decreased was due to the shift of ternary equilibrium system, allowing arsenic compound to distribute more to the extractant phase – the phase at which the operating volume was adjusted to higher (1x condensate : 4x extractant).

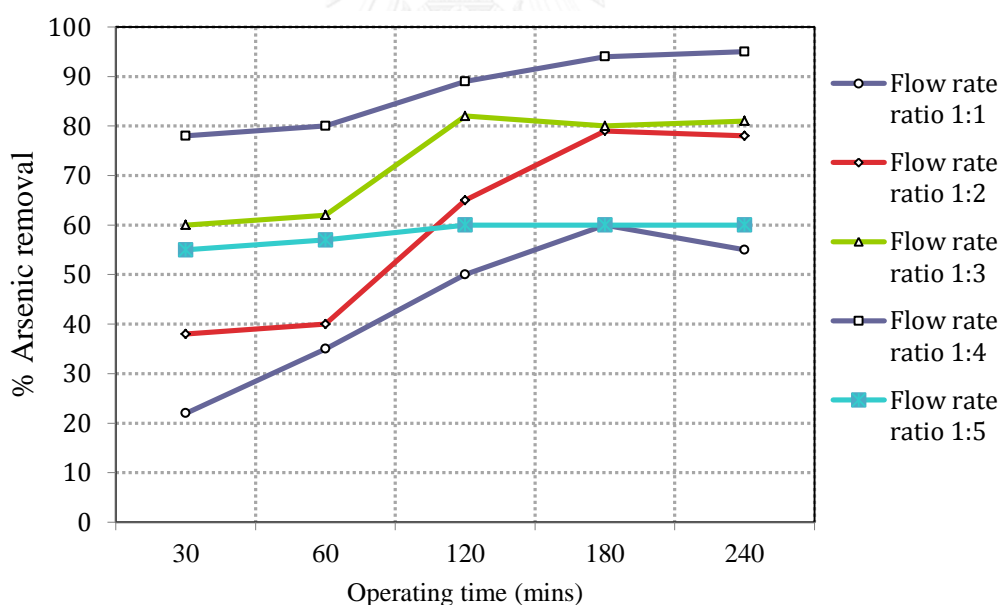


Figure A.11 The effects of volumetric-flowrate ratio of the condensate to the extractant on the percentage of arsenic removal using the mixture of 1M HCl and 20% (v/v) CH_3OH as the extractant at a pulse velocity of 20 mm/s

Fractional hold-up and interfacial area were determined with an interest to examine the behaviour of the varying flowrate ratio case.

As can be seen from the calculated data in Table A.4 that the dispersed phase hold up and the interfacial area have an increasing tendency with the progress of flowrate ratio from high to low. It stops when the ratio proceeds from 1:4 to 1:5 as both the hold-up and the interfacial area show insignificant change, exhibiting the sign of flow regime transition. And any further decrease in the flowrate ratio – by increasing the extractant (dispersed) phase –, it may leads to the column flooding where the terminal rise velocity of condensate (continuous) phase is less than the superficial velocity of the continuous phase. Hence, the condensate phase will start accumulating in the column at the continuous phase outlet, compromising the removal efficiency.

Table A.4 Calculated interfacial area from varied volumetric flowrate ratio

Flowrate ratio	davg (mm)	Hold-up	Interfacial area (m ² /m ³)
1:1	0.4049	0.45	67
1:2	0.4048	0.62	92
1:3	0.4047	0.78	109
1:4	0.4046	0.80	118
1:5	0.4045	0.81	120

A.5.5 Cycle Effect

Fig. A.12 shows the percentage of arsenic removal in each cycle, based on the operation at the pulse velocity of 20 mm/s and the volumetric-flowrate of the condensate to the extractant 1:4 ratio. In this experiment work, the fresh feed condensate (504 ppb arsenic) was introduced every cycle while the extractant solvent was reused. The arsenic removal percentages were reported in linear decline: 94, 85, 80, 60, 46 and 40 from the respective 1st – 6th cycle.

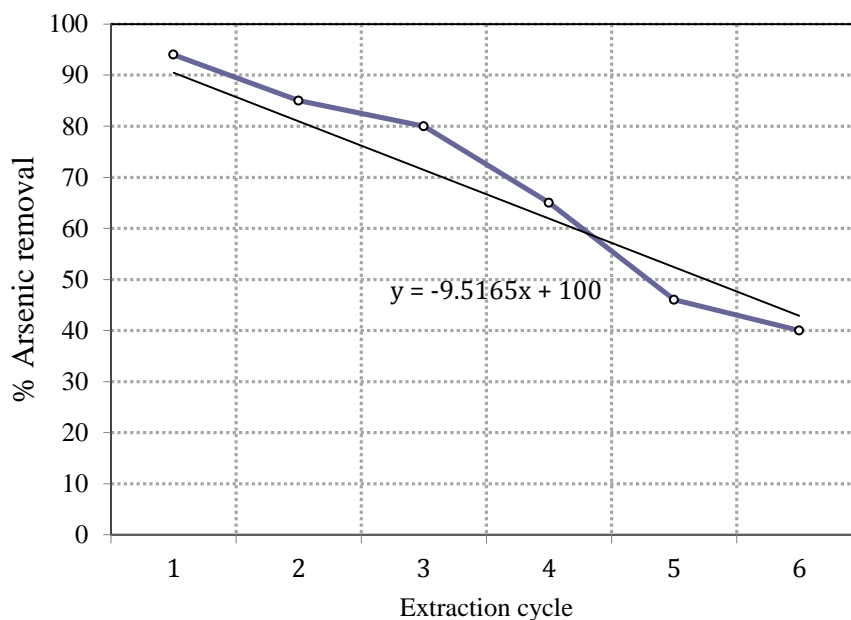


Figure A.12 The effects of removal cycle on the remained arsenic in the condensate using the mixture of 1 M HCl and 20% (v/v) CH_3OH as the extractant at a pulse velocity of 20 mm/s, the volumetric-flowrate of the condensate to the extractant 1:4

A.6 Conclusion

The arsenic removal using a mixture of hydrochloric acid and methanol via a pulsed sieve plate column was found with highly effective arsenic removal from the natural-gas condensate. The pulsed sieve plate column is one of the suitable units of operation to deal with organic condensate since the wet part is made of stainless steel, insusceptible to organic solvation. Moreover it utilises pulsation unit to

enhance mass transfer without the need of rotating mechanical internals to deal with viscous type liquid such as the natural-gas condensate in this case.

Operating parameters were examined to establish the optimum operating condition for the arsenic removal application using the pulsed sieve plate column. The best extractant solvent was found from the combined 1M hydrochloric acid and 20% (v/v) methanol. The suitable pulse velocity was 20 mm/s. The volumetric flowrate ratio was found optimum at 1:4 of the ratio between the condensate and the extractant. Lower than 1:4, e.g. 1:5, the drop in arsenic removal performance was observed. This was probably due to the operating flow regime entering into the unstable stage of column flooding – suggested by the calculated dispersed fractional hold-up.

The highest percentage of removal was found at 94% from the aforementioned operating condition. Under these conditions, the efficient mass transfer represented by the minimum calculated HTU_{oy} was calculated.

With the continuous operation in cycle mode, the removal percentages were observed at 94, 85, 80, 60, 46 and 40 from the respective 1st – 6th cycle, behaving in a linear decline trend. The operation was on the condition that the fresh feed (504

ppb arsenic) was introduced at the beginning of each cycle while the extractant solvent was reused.

A.7 Acknowledgments

The authors are grateful to Weerasuwan Co., Ltd. for their collaboration and the condensate, the Department of Chemical Engineering, Pathumwan Institute of Technology, Bangkok, Thailand for supporting the pulsed sieve plate column. Sincerely thanks also go to Thailand Research Fund (TRF), the Office of Small and Medium Enterprises Promotion (OSMEP), the Separation Laboratory, Department of Chemical Engineering, Chulalongkorn University, Bangkok, Thailand for the research grants and chemicals. More appreciation CU-Cluster Ratchadaphisak Somphot Endowment Fund for the partial supported.

A.8 Nomenclature

a : Interfacial area (m^2/m^3)

$C_{As, in}$: Concentration of arsenic in inlet feed (ppm)

$C_{As, out}$: Concentration of arsenic in outlet extract (ppm)

d_{vs}	: Surface mean diameter of dispersed drop size
HTU	: Height of transfer unit (cm)
H_d	: The fractional hold-up of the dispersed phase
L_c	: Flow rate of the continuous phase (m^3/s)
L_d	: Flow rate of the dispersed phase (m^3/s)
m	: The slope of equilibrium curve
NTU	: Number of transfer units
$PSPC$: Pulsed Sieve Plate Column
U	: Phase volume (cm^3)
u_0	: Characteristic velocity
V	: Phase Velocity (m/s)
x	: fraction of solute concentration in the continuous phase
y	: fraction of solute concentration in the dispersed phase
Z	: Effective height of extraction column (cm)

Subscripts

c	: Continuous phase
d	: Dispersed phase

- lm* : Log-mean
- oy* : Overall based on dispersed phase
- 1, 2 : Top and bottom conditions of column, respectively

A.9 Reference

- [1] http://en.wikipedia.org/wiki/Natural_gas 1/10/2010.
- [2] Krupp, E. M., Johnson, C., Rechsteiner, C., Moir, M., Leong, D. and Feldmann, J. (2007) Investigation into the determination of trimethylarsine in natural gas and its partitioning into gas and condensate phases using (cryotrapping)/gas chromatography coupled to inductively coupled plasma mass spectrometry and liquid/solid sorption techniques. *Spectrochimica Acta Part B*, 62: 970.
- [3] Puri, B. K. and Irgolic, K. J. (1989) Determination of arsenic in crude petroleum and liquid hydrocarbons. *Environmental Geochemistry and Health*, 11 : 95.
- [4] Tantichaipakorn, P. (1998) M.Eng. Thesis, Department of Chemical Engineering, Faculty of Engineering, Chulalongkorn University, Thailand,
- [5] http://www.newpointgas.com/naturalgas_arsenic.php 12/10/2010.

- [6] Clifford, D. (1999). Ion Exchange and Inorganic Adsorption. In American Water Works Association (Eds.), Water Quality and Treatment: A Handbook of Community Water Supplies, 5th ed. New York: McGraw-Hill.
- [7] Sangtumrong, S., Ramakul, P., Satayaprasert, C., Pancharoen, U. and Lothongkum, A.W. (2007) Purely Separation of Mixture of Mercury and Arsenic via Hollow Fiber Supported. J. Ind. Eng. Chem., 13: 751.
- [8] Prapasawat, T., Ramakul, P., Satayaprasert, C., Pancharoen, U. and Lothongkum, A.W. (2007) Separation of As(III) and As(V) by hollow fiber supported liquid membrane based on the mass transfer theory. Korean J. Chem. Eng., 25: 158.
- [9] Usman, M. R., Hussain, S. N., Rehman, L., Bashir, M. and Butt, M. A. (2006) Mass transfer performance in a pulsed sieve- plate extraction column. Proc. Pakistan Acad. Sci., 43: 173.
- [10] Yadav, R.L. and Patwardhan, A.W. (2008) Design aspects of pulsed sieve plate columns. Chem. Eng. J., 138: 389.
- [11] Meisam T.M. and Jaber S. (2009) Mass transfer coefficients in a pulsed packed extraction column. Chemical Engineering and Processing 48:1321

- [12] Laddha, G. S. and Degaleesan, T.E. (1978) Transport Phenomena in Liquid Extraction. McGraw-Hill.
- [13] Gottliesen, K., Grinbaum, B., Chen, D. and Geoff, W. S. (2000) The use of pulsed perforated plate extraction column for recovery of sulphuric acid from copper tank house electrolyte bleeds. *Hydrometallurgy*, 58: 203.
- [14] Kumar, A. and Hartland, S. (1999) Correlations for Prediction of Mass Transfer Coefficients in Single Drop Systems and Liquid-Liquid Extraction Columns. *Chemical Engineering Research and Design*, 77 : 372.
- [15] Pancharoen, U., Poonkum, W. and Lothongkum, A.W. (2009) Treatment of arsenic ions from produced water through hollow fiber supported liquid membrane. *J. of Alloys and Comp.*, 482: 328.
- [16] Lothongkum, A.W., Suren, S., Chaturabul, S., Thamphiphit, N. and Pancharoen, U. (2011) Simultaneous removal of arsenic and mercury from natural-gas-co produced water from the gulf of Thailand using synergistic extractant via HFSLM. *J. Membr. Sc.*, 369 (1-2): 350.
- [17] Delaney, D. D., (1988) United States Patent, 4752380.

- [18] Pizarro, I., Gómez, M., Cámara, C. and Palácios, M.A. (2003) Arsenic speciation in environmental and biological samples Extraction and stability studies. *Analytica Chimica Acta*, 495: 85.
- [19] Yuan, C., Jiang, G. and He, B. (2005) Evaluation of the extraction methods for methods for Arsenic speciation in rice straw. *J. Anal. At. Spectrom*, 20: 103.
- [20] Giraldo-Zuniga, A. D., Coimbra, Jane S.R., Minim, L.A. and Garcia Rojas, E. E. (2006) Dispersed phase hold-up in a Graesser raining bucket contactor using aqueous two-phase systems. *J. Food Engineering*, 72: 302.
- [21] <http://www.colby.edu/chemistry/webmo/methanol.html> 9/9/2010.
- [22] <http://www.colby.edu/chemistry/webmo/ethanol.html> 6/8/2010

Mr. Srestha Chaturabul obtained his Bachelor Degree of Petroleum Engineering from Chulalongkorn University in 1998 and Master degree of Chemical Engineering also from Chulalongkorn University in 2006. He pursued his graduate study in Doctoral degree at Separation Technology Laboratory, Department of Chemical Engineering, Faculty of Engineering, Chulalongkorn University since 2006 and received scholarship from the Thailand Research Fund and Chulalongkorn University under the Royal Golden Jubilee Ph.D. Program.

[1] S. Chaturabul, K. Wongkaew, U. Pancharoen, Selective Transport of Palladium through a Hollow Fiber Supported Liquid Membrane and Prediction Model Based on Reaction Flux, *Separation Science and Technology* 48 (2012) 93-104.

[2] S. Chaturabul, W. Srirachat, T. Wannachod, P. Ramakul, U. Pancharoen, S. Kheawhom, Separation of mercury(II) from petroleum produced water via hollow fiber supported liquid membrane and mass transfer modeling, *Chemical Engineering Journal* 265 (2015) 34-46.

[3] S. Chaturabul, T. Wannachod, N. Leepipatpiboon, U. Pancharoen, S. Kheawhom, Mass transfer resistance of simultaneous extraction and stripping of mercury(II) from petroleum produced water via HFSLM, *Journal of Industrial and Engineering Chemistry* 21 (2015) 1020-1028.

[4] S. Chaturabul, T. Wannachod, V. Mohdee, U. Pancharoen, S. Phatanasri, An investigation of Calix[4]arene nitrile for mercury(II) treatment in HFSLM application, *Chemical Engineering and Processing: Process Intensification* 89 (2015) 35-40.

[5] P. Wannachod, S. Chaturabul, U. Pancharoen, A.W. Lothongkum, W. Patthaveekongka, *J. Alloy. Comp.* 509 (2011) 354-361.

